NASA Contractor Report 166528

A Computer Program for the Calculation of Three-Dimensional Transonic Nacelle/Inlet Flowfields

(NASA-CR-166528) A COMPUTER PROGRAM FOR THE CALCULATION OF THREE-DIMENSIONAL TRANSONIC NACELLE/INLET FLOWFIELDS Final Report (Lockheed-Georgia Co., Marietta.) 102 p HC A06/MF A01 CSCL 01A G3/02

N84-13159

Unclas 43195

Joseph Vadyak
Essam H. Atta

Contract NAS2-11285
November 1983

NASA

NASA Contractor Report 166528

A Computer Program for the Calculation of Three-Dimensional Transonic Nacelle/Inlet Flowfields

Joseph Vadyak
Essam H. Atta
Lockheed-Georgia Company
Marietta, Georgia

Prepared for Ames Research Center
under Contract NAS2-11285

National Aeronautics and
Space Administration

Ames Research Center
Moffett Field, California 94035

TABLE OF CONTENTS

SECTION		PAGE
I.	INTRODUCTION	2
II.	COMPUTATIONAL METHOD	4
	1. INTRODUCTION	4
	2. GRID TOPOLOGY AND GENERATION	4
	3. GOVERNING EQUATIONS FOR THE INVISCID FLOW	8
	4. NUMERICAL ALGORITHM	11
	4.1 BASIC FINITE-DIFFERENCE SCHEME	11
	4.2 BOUNDARY CONDITIONS	14
	4.3 INITIALIZATION	15
	4.4 NUMERICAL STABILITY	16
	5. NUMERICAL RESULTS	16
III.	SUBROUTINE DESCRIPTIONS	33
	1. INTRODUCTION	33
	2. SUBROUTINE DESCRIPTIONS FOR THE NGRIDA GRID GENERATION PROGRAM	33
	3. SUBROUTINE DESCRIPTIONS FOR THE NACELLE FLOW SOLUTION PROGRAM	35
IV.	INPUT PARAMETERS AND OUTPUT INTERPRETATION	39
	1. INTRODUCTION	39
	2. NGRIDA GRID GENERATION PROGRAM INPUT PARAMETERS	39
	2.1 NAMELIST LIST1	39
	2.2 NAMELIST LIST2	47
	2.3 NAMELIST LIST3	48
	2.4 NAMELIST LIST4	50
	2.5 PARAMETER STATEMENT SPECIFICATION	51
	2.6 FILE USAGE	51
	3. NGRIDA PROGRAM OUTPUT INTERPRETATION	52
	4. NACELLE FLOW SOLUTION PROGRAM INPUT PARAMETERS	52
	4.1 NAMELIST LIST1	53
	4.2 NAMELIST LIST2	58
	4.3 NAMELIST LIST3	60
	4.4 NAMELIST LIST4	62
	4.5 PARAMETER STATEMENT SPECIFICATION	63
	4.6 FILE USAGE	63
	5. NACELLE PROGRAM OUTPUT INTERPRETATION	63
V.	SAMPLE CASES AND SUGGESTIONS FOR USAGE	65
	1. INTRODUCTION	65
	2. NGRIDA GRID GENERATION PROGRAM SAMPLE CASES	65

2.1 SAMPLE CASE NO. 1 65
2.2 SAMPLE CASE NO. 2 67
2.3 SAMPLE CASE NO. 3 67
2.4 SAMPLE CASE NO. 4 67
3. NACELLE FLOW ANALYSIS PROGRAM SAMPLE CASES . 78
3.1 SAMPLE CASE NO. 1 78
3.2 SAMPLE CASE NO. 2 82
3.3 SAMPLE CASE NO. 3 82
3.4 SAMPLE CASE NO. 4 91
4. SUGGESTIONS FOR USAGE. 91
4.1 PARAMETER STATEMENT USAGE 91
4.2 NGRIDA PROGRAM USAGE. 95
4.3 NACELLE PROGRAM USAGE 95

REFERENCES 97

A COMPUTER PROGRAM FOR THE CALCULATION OF THREE-DIMENSIONAL TRANSONIC NACELLE/INLET FLOWFIELDS

Joseph Vadyak and Essam H. Atta
Advanced Flight Sciences Department
Lockheed-Georgia Company
Marietta, Georgia 30063

SUMMARY

A highly efficient computer analysis has been developed for predicting transonic nacelle/inlet flowfields. This algorithm can compute the three-dimensional transonic flowfield about axisymmetric (or asymmetric) nacelle/inlet configurations at zero or nonzero incidence. The flowfield is determined by solving the full-potential equation in conservative form on a body-fitted curvilinear computational mesh. The difference equations are solved using the AF2 approximate factorization scheme.

This report presents a discussion of the computational methods used to both generate the body-fitted curvilinear mesh and to obtain the inviscid flow solution. Computed results and correlations with existing methods and experiment are presented. Also presented are discussions on the organization of the grid generation (NGRIDA) computer program and the flow solution (NACELLE) computer program, descriptions of the respective subroutines, definitions of the required input parameters for both algorithms, a brief discussion on interpretation of the output, and sample cases to illustrate application of the analysis.

The isolated nacelle program developed herein has also been combined with the NASA-Ames TWING transonic wing flow analysis program to produce a wing/nacelle multicomponent flow analysis algorithm. The theory and usage of the wing/nacelle multicomponent program is discussed in a separate report.

SECTION I

INTRODUCTION

Accurate isolated nacelle/inlet flowfield predictions are required for nacelle contour optimization for both axisymmetric and asymmetric configurations at zero and nonzero incidence. The prediction methods must be capable of analyzing three-dimensional transonic flowfields with the inclusion of embedded shock waves. The computational analyses which are developed must not only be accurate but also efficient enough to be used repetitively in parametric design studies.

The objective of this investigation was to develop an accurate and highly-efficient method for calculating the three-dimensional transonic flowfield about axisymmetric (or asymmetric) nacelle/inlet configurations at zero or nonzero incidence. The solution is obtained by solving the full-potential equation in conservation law form on a three-dimensional body-fitted curvilinear mesh which is numerically generated. The use of the conservative form of the equation ensures that mass continuity is satisfied when capturing embedded shock waves. The difference equations are solved using the AF2 approximate factorization algorithm[1]. The AF2 algorithm has been applied to the computation of two-dimensional transonic airfoil flows by Holst[2] and to the computation of three-dimensional transonic wing flows by Holst and Thomas[3]. Increases in convergence speed by factors of 4 to 7 have been realized using the AF2 scheme instead of using the standard transonic relaxation scheme, successive-line-over-relaxation.

In the present investigation, the numerically-generated body-fitted grid is determined using a separate Fortran computer program called NGRIDA. The NGRIDA program can generate the computational mesh for axisymmetric nacelle/inlet configurations. It can be modified to be applied in a meridional plane sense to obtain the computational mesh for asymmetric nacelle/inlet configurations.

The inviscid flow solution is obtained using a separate Fortran computer program called NACELLE. The NACELLE program uses the computational grid generated by NGRIDA or an alternate program. The NACELLE code can determine the flowfield solution for axisymmetric or asymmetric nacelle/inlet configurations operating at zero or nonzero incidence in a subsonic or transonic free-stream flow.

The development of the isolated nacelle algorithm represents part of an overall effort to develop a combined wing/nacelle flow analysis program. The approach taken in developing the multicomponent algorithm is to use a component-adaptive grid embedding scheme in which the global computational grid is composed of a series of overlapped component grids, where each component grid is optimized for a particular geometry such as the wing or nacelle. The AF2 algorithm is used to determine the full-potential equation solution on each grid with trivariate interpolation being used to transfer property information between the component grids. To implement this approach for a wing/nacelle configuration, the NASA-Ames TWING

transonic wing flow analysis program[3] has been combined with the NACELLE transonic nacelle flow analysis program presented herein. Preliminary results employing this scheme are reported by Atta and Vadyak[4]. A report detailing the theory and usage of the combined multicomponent algorithm is given in Reference 5.

SECTION II

COMPUTATIONAL METHOD

1. INTRODUCTION

The three-dimensional body-fitted computational grid is determined using the NGRIDA computer program which employs a numerical mesh generation technique. The full-potential equation solution is obtained on the mesh generated by the NGRIDA program using the NACELLE flow analysis program. The efficient AF2 approximate factorization scheme is used by the NACELLE algorithm in solving the system of finite-difference equations.

In this section, the computational methods used to generate the curvilinear mesh and to obtain the inviscid flow solution are presented. Computed results and comparison with existing axisymmetric flow analysis methods and three-dimensional flow experimental data are presented to illustrate application of the analysis.

2. GRID TOPOLOGY AND GENERATION

The flow solution is determined on a three-dimensional body-fitted curvilinear computational mesh. The computational mesh is obtained by using two-dimensional numerical grid generation techniques for a series of meridional planes which are splayed circumferentially around the body (a meridional plane is a plane containing the longitudinal axis of the inlet).

Figure 1 illustrates the C-type nacelle/inlet grid topology for a semi-infinite nacelle extended in the downstream direction. The base Cartesian coordinates are denoted by x, y, and z. Figure 1a shows the meridional plane grid topology, whereas Figure 1b illustrates the grid as viewed along the longitudinal axis of the inlet which is the x axis. The computational curvilinear coordinates are denoted by ξ, η, and ζ. The ξ coordinate is in the wraparound direction, initiates at the external outflow surface, and terminates at the compressor face outflow surface. The η coordinate is in the circumferential direction, initiates at the $\theta = 0$ meridional plane, and terminates at the $\theta = 2\pi$ meridional plane. The ζ coordinate is in the radial direction, initiates at the outer computational boundary (or centerline boundary), and terminates at the body surface. The $\theta = 0$ and $\theta = 2\pi$ meridional planes are coincident for isolated nacelle configurations. If a pylon were present, then the pylon geometry would be contained between these two meridional stations. The (x-y) coordinate plane is the symmetry plane for angle of attack cases.

The surface grid points are clustered in the region of the nacelle hilite (leading edge point of the nacelle). The clustering is achieved by using a geometric stretching function which is expressed in terms of the arc length measured along the body from the hilite point in a given meridional plane. The stretching factor α_s is used to compute the ratio of arc lengths between successive pairs of surface grid points as given by the

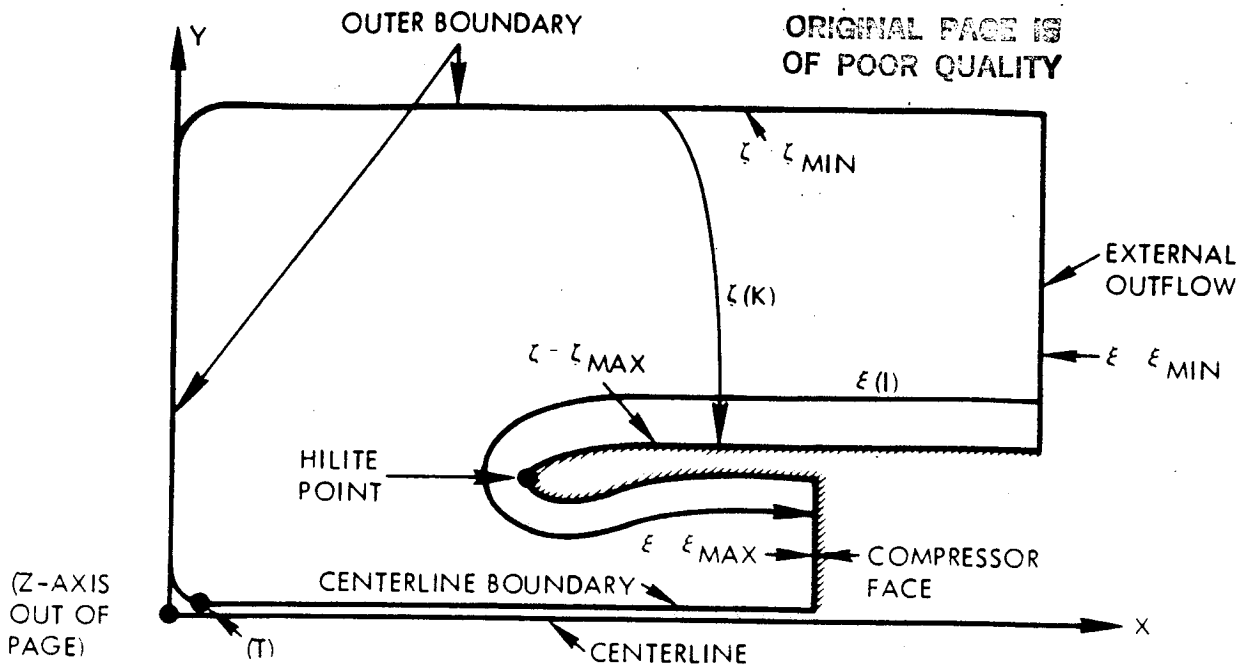

(a) MERIDIONAL PLANE GRID TOPOLOGY

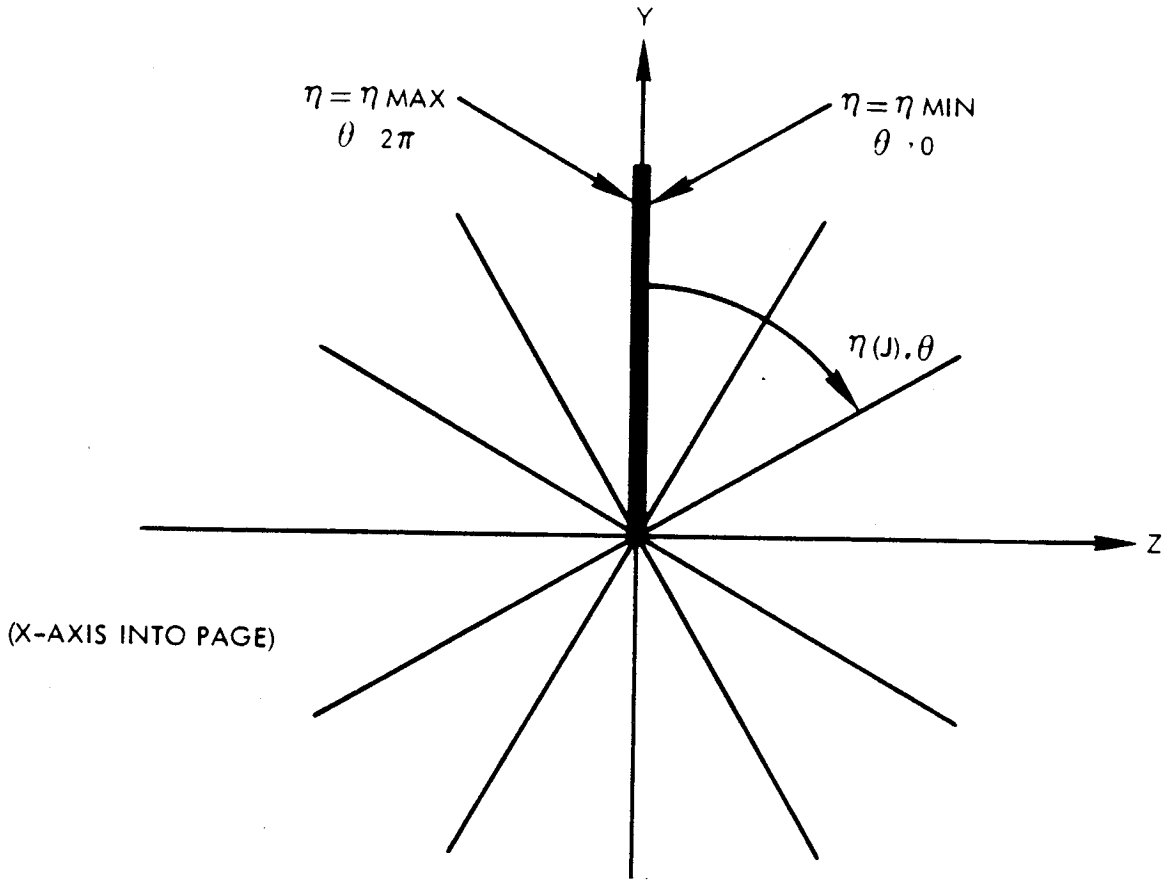

(b) GRID VIEWED ALONG X-AXIS

Figure 1. Grid topology.

expression

$$\alpha_s = \Delta S_n / \Delta S_{n-1} \tag{1}$$

where ΔS_n is the arc length between points n and n+1, and ΔS_{n-1} is the arc length between points n-1 and n, as shown in Figure 2. Independent values of α_s may be used for locating surface grid points on the external and internal nacelle contours. The outer computational boundary point distribution is determined by using either an angular distribution function expressed in terms of an angle measured about the nacelle hilite, or by again using an arc length distribution along the outer boundary.

Once the surface and outer boundary mesh point distributions have been determined, the interior mesh point locations are computed using the NASA-Ames GRAPE[6] algorithm. The GRAPE algorithm determines the interior field point coordinates by iteratively solving two-coupled Poisson equations. For axisymmetric geometries, this two-dimensional grid generation procedure is applied for only one meridional plane, and the grid point locations on the remaining meridional planes are found by using simple reflection techniques. For asymmetric geometries, the two-dimensional grid generation algorithm can be applied for each meridional plane.

Let x and y denote the Cartesian axial and radial coordinates, respectively, for a selected meridional plane, and let ξ and ζ denote the wraparound and radial curvilinear coordinates, respectively, for that plane. The interior grid point (x, y) distribution for the meridional plane is obtained by solving the following Poisson equations:

$$\alpha x_{\xi\xi} - 2\beta x_{\xi\zeta} + \gamma x_{\zeta\zeta} = -J_M^2 (P\, x_\xi + Q x_\zeta) \tag{2}$$

$$\alpha y_{\xi\xi} - 2\beta y_{\xi\zeta} + \gamma y_{\zeta\zeta} = -J_M^2 (P\, y_\xi + Q y_\zeta) \tag{3}$$

In equations (2) and (3), the parameters α, β, γ, and J_M are defined as

$$\alpha = x_\zeta^2 + y_\zeta^2 \tag{4}$$

$$\beta = x_\xi\, x_\zeta + y_\xi\, y_\zeta \tag{5}$$

$$\gamma = x_\xi^2 + y_\xi^2 \tag{6}$$

and

$$J_M = x_\xi\, y_\zeta - x_\zeta\, y_\xi \tag{7}$$

The parameters P and Q are user-determined forcing functions which control grid point spacing and orthogonality near the computational boundaries. Equations (2) and (3) are solved numerically in the GRAPE algorithm using a successive-line-over-relaxation scheme. The boundary grid point locations are supplied to the GRAPE algorithm and are used as Dirichlet boundary conditions. Initial estimates of the interior field point locations are

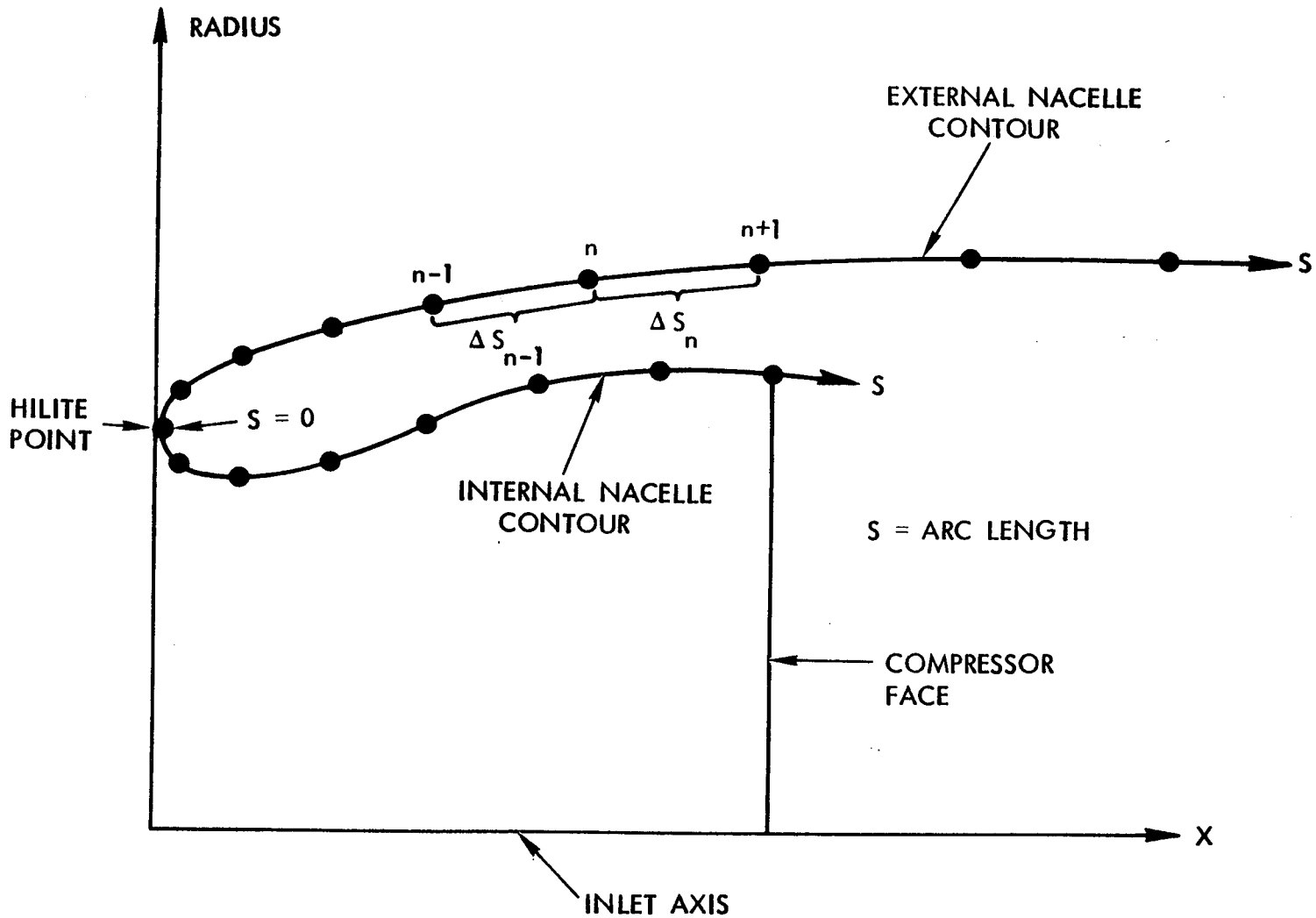

Figure 2. Surface grid point clustering.

required to start the relaxation procedure.

The GRAPE two-dimensional grid generation algorithm is contained within the NGRIDA program and is used solely to obtain the interior grid point locations. The boundary point locations are computed in NGRIDA and are supplied to the GRAPE algorithm to be used as boundary conditions. After the interior field point coordinates have been determined by GRAPE, point reordering, and grid translation, scaling, and reflection are performed in NGRIDA. The detailed theory and operation of the GRAPE algorithm are discussed in Reference 6.

Figure 3 illustrates the rectangular computational space domain which corresponds to the physical space domain shown in Figure 1. The physical space boundaries transform into boundaries in computational space. This allows for accurate and straightforward boundary condition implementation. The mesh points are equally spaced in computational space thereby permitting the use of standard finite-difference formulae in the flow solution analysis.

Figure 4 illustrates a typical meridional plane grid. The inlet centerline, which is the x axis, represents a singularity in the three-dimensional grid mapping. The computational grid boundary is displaced a small distance away from the x axis. An extrapolation and averaging technique, described later, is used to obtain flow properties on the centerline. Also, it has been found to be computationally advantageous to adjust the normal spacing near the external outflow surface to make a uniform radial point distribution along that surface. This produces a more favorable cell aspect ratio in this region, and thereby enhances stability and convergence in the flow solution algorithm.

3. GOVERNING EQUATIONS FOR THE INVISCID FLOW

The inviscid flow gas dynamic model is based on the assumption of steady potential flow which requires that the flow be both irrotational and isentropic. The governing equations for steady three-dimensional potential flow are given by

$$\left(\frac{\rho U}{J}\right)_{\xi} + \left(\frac{\rho V}{J}\right)_{\eta} + \left(\frac{\rho W}{J}\right)_{\zeta} = 0 \tag{8}$$

$$\rho = \left[1 - \frac{\gamma-1}{\gamma+1}\left(U\,\phi_{\xi} + V\,\phi_{\eta} + W\,\phi_{\zeta}\right)\right]^{\frac{1}{\gamma-1}} \tag{9}$$

where ξ, η, and ζ denote the system of curvilinear coordinates, U, V, and W are the contravariant velocity components in the ξ, η, and ζ directions, respectively, ρ is the density, J is the Jacobian of transformation from the Cartesian coordinate system (x, y, z) to the general curvilinear coordinate system (ξ, η, ζ), Φ is the velocity potential function, and γ is

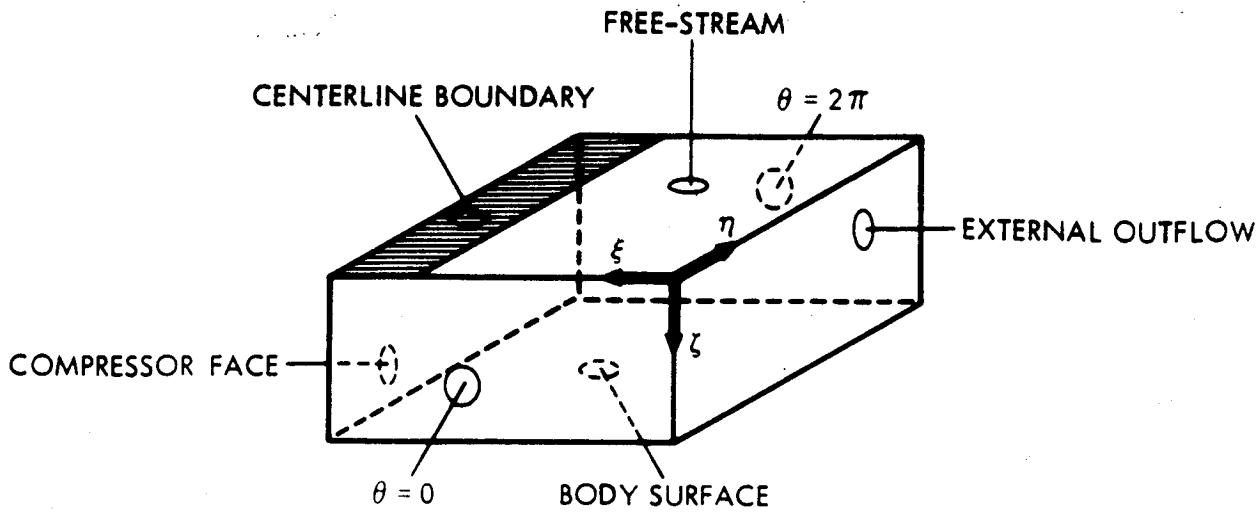

Figure 3. Computational domain.

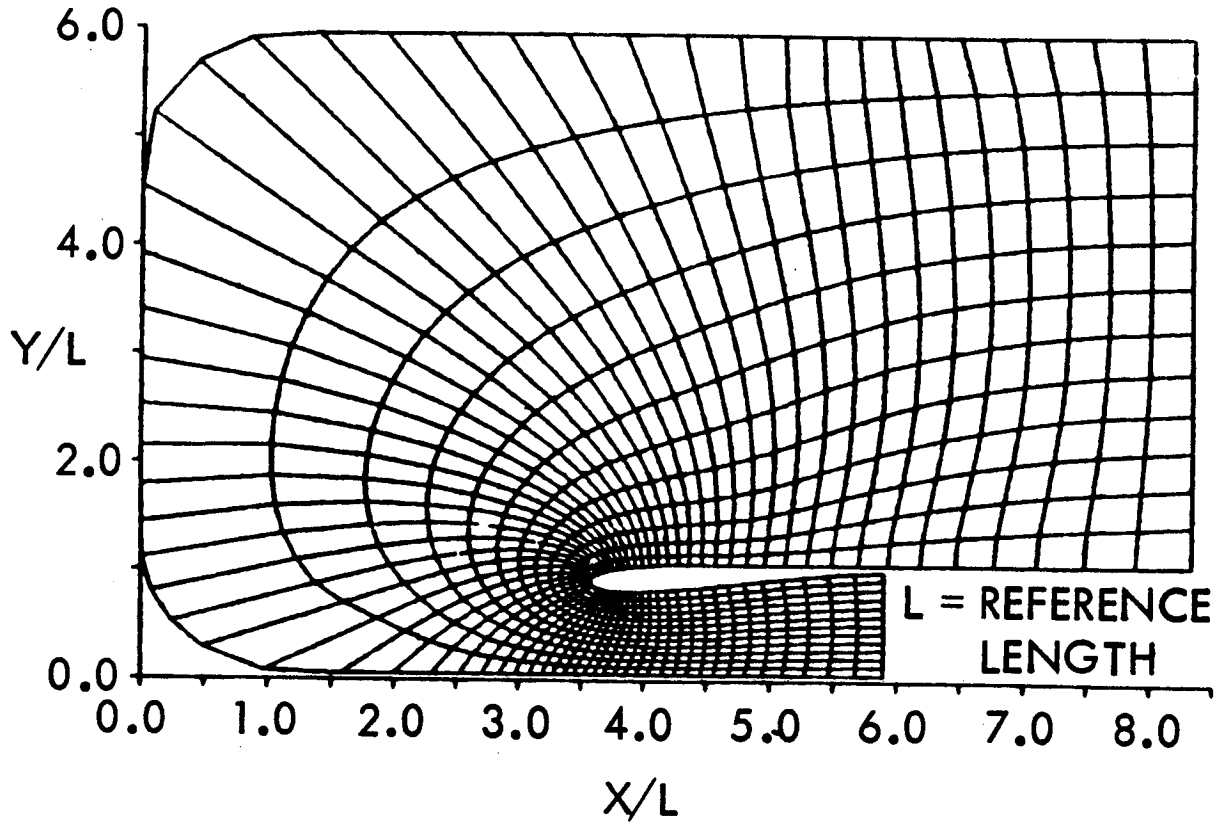

Figure 4. Meridional plane grid.

the specific heat ratio. The density and contravariant velocity components are normalized by the stagnation density and critical sonic speed, respectively.

Equation (8) is the full-potential equation in strong conservation law form. It expresses mass continuity for steady three-dimensional flows. Equation (9) expresses entropy conservation and is used to compute the density given the velocity potential field.

The contravariant velocity components can be expressed in terms of the Cartesian velocity components as

$$U = u\xi_x + v\xi_y + w\xi_z \tag{10}$$

$$V = u\eta_x + v\eta_y + w\eta_z \tag{11}$$

$$W = u\zeta_x + v\zeta_y + w\zeta_z \tag{12}$$

where u, v, and w denote the nondimensional velocity components along the x, y, and z Cartesian coordinate axes, respectively. The contravariant velocity components can be also expressed in terms of the velocity potential ϕ as

$$U = A_1\phi_\xi + A_4\phi_\eta + A_5\phi_\zeta \tag{13}$$

$$V = A_4\phi_\xi + A_2\phi_\eta + A_6\phi_\zeta \tag{14}$$

$$W = A_5\phi_\xi + A_6\phi_\eta + A_3\phi_\zeta \tag{15}$$

The metric parameters A_i (i = 1 to 6) and the Jacobian of transformation J are given by

$$A_1 = \xi_x^2 + \xi_y^2 + \xi_z^2 \qquad A_4 = \xi_x\eta_x + \xi_y\eta_y + \xi_z\eta_z$$

$$A_2 = \eta_x^2 + \eta_y^2 + \eta_z^2 \qquad A_5 = \xi_x\zeta_x + \xi_y\zeta_y + \xi_z\zeta_z \tag{16}$$

$$A_3 = \zeta_x^2 + \zeta_y^2 + \zeta_z^2 \qquad A_6 = \eta_x\zeta_x + \eta_y\zeta_y + \eta_z\zeta_z$$

$$J = \xi_x\eta_y\zeta_z + \xi_y\eta_z\zeta_x + \xi_z\eta_x\zeta_y - \xi_z\eta_y\zeta_x$$

$$-\xi_y\eta_x\zeta_z - \xi_x\eta_z\zeta_y \tag{17}$$

The following metric relations are also required in defining the mapping from physical space to computational space:

$$\xi_x = J(y_\eta z_\zeta - y_\zeta z_\eta) \quad \eta_x = J(y_\zeta z_\xi - y_\xi z_\zeta) \quad \zeta_x = J(y_\xi z_\eta - y_\eta z_\xi)$$

$$\xi_y = J(x_\zeta z_\eta - x_\eta z_\zeta) \quad \eta_y = J(x_\xi z_\zeta - x_\zeta z_\xi) \quad \zeta_y = J(x_\eta z_\xi - x_\xi z_\eta) \tag{18}$$

$$\xi_z = J(x_\eta y_\zeta - x_\zeta y_\eta) \quad \eta_z = J(x_\zeta y_\xi - x_\xi y_\zeta) \quad \zeta_z = J(x_\xi y_\eta - x_\eta y_\xi)$$

The metric parameters are obtained numerically using standard second-order or fourth-order accurate finite-difference formulae to compute derivatives of the form x_ξ, x_η, x_ζ, y_ξ, etc. Then using the metric relations given by equations (18), the inverse quantities ξ_x, η_x, etc., are determined. Substitution of these values into equations (16) and (17) yields the A_i and Jacobian J.

4. NUMERICAL ALGORITHM

4.1 BASIC FINITE-DIFFERENCE SCHEME

The present numerical algorithm is based on the finite-difference formulation used by Holst and Thomas[3] in computing transonic wing flows. In this algorithm, the full-potential equation residual is given by

$$L\phi_{i,j,k} = \overleftarrow{\delta}_\xi \left(\frac{\tilde{\rho U}}{J}\right)_{i+\frac{1}{2},j,k} + \overleftarrow{\delta}_\eta \left(\frac{\bar{\rho V}}{J}\right)_{i,j+\frac{1}{2},k} + \overleftarrow{\delta}_\zeta \left(\frac{\hat{\rho W}}{J}\right)_{i,j,k+\frac{1}{2}} \tag{19}$$

where $L\phi_{i,j,k}$ denotes the residual operator, and i, j, and k denote the grid point indices in the ξ (wraparound), η (circumferential), and ζ (radial) directions, respectively. The magnitude of the residual $L\phi_{i,j,k}$ approaches zero as convergence is attained. The operators $\overleftarrow{\delta}_\xi$ ( ), $\overleftarrow{\delta}_\eta$ ( ), and $\overleftarrow{\delta}_\zeta$ ( ) are first-order accurate backward finite-difference operators (applied at midpoints) for the ξ, η, and ζ directions, respectively. The terms $\tilde{\rho}$, $\bar{\rho}$, and $\hat{\rho}$ are upwind-biased density coefficients given by expressions of the form

$$\tilde{\rho}_{i+\frac{1}{2},j,k} = [(1-\nu)\rho]_{i+\frac{1}{2},j,k}$$

$$+ \nu_{i+\frac{1}{2},j,k}\, \rho_{i+\frac{1}{2}+r,j,k} \qquad (20)$$

where r denotes an upwind point along the ξ direction, and ν is an artificial viscosity coefficient. In equation (20), the physical density ρ is computed using equation (9) with central differences used for determining the derivatives of ϕ. The artificial viscosity coefficient is given by

$$\nu = 0 \;:\; M_{i,j,k} < 1$$

$$\nu = C(M^2_{i,j,k} - 1) \;:\; M_{i,j,k} > 1 \qquad (21)$$

where M is the local Mach number, and C is a user-specified constant. The artificial viscosity coefficient C typically ranges from 1.0 to 2.0, with the larger values producing greater upwinding. Expressions similar to equation (20) hold for $\bar{\rho}$ and $\hat{\rho}$ which effect upwinding in the η and ζ directions, respectively.

The finite-difference equations are solved using the AF2 approximate factorization scheme which has proved to be significantly more efficient than successive-line-overrelaxation schemes[3]. The AF2 algorithm is written in a three-step form as:

First-Step:

$$\left(\alpha - \frac{1}{A_k}\, \vec{\delta}_\eta A_j \overleftarrow{\delta}_\eta\right) g^n_{i,j} = \alpha\omega L\phi^n_{i,j,k} \qquad (22)$$

$$+ A_{k+1}\, f^n_{i,j,k+1}$$

Second-Step:

$$\left(A_k \mp \beta_\xi \overleftrightarrow{\delta}_\xi - \frac{1}{\alpha}\, \vec{\delta}_\xi A_i \overleftarrow{\delta}_\xi\right) f^n_{i,j,k} = g^n_{i,j} \qquad (23)$$

Third-Step:

$$(\alpha + \overleftarrow{\delta}_\zeta) C^n_{i,j,k} = f^n_{i,j,k} \qquad (24)$$

In equations (22) to (24), α is a time-like factorization parameter chosen to maintain stability and attain fast convergence, β_ξ is a factor that controls the amount of dissipation required in regions of supersonic flow, ω is a relaxation factor, n is the iteration number, $L\phi_{i,j,k}$ is the mass residual [defined by equation (19)], f and g are intermediate functions which are obtained during the solution process, and $C^n_{i,j,k}$ is the potential function correction given by

$$C^n_{i,j,k} = \phi^{n+1}_{i,j,k} - \phi^n_{i,j,k} \tag{25}$$

The terms A_i, A_j, and A_k are defined by

$$A_i = (\tilde{\rho}A_1/J)^n_{i-\frac{1}{2},j,k} \tag{26}$$

$$A_j = (\bar{\rho}A_2/J)^n_{i,j-\frac{1}{2},k} \tag{27}$$

$$A_k = (\hat{\rho}A_3/J)^n_{i,j,k-\frac{1}{2}} \tag{28}$$

In Steps 1 and 2 the g and f functions are obtained by solving a tridiagonal system of equations while in Step 3 the correction $C^n_{i,j,k}$ is obtained by solving a bidiagonal system of equations.

The iterative relaxation procedure can be viewed as a time-marching integration algorithm in pseudotime. Using this analogy, the factorization parameter α appearing in equations (22), (23), and (24) can be regarded as the reciprocal of the marching pseudotime step. To eliminate all components of the error frequency spectrum, it is generally preferable to employ a variable time step which sequentially varies with iteration number. The small values of α are particularly effective in reducing the low frequency errors, while the large values of α are effective in reducing the high frequency errors.

The factorization parameter α is computed using a repeating sequence which is based on iteration number[1]. The α sequence that is the most frequently employed is given by

$$\alpha_k = \alpha_h \left(\alpha_l/\alpha_h\right)^{\frac{k-1}{M-1}} \qquad (k = 1,2,\cdots,M) \tag{29}$$

where α_l is the lower limit of α, α_h is the upper limit, and α_k is the value of α for the kth element of the sequence. For all cases presented herein, the number of elements in the sequence M was equal to 8. The optimum values of α_l and α_h are generally determined by numerical experiment. For a (67x13x13)-point grid, factorization parameter limits of

$\alpha_l = 0.175$ and $\alpha_h = 6.0$ were used. The relaxation parameter ω is typically equated to 1.0. The time-like dissipation factor β_ξ is typically set to 0.1. The use of β_ξ ensures diagonal dominance in the ξ-difference equation tridiagonal matrix. The artificial viscosity coefficient C generally varies between 1.0 and 2.0.

4.2 BOUNDARY CONDITIONS

The density and potential function on the outer boundary (see Figure 1) are held at their initial free-stream values during the course of the iterative solution procedure. As mentioned before, the grid centerline boundary is offset a small distance from the centerline (x axis) to avoid the mapping singularity. To determine property values on the centerline, an extrapolation and averaging procedure is employed. For each meridional plane, the potential function values at interior mesh points are used to linearly extrapolate for the potential values on the centerline. A circumferential averaging of the extrapolated values is then performed for each wraparound station on the centerline. The potential values for points on each meridional plane centerline boundary are then updated by interpolation using property information from the centerline and interior field points. The updating of the properties on the grid centerline boundary is performed for every iteration. The property values on the outer and centerline boundaries are then used as Dirichlet boundary conditions for the ensuing iteration. Slight improvements in convergence speed can be realized by smoothing property values in the region of point (T) (see Figure 1), which delineates the transition point between the outer and centerline boundaries.

At the body surface, the contravariant velocity W_s in the ζ-coordinate direction is specified. The velocity W_s is identically zero for a purely inviscid calculation as this satisfies the flow tangency condition. To account for boundary layer displacement effects, an effective W_s can be calculated from the computed boundary layer growth and can then be applied as a surface transpiration velocity boundary condition. Once W_s is specified, the term ϕ_ζ is calculated from

$$\phi_\zeta = (W_s - A_5\phi_\xi - A_6\phi_\eta)/A_3 \tag{30}$$

where the derivatives ϕ_ξ and ϕ_η are found using second-order differencing in the ζ= constant boundary surface.

At both the compressor face and external outflow surfaces, the contravariant velocity U_o in the ξ-coordinate direction is specified. Given the local Cartesian velocity components u, v, and w, and the metric quantities ξ_x, ξ_y, and ξ_z, U_o can be determined using equation (10). At the compressor face, the flow is assumed to be uniform and in the axial (x) direction. The local flow velocity and density are fixed by specification of the required engine mass flow rate. At the external outflow surface, it is assumed that the free-stream velocity components are recaptured. This assumption is good far from the body surface, but is only approximate as the surface is approached. Locating the external outflow surface far

enough downstream minimizes the effect of this approximation. Once U_o has been determined, the term ϕ_ξ is calculated from

$$\phi_\xi = (U_o - A_4\phi_\eta - A_5\phi_\zeta)/A_1 \tag{31}$$

where the derivatives ϕ_ζ and ϕ_η are found using second-order differencing in the ξ = constant boundary surface.

At the mesh corner points ($\xi = \xi_{min}$; $\zeta = \zeta_{max}$) and ($\xi = \xi_{max}$; $\zeta = \zeta_{max}$), two boundary conditions are enforced since both U and W are fixed. In these cases, ϕ_η is computed using second-order differencing, and the derivative ϕ_ζ is found from

$$\phi_\zeta = \frac{A_5 (U_o - A_4\phi_n) - A_1 (W_s - A_6\phi_n)}{A_5^2 - A_1 A_3} \tag{32}$$

The term ϕ_ξ is then calculated using equation (31).

In calculating the residual values for points on the body and outflow surfaces, the surface contravariant velocity along the direction normal to the surface is used directly.

Boundary conditions are also required for the intermediate functions f and g. For isolated nacelle geometries, periodic boundary conditions are used in the η-coordinate direction. In the ξ-coordinate direction, the condition $f_\xi = 0$ is imposed at both the compressor face and external outflow surfaces.

4.3 INITIALIZATION

Significant improvements in convergence speed have been realized by initializing the potential function field using different procedures for the external flow and the internal flow. The potential field initialization for the external flow is performed using free-stream velocity components. For the internal flow initialization, the local velocity is assumed to be axial and is computed using a Mach number which is determined from the implicit relation

$$M\left(1 + \frac{\gamma-1}{2} M^2\right)^{\frac{-(\gamma+1)}{2(\gamma-1)}} = \left(\frac{A_{cf}}{A}\right) M_{cf} \left(1 + \frac{\gamma-1}{2} M_{cf}^2\right)^{\frac{-(\gamma+1)}{2(\gamma-1)}} \tag{33}$$

where M and M_{cf} denote the local and compressor face Mach numbers, respectively, and A and A_{cf} denote the local and compressor face flow areas, respectively. Equation (33) was obtained using one-dimensional gas dynamic formulae and simply expresses mass continuity for the captured

stream tube. To determine the internal potential field, a trapezoidal rule integration is used. The compressor face Mach number M_{cf} is fixed by specification of the engine mass flow rate. Generally, M_{cf} is directly entered in the program or is determined by specification of the inlet capture ratio. The free-stream Mach number M_∞ and the compressor face Mach number M_{cf} can differ significantly at cruise conditions.

4.4 NUMERICAL STABILITY

During the course of program development, it was found necessary to impose a velocity potential function under-relaxation in the iterative process when calculating the solution at points near the centerline. The centerline represents singularity in the three-dimensional grid mapping. Without the under-relaxation, somewhat large potential function corrections would occur at mesh points near the centerline.

A von Neumann linear stability analysis was conducted for the three-dimensional AF2 algorithm using the conservative form of the full-potential equation expressed in curvilinear coordinates. Simplified and linearized forms of the residual and AF2 correction operators were obtained by assuming that flow was subsonic ($\rho \approx 1$), that there was a slow spatial variation of the metrics ($A_{1\xi} \approx 0$, etc.), and that the grid was approximately orthogonal. Expressions were derived for the amplification factor in terms of A_1, A_2, A_3, J, α, and ω. The analysis indicated unconditional linear stability if $0 < \omega < 2$ and $\alpha > 0$. When numerical values for the metric terms were substituted into the amplification factor expressions, low amplification factor values were obtained for the external flow mesh points and for the internal flow mesh points near the body surface. Higher amplification factor values were obtained near the centerline. Fastest convergence is attained if the amplification factor magnitude is near zero.

To compensate for this effect, a simple potential function correction under-relaxation scheme was incorporated for mesh points close to the centerline. The potential function updating is thereby performed using

$$\phi^{n+1}_{i,j,k} = \phi^{n}_{i,j,k} + \sigma C^{n}_{i,j,k} \tag{34}$$

where $\sigma < 1.0$ at mesh points close to the centerline and $\sigma = 1.0$ elsewhere (standard algorithm). Generally, σ is varied with the radial distance from the centerline. For mesh points close to the centerline, σ is small (i.e., $\sigma \approx .2$), and as the radial distance is increased so is σ increased, finally reaching the value of 1.0 at a distance sufficiently far from the centerline.

5. NUMERICAL RESULTS

Selected numerical results are now presented to illustrate application of the analysis. Both axisymmetric and asymmetric nacelle/inlet configurations operating at zero and nonzero incidence are

considered.

The first set of computed results are for a recently-designed Lockheed-Georgia axisymmetric nacelle/inlet configuration (GELAC1 inlet). Figure 5 illustrates the computed Mach number distributions (without viscous correction) for both the external and internal nacelle surfaces. The results shown are for a free-stream Mach number M_∞ of 0.8, an effective compressor face Mach number M_{cf} of 0.35, and an incidence α of 0 degrees. Plotted is the surface Mach number M versus the distance (ΔX) from the nacelle hilite. Since the geometry is axisymmetric and the angle of attack is zero, the flowfield will be axisymmetric. Also shown on Figure 5 are the results of the Jameson FLO-49 axisymmetric flow nacelle code[7]. The Jameson code is a two-dimensional full-potential finite-volume nacelle algorithm which uses successive-line-over-relaxation (SLOR) with multigrid convergence acceleration. It is limited to predicting the flow for axisymmetric nacelles at zero incidence. Referring to Figure 5, it can be seen that the two analyses agree very well. The Jameson program computation employed a grid with 128 wraparound stations and 32 radial stations. The three-dimensional nacelle program computation employed a grid with 67 wraparound stations, 13 circumferential stations, and 13 radial stations.

When an axisymmetric inlet is operated at incidence, cross flow develops and the flowfield becomes three-dimensional. Figure 6 illustrates the computed surface Mach number distribution when the GELAC1 inlet is operated at α = 3 (deg) while maintaining M_∞ = 0.8 and M_{cf} = 0.35. This figure illustrates the solution for the leeward (θ= 0), transverse [θ = 90 (deg)], and windward [θ = 180 (deg)] meridians. As the inlet is put at incidence, the stagnation point on the leeward meridian moves to increase the amount of flow expansion and subsequent peak Mach number and shock strength on the external surface, and to reduce the peak Mach number on the internal surface. The opposite effect occurs on the windward meridian.

Figure 7 illustrates the computed surface Mach number distribution for a Lockheed-California axisymmetric inlet design (CALAC4 inlet) operating at α = 0 (deg). Again, the free-stream and compressor face Mach numbers were maintained at 0.8 and 0.35, respectively. The results of the Jameson FLO-49 program are also presented on Figure 7 for the zero incidence case. The FLO-49 computation employed a (64 x 16)-point grid. Good agreement is obtained between the two analyses.

Figures 8 through 12 show correlations between analysis and experimental data[8] for the CALAC4 inlet. In Figure 8, the computed surface pressure coefficient C_p and wind tunnel data are compared for a case with M_∞ = 0.6, α = 1.083 (deg), and an inlet capture ratio Q of 0.505. The capture ratio is defined as the ratio of free-steam capture area to the inlet hilite area. Figure 8 illustrates the results for both the external and internal surfaces for both the leeward and windward meridians. The agreement between the results of the numerical analysis and experiment is very good. The numerical results illustrated in Figure 8 were obtained using a computational grid with 67 wraparound stations, 25 circumferential stations, and 16 radial stations. The same case was executed using a (67X13X13)-point grid. The resulting surface solutions for the two grids were almost identical except that the C_p peak on the windward meridian's

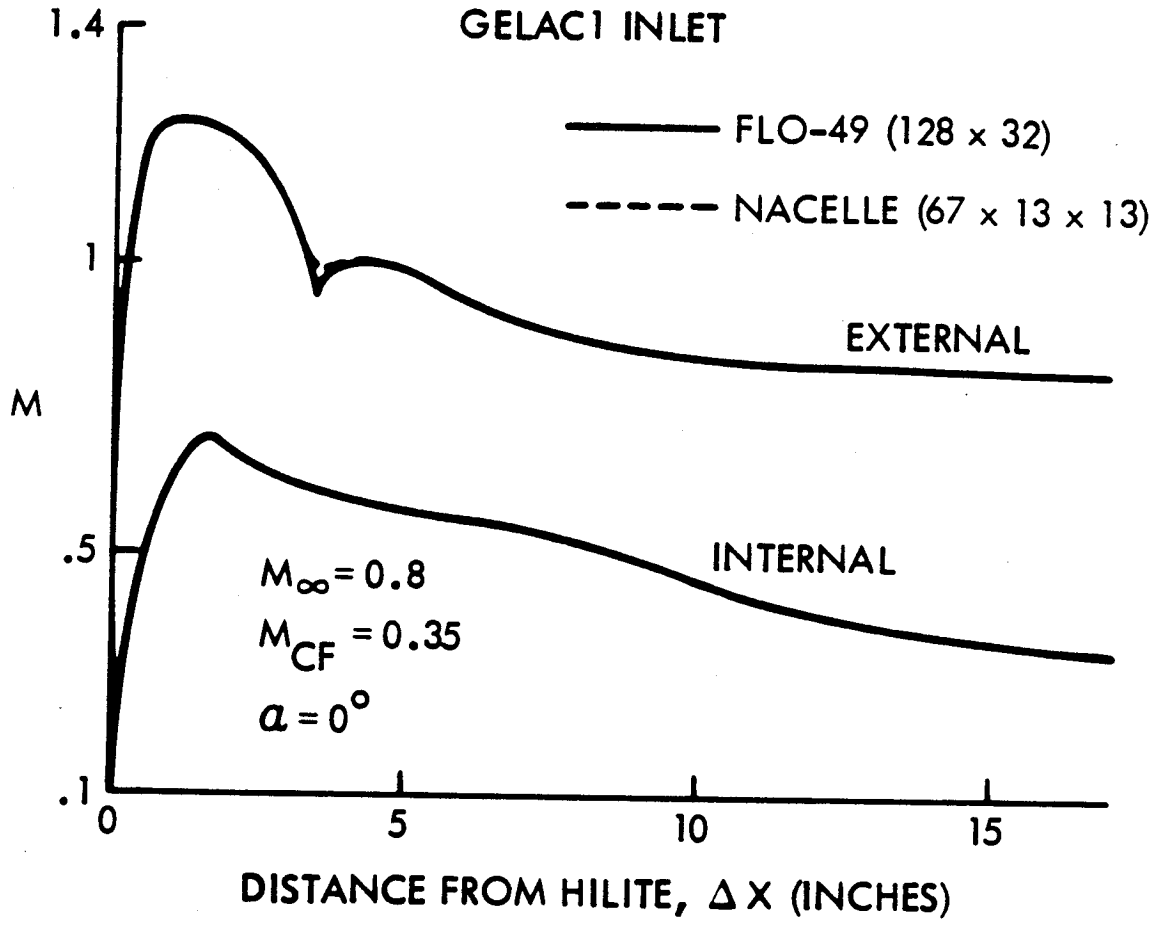

Figure 5. Solution for GELAC1 Inlet at $M_\infty = 0.8$ and $\alpha = 0$.

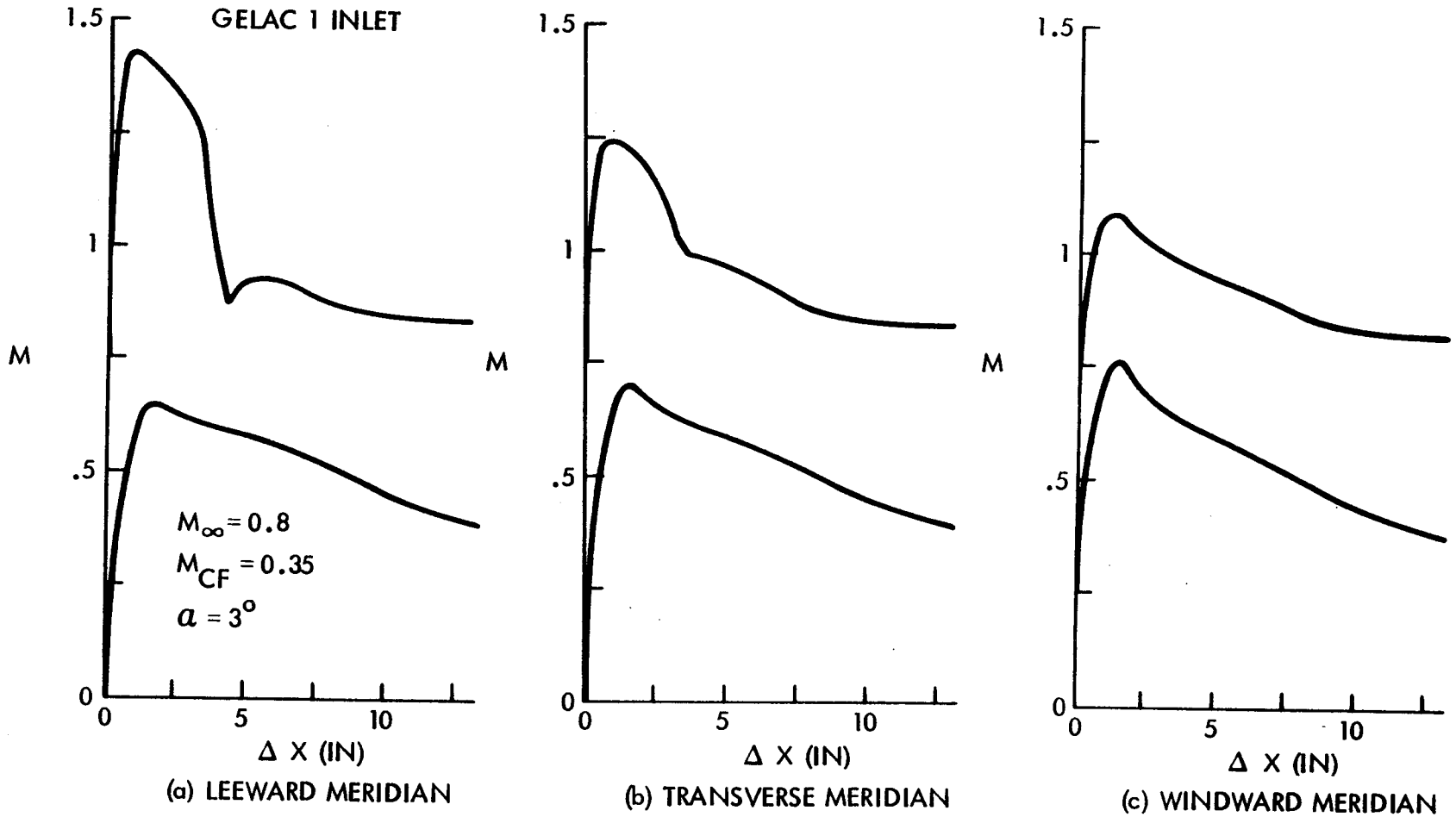

Figure 6. Solution for GELAC1 Inlet at M_∞ = 0.8 and α = 3 (deg).

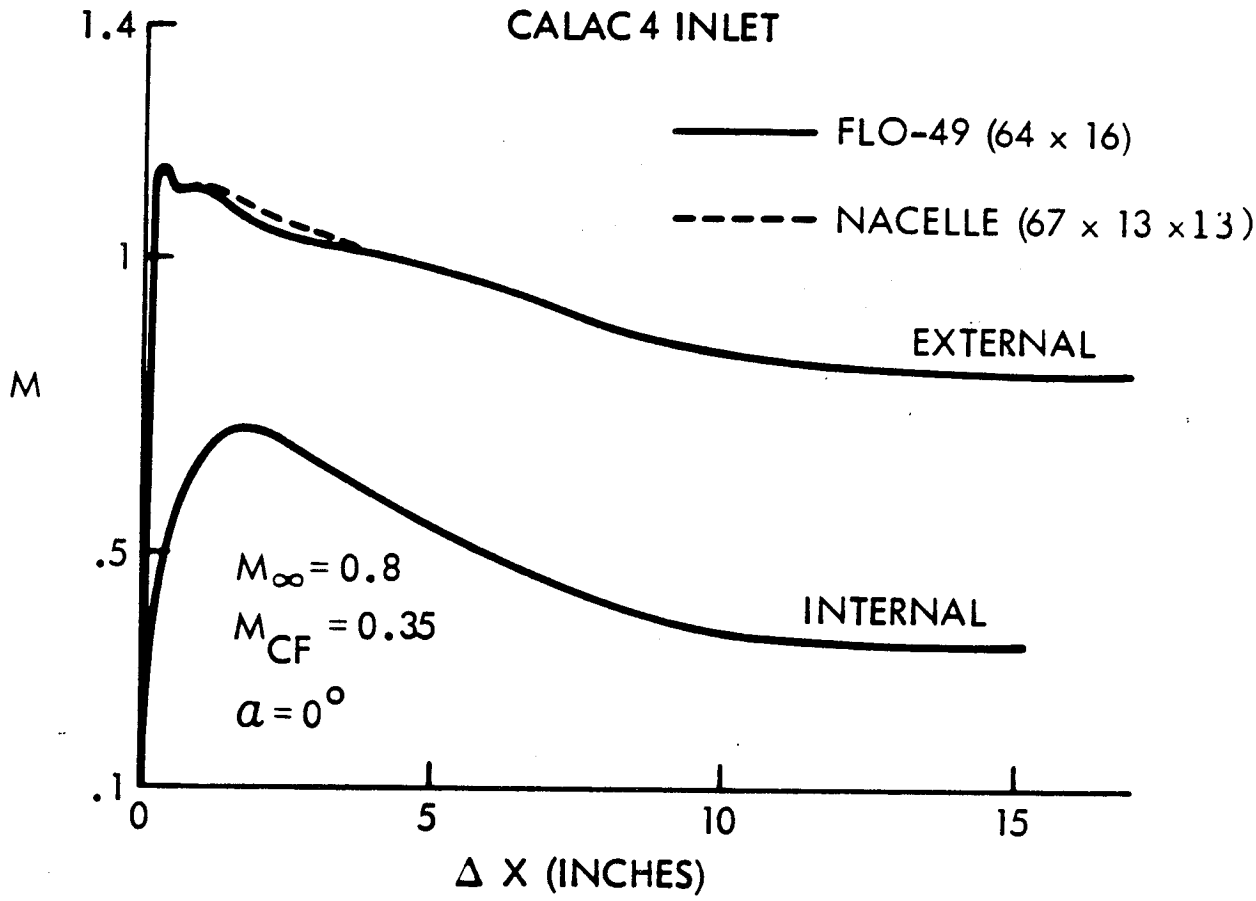

Figure 7. Solution for CALAC4 Inlet at M_∞ = 0.8 and α = 0.

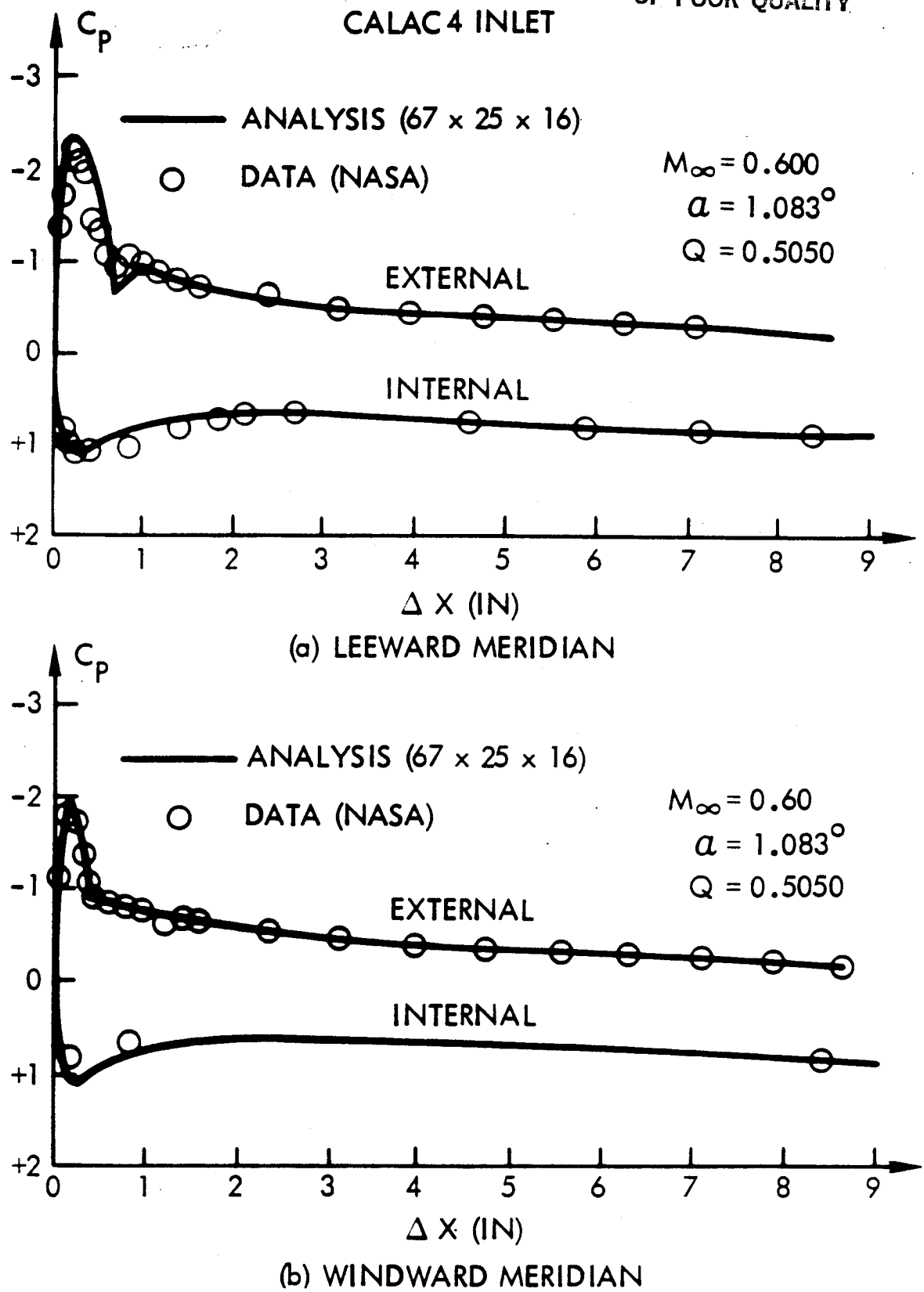

Figure 8. Comparison of analysis and experiment for CALAC4 Inlet at M_∞ = 0.6 and α = 1.083 (deg).

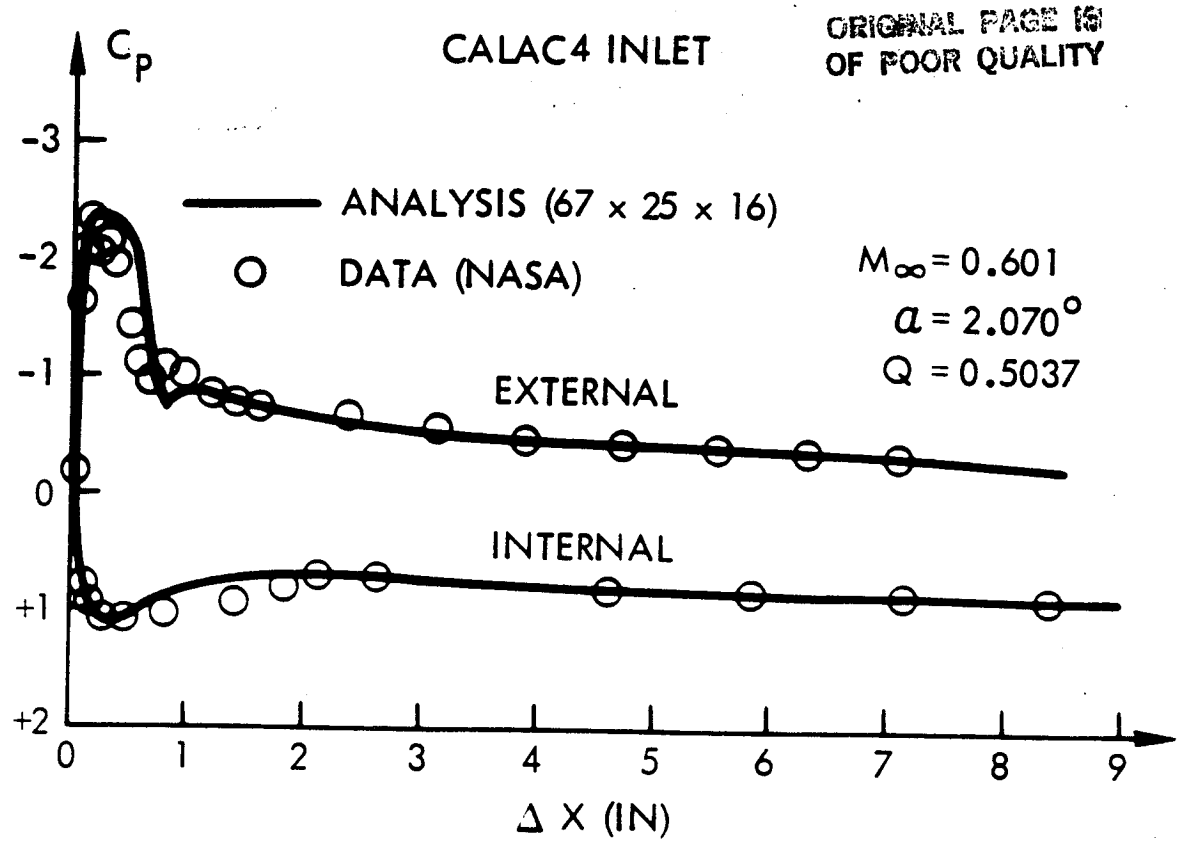

(a) LEEWARD MERIDIAN

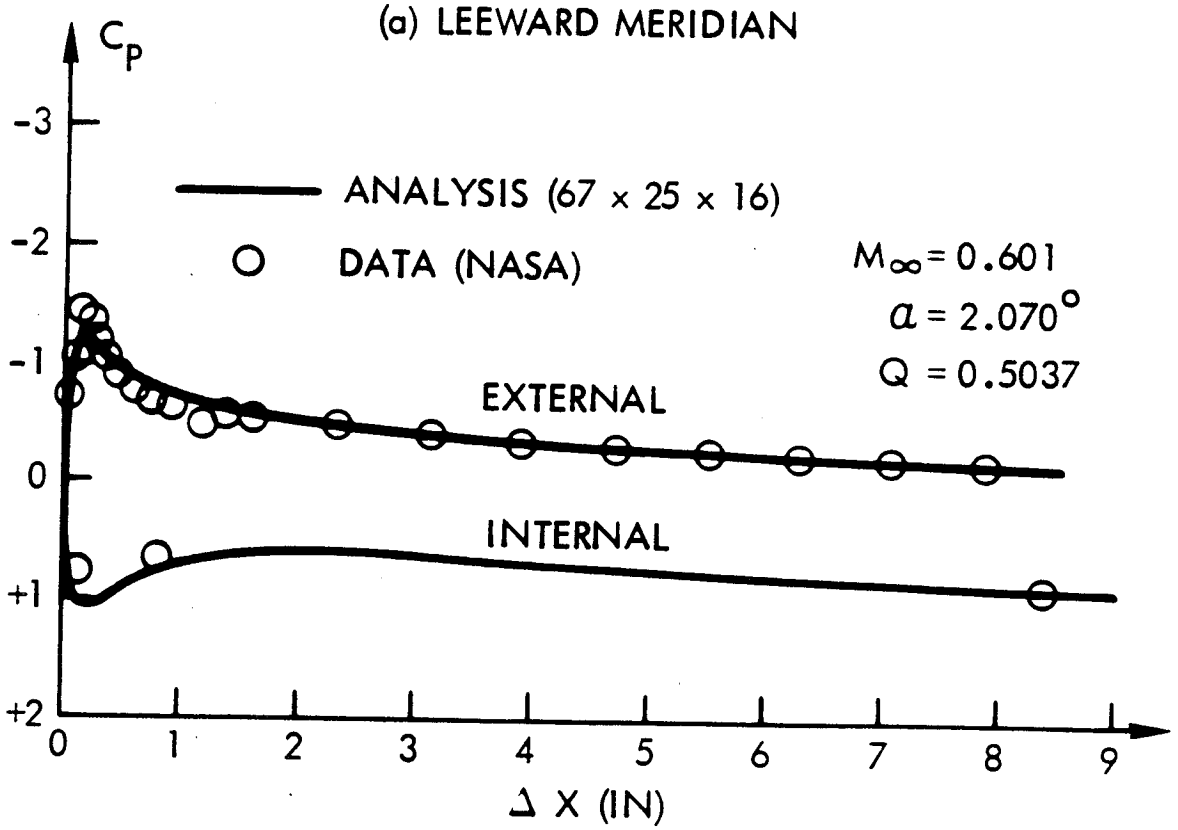

(b) WINDWARD MERIDIAN

Figure 9. Comparison of analysis and experiment for CALAC4 Inlet at M_∞ = 0.601 and α = 2.070 (deg).

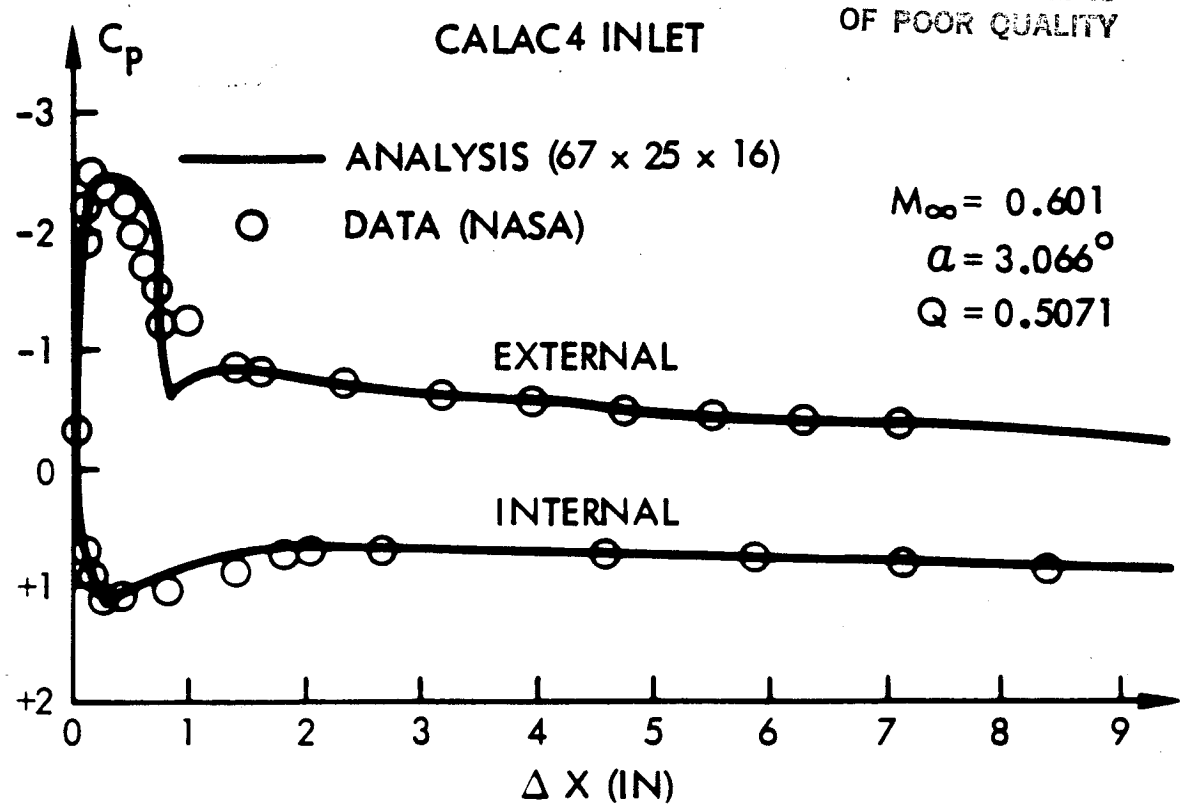

(a) LEEWARD MERIDIAN

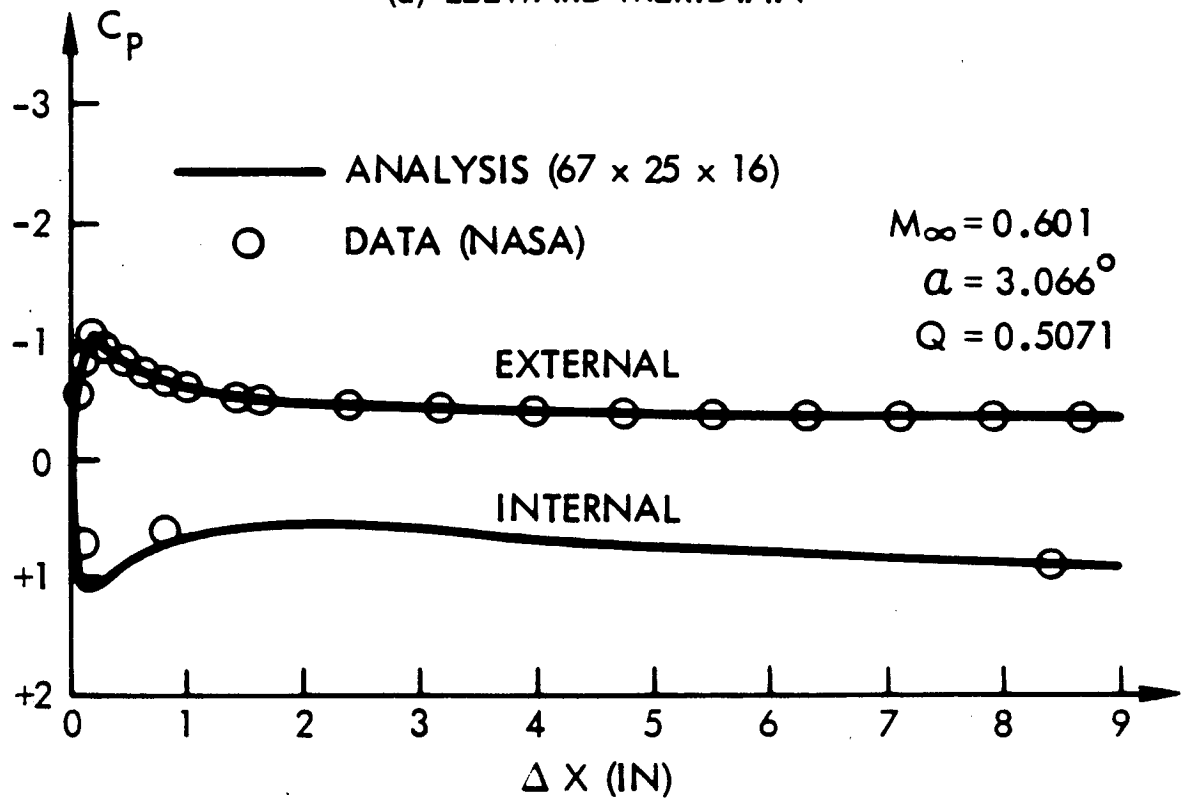

(b) WINDWARD MERIDIAN

Figure 10. Comparison of analysis and experiment for CALAC4 Inlet at M_∞ = 0.601 and α = 3.066 (deg).

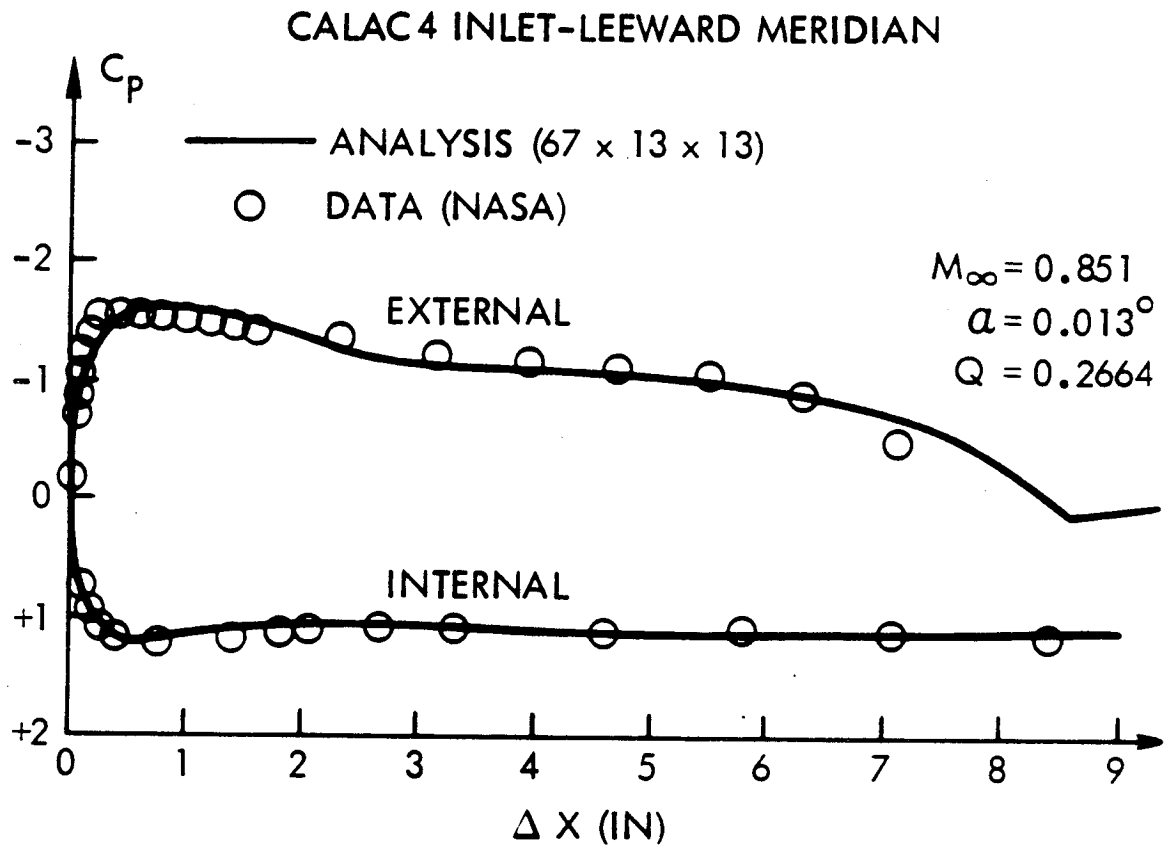

Figure 11. Comparison of analysis and experiment for CALAC4 Inlet at M_∞ = 0.851 and α = 0.013 (deg).

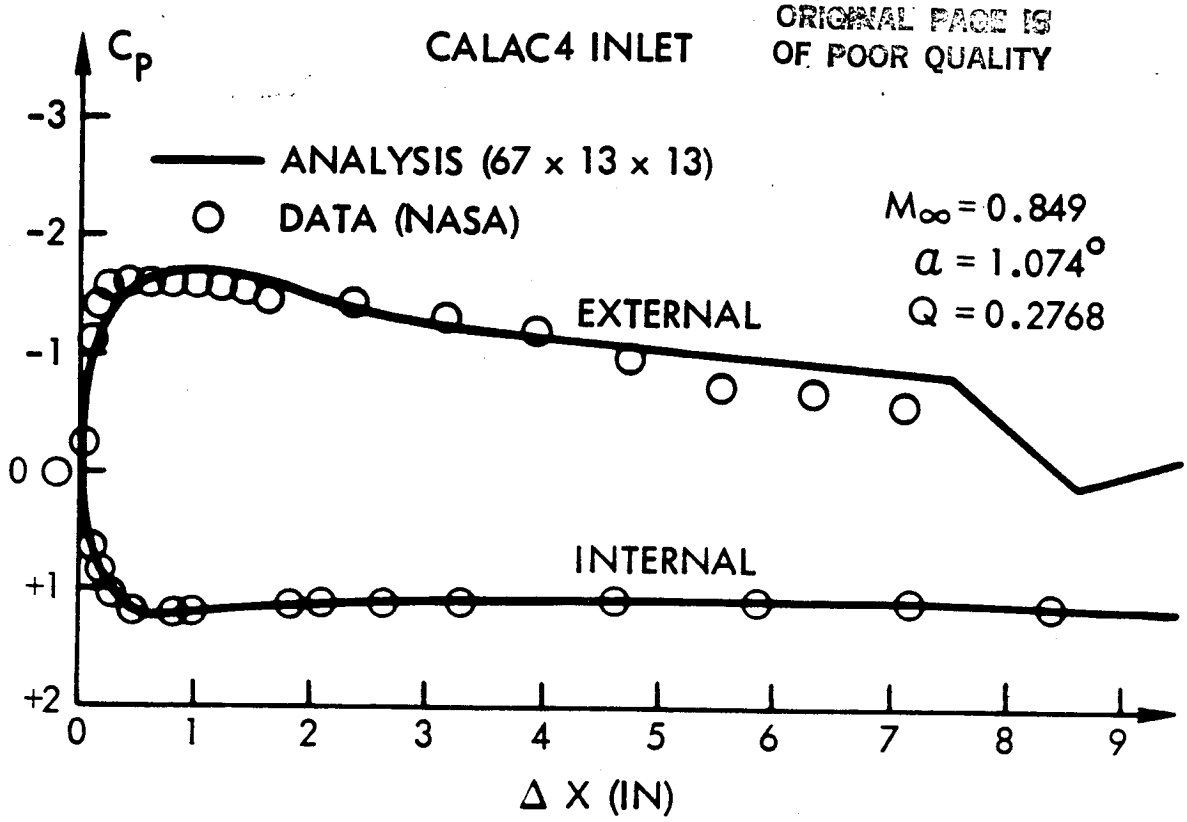

(a) LEEWARD MERIDIAN

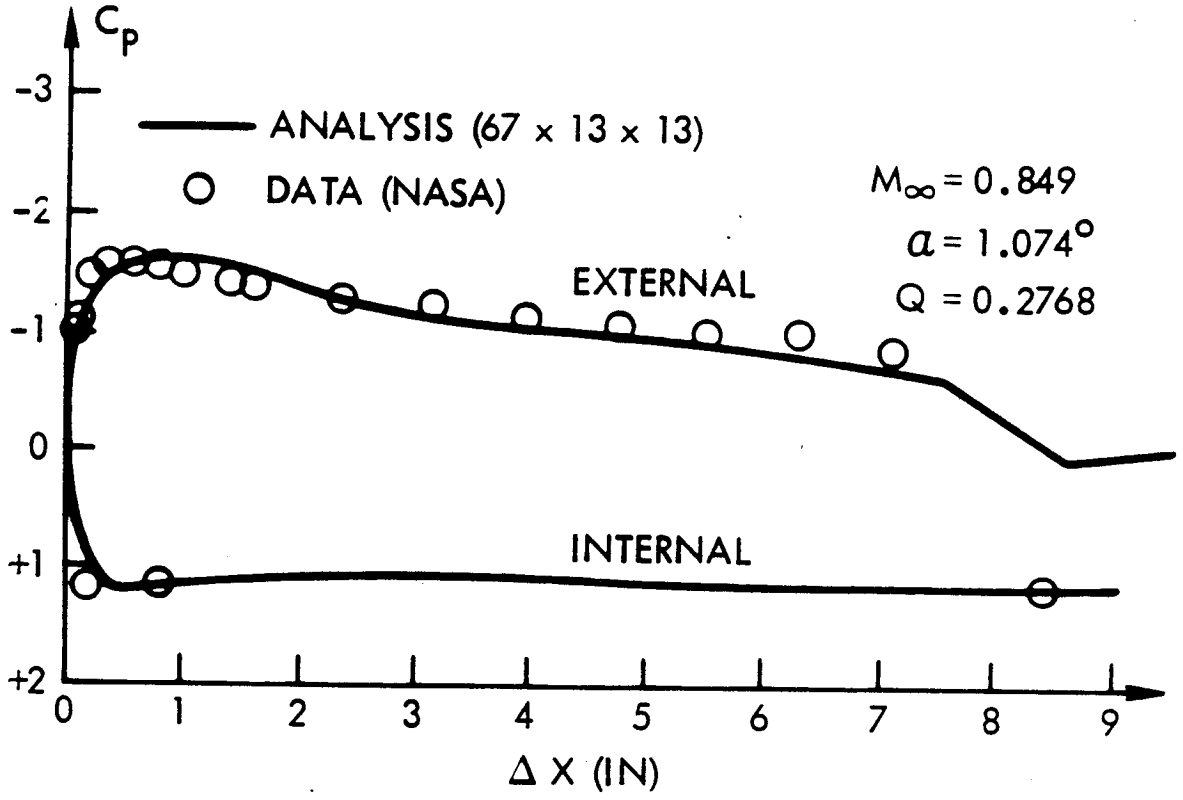

(b) WINDWARD MERIDIAN

Figure 12. Comparison of analysis and experiment for CALAC4 Inlet at M_∞ = 0.849 and α = 1.074 (deg).

external surface was better predicted using the finer grid. Figures 9 and 10 compare analysis versus experiment maintaining the Mach number and capture ratio approximately constant but increasing the angle of attack to α = 2.07 (deg) and 3.066 (deg), respectively.

Figure 11 illustrates the computed surface pressure coefficient distribution and experimental data for the CALAC4 inlet operating at the conditions of M_∞ = 0.851, α = 0.013 (deg), and Q = 0.2664. This represents a difficult test case because of the low capture ratio which requires that most of flow be spilled around the external cowling thereby generating a large region of supersonic flow. The Mach number corresponding to the peak negative pressure coefficient is approximately 2.1. Nonetheless, excellent agreement is obtained with the data using a (67X13X13)-point grid. Figure 12 illustrates the solution when the incidence has been increased to α = 1.074 (deg). These low capture ratio cases required increasing the artificial viscosity and time-like dissipation coefficients beyond their default values. This ensures numerical stability but decreases convergence speed.

Figures 13, 14, and 15 illustrate the rapid convergence properties of the present approximate factorization algorithm. The variation of the number of supersonic points (NSP) with iteration number is plotted in Figure 13 for the flow field solution of the CALAC4 inlet operating at a free-stream Mach number of 0.8, a compressor face Mach number of 0.35, and α = 3 (deg) angle of attack. For this case, convergence, which corresponds to a three-order of magnitude reduction in maximum residual, was attained in 139 iterations. The value of NSP increases very quickly with iteration number. After 25 iterations, the NSP level has already achieved 90% of its final value. Figure 14 illustrates error reduction as a function of iteration number again for the α = 3 (deg) incidence case of Figure 13. On the ordinate axis is plotted the log of the ratio of the absolute value of the maximum residual on the current iteration to that on the first iteration. (The results were plotted every 20 iterations). At approximately 60 iterations, the maximum residual has been reduced by two orders of magnitude. Figure 15 presents the evolution of the surface solution with iteration number for the flow field computation of the GELAC1 inlet operating at M_∞ = 0.8, M_{cf} = 0.35, and α = 1 (deg). Shown in this figure are the computed solutions at 50, 80, and 158 iterations for the leeward and transverse meridians. The solution at 158 iterations represents the final converged solution at which point the maximum residual has been reduced by three orders of magnitude. After 50 iterations, a good approximation to the fully converged solution has been attained. The difference between the fully converged solution and that at 80 iterations is very minor. A characteristic of the AF2 algorithm is the rapid development of the surface Mach number and pressure distributions, as evidenced by Figure 15.

Flow computations have also been performed for an asymmetric nacelle/inlet configuration. The configuration under study is a recent Lockheed drooped-inlet design in which the inlet contour has circumferential variation both in section shape and in length from the hilite point to the compressor face. The front of the inlet is tilted downward with respect to the engine centerline for the purpose of aligning the inlet with the local flow direction underneath the wing. This reduces

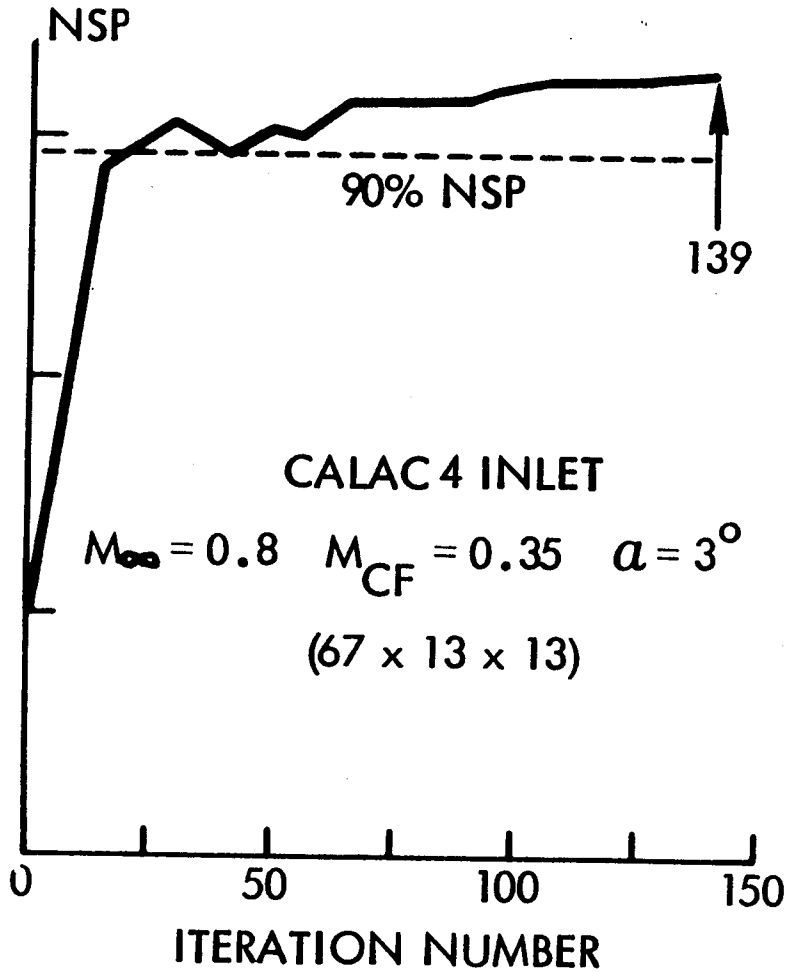

Figure 13. Number of supersonic points (NSP) vs. iteration number.

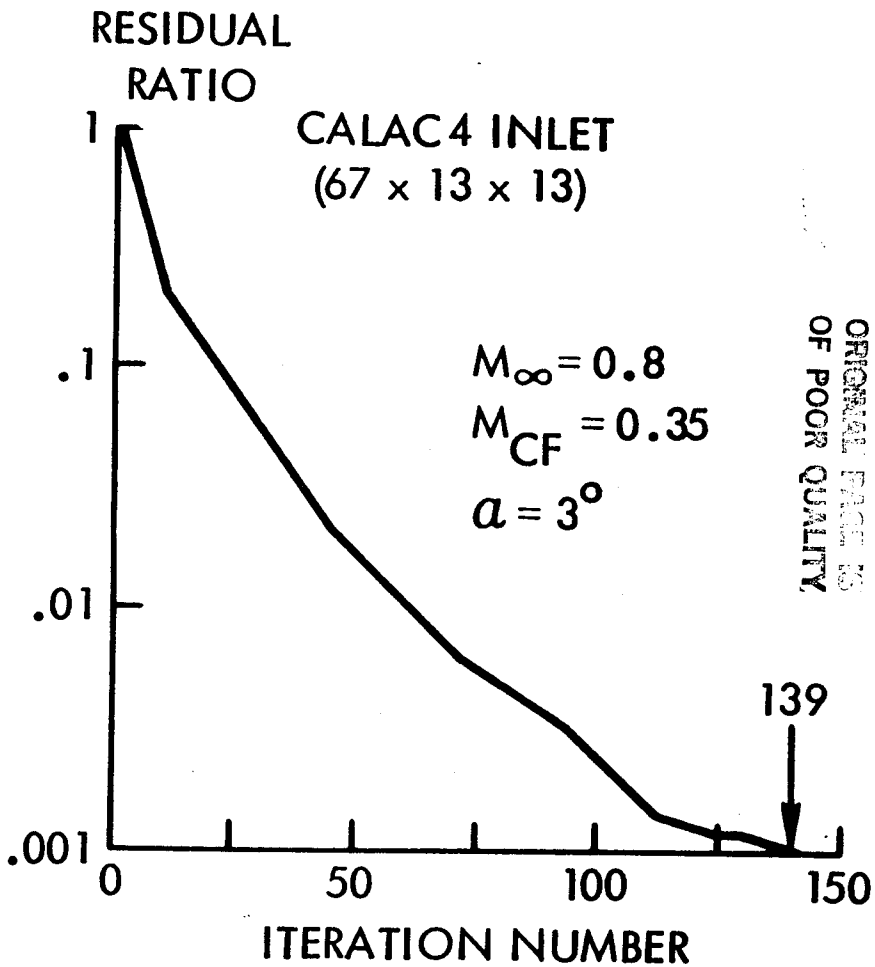

Figure 14. Error vs. iteration number.

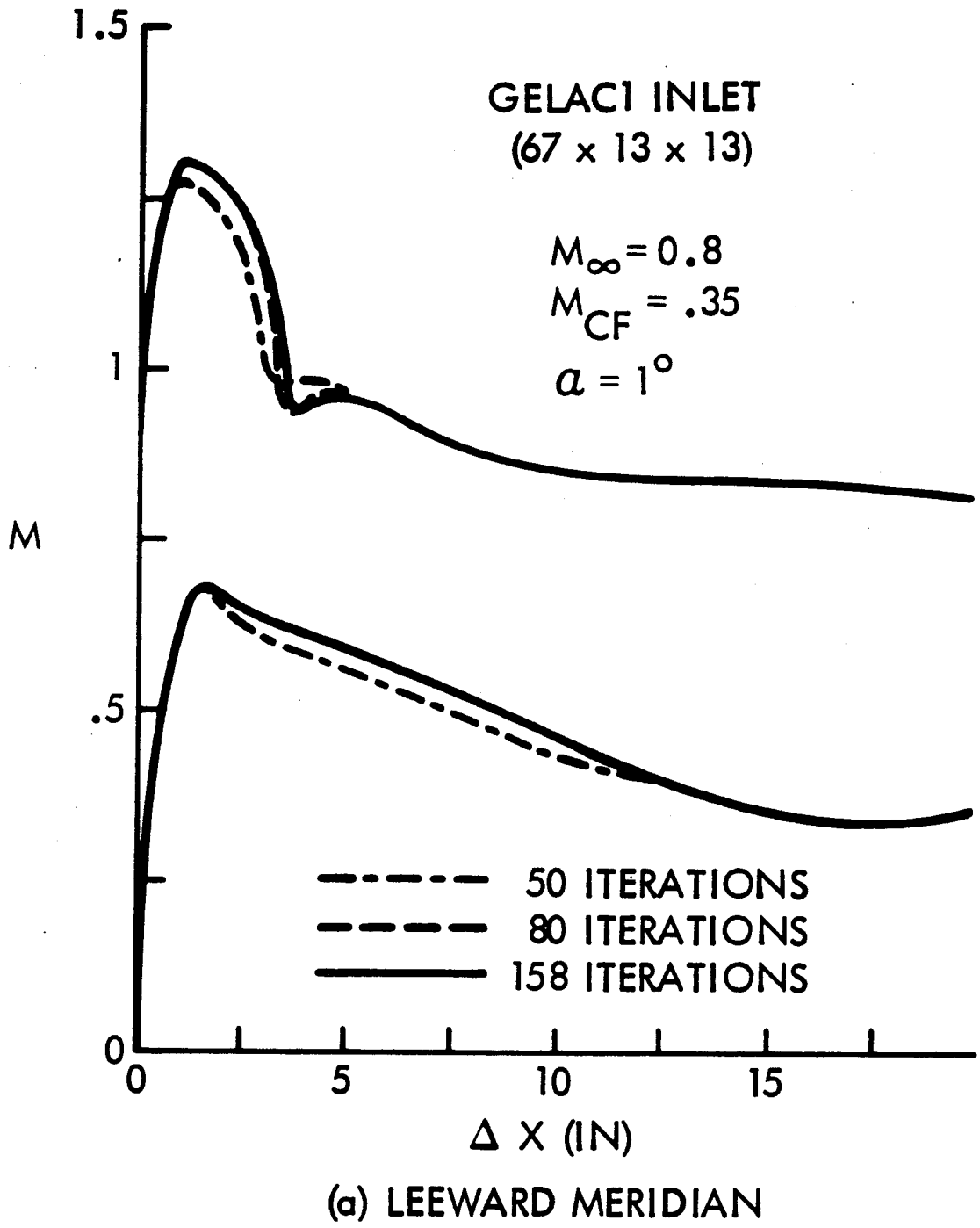

Figure 15. Evolution of surface solution with iteration number.

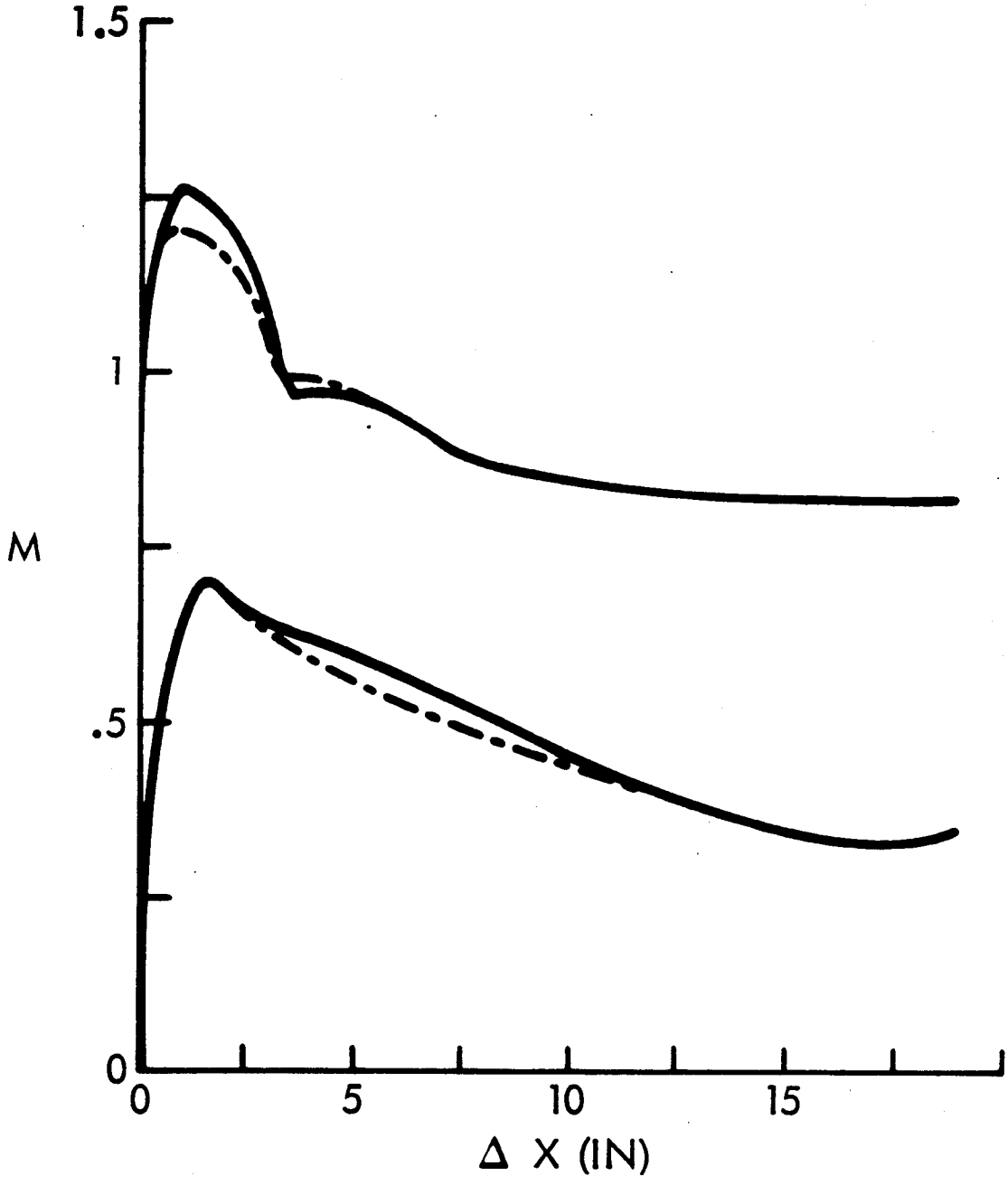

(b) TRANSVERSE MERIDIAN

Figure 15. Continued.

cruise drag while maintaining the engine thrust vector in the proper orientation. Figure 16 illustrates the nacelle/inlet contours for the top (θ = 0) and bottom [θ = 180 (deg)] circumferential stations. The nacelle has one plane of geometric symmetry, and thereby the computational grid is generated for one half of the computational domain and then reflected about the symmetry axis to obtain the other half.

For an asymmetric nacelle, the flow will be three-dimensional even at zero incidence. Computed surface Mach number contours for the top (θ = 0) and bottom [θ = 180 (deg)] meridians of the asymmetric nacelle are presented in Figure 17. These results are for a free-stream Mach number M_∞ of 0.8, a compressor face Mach number M_{cf} of 0.35, and zero incidence (α = 0). Asymmetry exists in the computed solution with the lower external surface producing a higher local Mach number than the top meridian at this angle of attack.

Typical computation times for three-dimensional flow solutions using the nacelle/inlet algorithm are 15-25 minutes for subcritical cases and 35-50 minutes for supercritical cases on a VAX-11/780 super-mini-computer using a (67 x 13 x 13)-point computational grid. The algorithm has also been executed on the NASA-Ames CRAY-1 Class VI vector processor. Typical computation times for three-dimensional supercritical flow solutions using the CRAY-1 are on the order of 90 seconds of CPU time. No special effort has yet been made in vectorizing the program for use on the CRAY-1. Consequently, substantial improvements in the required execution time can be realized by restructuring the scalar code to benefit more fully from the CRAY vector-processing capabilities. It is estimated that by doing this the execution time could be reduced by a factor of 5 to 6.

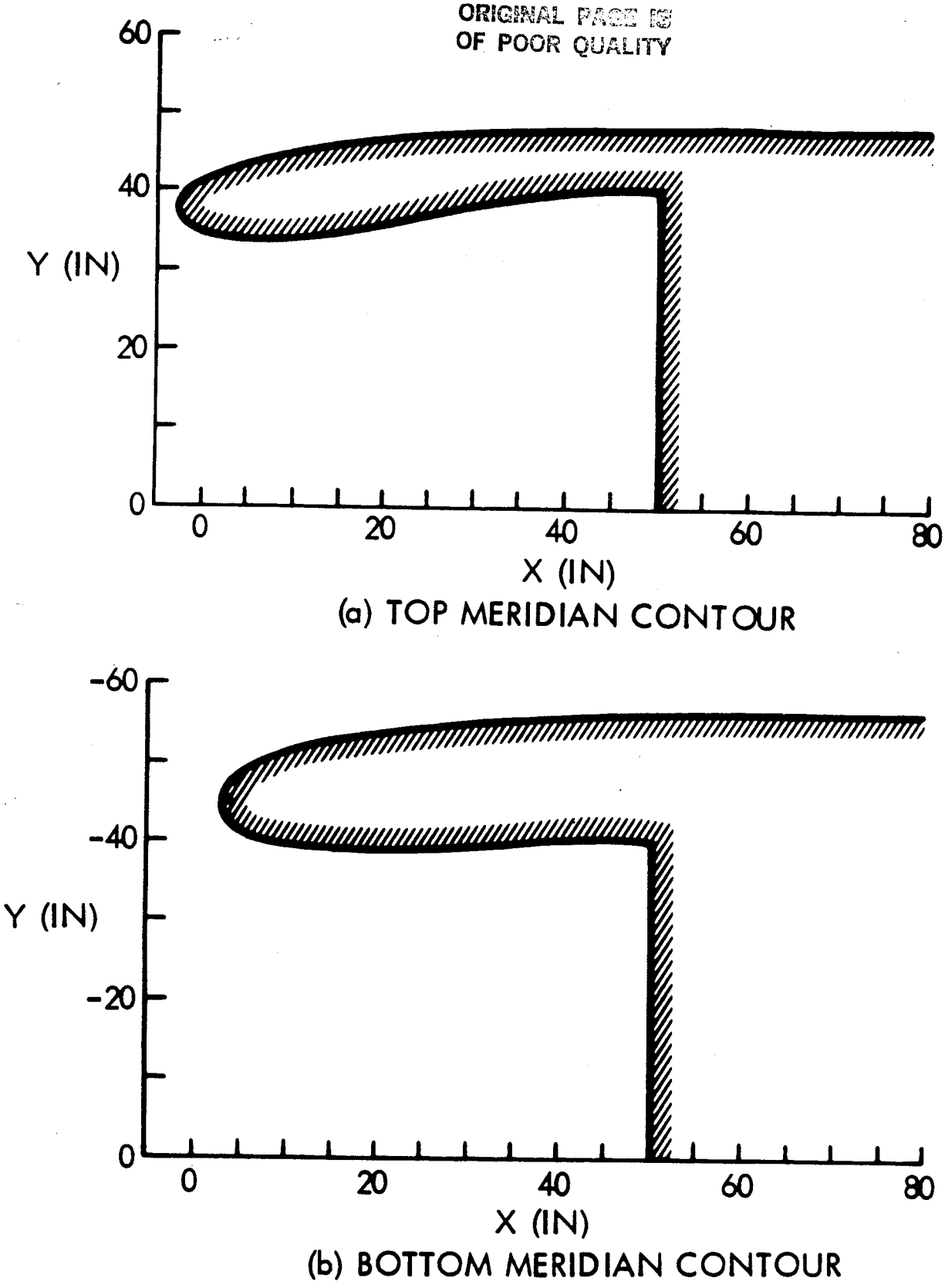

Figure 16. Asymmetric nacelle/inlet meridian contours.

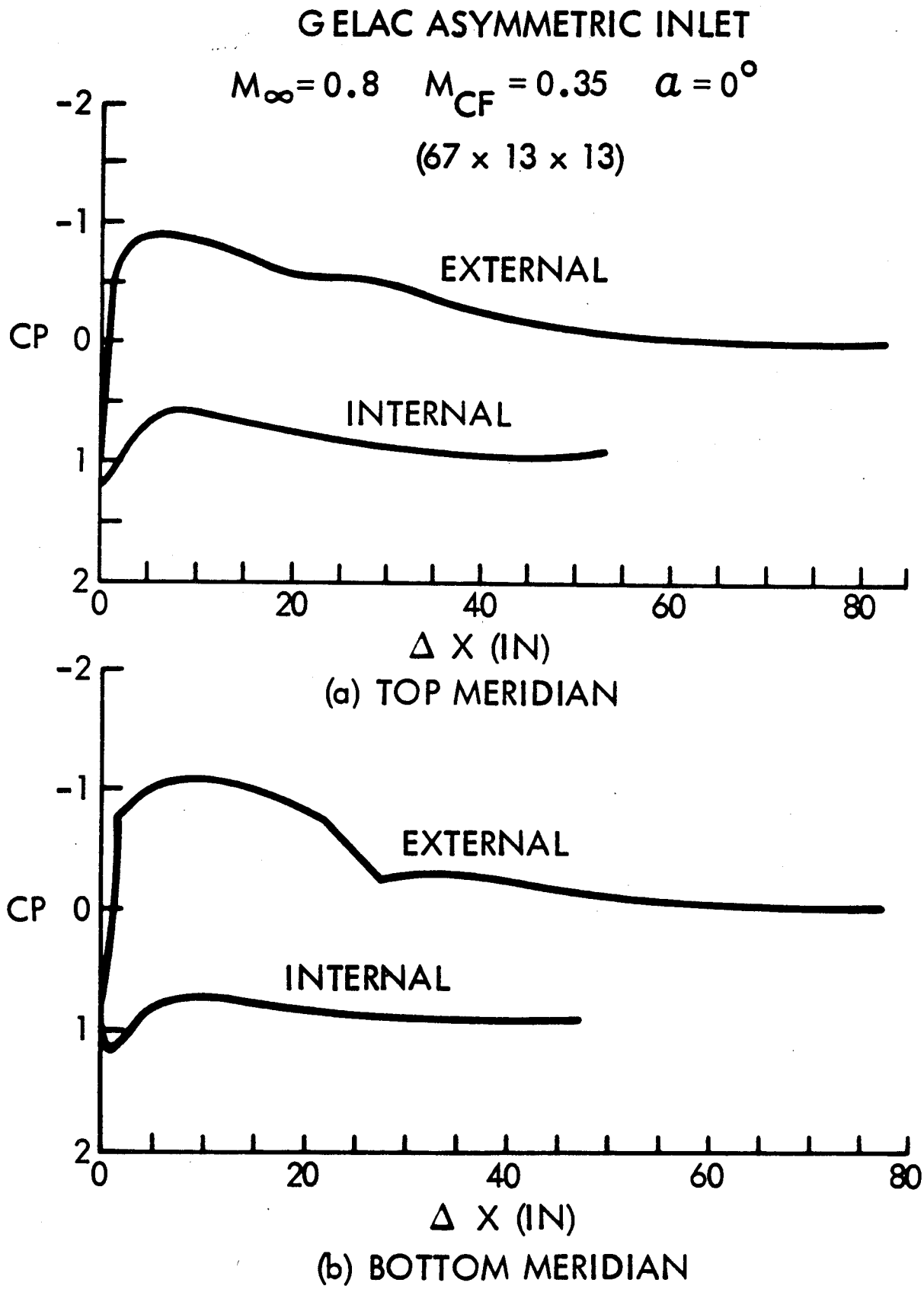

Figure 17. Solution for asymmetric inlet at $M_\infty = 0.8$ and $\alpha = 0$.

SECTION III

SUBROUTINE DESCRIPTIONS

1. INTRODUCTION

In this section, a brief description is given of the function of each subroutine in both the NGRIDA grid generation Fortran program and the NACELLE flow solution Fortran program. This information supplements the information available in the form of comment statements within the respective programs.

2. SUBROUTINE DESCRIPTIONS FOR THE NGRIDA GRID GENERATION PROGRAM

NGRIDA. This program routine is the main control routine in the NGRIDA grid generation program. Routine NGRIDA first calls SUBROUTINE NINPUT for data input, parameter initialization, and printing of preliminary information. SUBROUTINE GENER is then called to control the actual numerical generation of the surface-fitted computational grid.

NINPUT. This subroutine is used to enter the input data, perform parameter initialization, and print preliminary information. The input data are entered by specification of the four NAMELISTS LIST1, LIST2, LIST3, and LIST4. All input parameters have specified default values, and a default axisymmetric nacelle/inlet geometry data set has been loaded onto DATA statements within the program. At the end of SUBROUTINE NINPUT, the input namelist data are printed to initiate the computer output. SUBROUTINE NINPUT is called from routine NGRIDA.

CUBICS. This subroutine determines the coefficients for a set of cubic spline polynomials which are used to interpolate for the surface geometry given the axial positions and corresponding surface radii for N tabular data points. The use of cubic splines ensure continuity of surface radius, slope, and curvature for the interpolated geometry. The spline coefficients are found in terms of the surface curvature values at each of the supplied tabular data points. A sparse system of simultaneous linear equations, which determines the curvature values, is solved by calling SUBROUTINE GELG. SUBROUTINE CUBICS is called from SUBROUTINE GENER.

GENER. This subroutine contains the main control logic for numerically generating the curvilinear computational grid. The initial step in GENER is to generate the cubic spline polynomial coefficients for both the external and internal nacelle surfaces by calling SUBROUTINE CUBICS. The cubic spline polynomials are used to interpolate for the surface geometry. At this stage, the arc length measured from the nacelle hilite is determined at each of the user-supplied tabular data points that define the geometry. From a set of user-supplied stretching factors which effect clustering around the hilite, the arc length distributions for the final surface grid point locations are determined. From the surface grid point arc length distributions, the axial and radial coordinates of the final surface grid points are found by interpolation using the cubic spline polynomials. At this stage, the outer computational boundary grid point

distribution is determined by one of two options. The first option determines the outer boundary point locations by using an angular distribution where the boundary points are located on rays spaced in equal angular increments around the nacelle hilite. The second option determines the outer boundary point locations by using an arc length distribution with the spacing between points being controlled by user-supplied stretching parameters. At this stage, a file is written for the GRAPE algorithm which determines the interior field point locations by iteratively solving two coupled Poisson equations. After the GRAPE algorithm has been executed, conversion of the data format and plotting of the finished grid is performed by calling SUBROUTINE CONVERT. At this stage, a reflection of the grid point coordinates is performed to determine the point distributions on the remaining meridional planes. Finally, certain transition point indices are determined and the grid point distribution is printed and also stored on a disk file for input to the flow solution program. SUBROUTINE GENER is called from routine NGRIDA.

CONVERT. This subroutine is used to convert the output from the GRAPE algorithm into a format which is acceptable by the NACELLE flow solution algorithm. The GRAPE-generated grid point coordinates are entered through a binary read of TAPE 7. The corners on the leading edge of the grid are then rounded and point reordering is performed to make the grid generator output consistent with the input format required by the NACELLE program. Translation and scaling of the grid are then performed. If desired, plotting of the finished grid is performed. The plotting routines use the ISSCO-DISSPLA[9] Fortran library of plot functions. If this subroutine library is not available, then the plotting section of the code will have to be modified to be compatible with the user's particular installation. SUBROUTINE CONVERT is called from SUBROUTINE GENER.

GELG. This subroutine is used for solving a system of simultaneous linear equations. The system is solved using Gaussian elimination with complete pivoting. This subroutine is IBM Library SUBROUTINE GELG. SUBROUTINE GELG is called from SUBROUTINE CUBICS.

The remaining subroutines in the NGRIDA grid generation program comprise the GRAPE algorithm. Cursory descriptions of the functions of these subroutines are presented herein. Detailed subroutine descriptions are given in Reference 6.

GRAPE. This subroutine is the main control routine in the GRAPE algorithm. SUBROUTINE GRAPE is called from SUBROUTINE GENER after the boundary grid point locations have been determined. SUBROUTINE GRAPE determines the interior field point locations by calling in turn SUBROUTINES INPUT, INCHK, INNER, OUTER, SOLVE, and OUTPUT. The grid point locations are transmitted back to SUBROUTINE GENER through use of a scratch disk file.

CKSMTH. This GRAPE algorithm subroutine is used to check for smoothness in an input array by passing a parabola through the three nearest neighbors of a point and then observing the difference between the actual value and that interpolated from the parabola.

CSPLIN. This GRAPE algorithm subroutine is used to perform cubic spline curve fitting.

IC. This GRAPE algorithm subroutine is used to initialize the grid coordinate and forcing function arrays prior to starting the iterative relaxation procedure to determine the interior grid point locations.

INCHK. This GRAPE algorithm subroutine is used to test for errors on selected input parameters for the GRAPE program.

INNER. This GRAPE algorithm subroutine is used to locate grid points on the inner computational boundary.

INPUT. This GRAPE algorithm subroutine is used to enter the input data that is required for execution of the GRAPE program.

INTERP. This GRAPE algorithm subroutine is used to interpolate from the coarse grid solution to obtain initial conditions for the fine grid solution.

OUTER. This GRAPE algorithm subroutine is used to locate grid points on the outer computational boundary.

OUTPUT. This GRAPE algorithm subroutine is used to print the finished grid point coordinates.

RELAX. This GRAPE algorithm subroutine is used to solve the governing Poisson equations using a successive-line-over-relaxation iteration scheme.

SOLVE. This GRAPE algorithm subroutine is used to control the coarse and fine grid solutions of the governing Poisson equations.

TRIB. This GRAPE algorithm subroutine is used to solve a tridiagonal system of simultaneous linear equations with fixed boundary conditions.

TRIP. This GRAPE algorithm subroutine is used to solve a tridiagonal system of simultaneous linear equations with periodic boundary conditions.

3. SUBROUTINE DESCRIPTIONS FOR THE NACELLE FLOW SOLUTION PROGRAM

NACELLE. This program routine is the main control routine in the NACELLE flow analysis program. Routine NACELLE first calls SUBROUTINE NINPUT for data input, initialization of certain parameters, and printing of preliminary information. SUBROUTINE NINIT is then called to perform selected parameter initialization, determination of outflow velocities, and potential field initialization. Finally, SUBROUTINE NSOLVE is called which applies the AF2 iteration scheme to obtain the inviscid solution.

NINPUT. This subroutine is used to enter the input data, perform initialization of selected parameters, and print preliminary information. The input data are entered by specification of the four NAMELISTS LIST1, LIST2, LIST3, and LIST4. Most of the input parameters have specified default values. At the end of SUBROUTINE NINPUT, the input namelist data are printed to initiate the computer output. SUBROUTINE NINPUT is called from routine NACELLE.

NINIT. This subroutine is used to initialize selected parameters employed in the computation. SUBROUTINE NINIT first computes functions of the specific heat ratio and binomial expansion coefficients used in the computation of the physical density. SUBROUTINE METRIC is then called to determine the metric parameters used in the grid mapping from physical space to computational space. At this stage, the free-stream velocity magnitude and Cartesian velocity components are computed along with the appropriate outflow boundary condition parameters. Finally, the potential field is initialized using one of two options. In the first option, the initialization is performed using velocity components based on the free-stream Mach number. In the second option, the external flow field points are initialized using free-stream velocity components, whereas the internal flow field points are initialized using velocities based on a local Mach number which itself is found from the area ratio and compressor face Mach number using one-dimensional gas dynamic formulae. SUBROUTINE NINIT is called from routine NACELLE.

SECANT. This subroutine is used to determine the local internal flow Mach number using one-dimensional gas dynamic formulae which express mass continuity for the captured streamtube. A reference area and Mach number are supplied, and from the local flow area the local Mach number is determined. A secant iteration scheme is used to numerically determine the zero of the governing implicit relation. SUBROUTINE SECANT is called from SUBROUTINE NINIT and determines the compressor face Mach number from the user-supplied capture ratio. It also determines the local Mach number from the compressor face Mach number and the ratio between the local and compressor face areas. SUBROUTINE SECANT is called from SUBROUTINE NINIT.

METRIC. This subroutine is used to compute the metric parameters for all points in the computational mesh. The metric coefficients define the three-dimensional grid mapping from physical space to computational space. The metric coefficients are computed using either second-order accurate or fourth-order accurate finite-difference formulae. The physical grid point locations are entered through a binary read of a disk file (TAPE 10). An option exists to calculate and print the finite-difference scheme amplification factor values as determined from a von Neumann linear stability analysis. SUBROUTINE METRIC is called from SUBROUTINE NINIT.

NRO. This subroutine is used to calculate the physical density coefficients at the ξ-half points and the ξ-end points in the computational mesh. From the current potential function field, the derivatives of the velocity potential in the ξ, η, and ζ directions are computed using second-order accurate finite-difference formulae. The potential function derivatives are then used in a form of the isentropic energy equation to determine the density. At the body surface, the flow tangency condition is used in computing the density. At the internal and external outflow surfaces, the density is assumed known from the prescribed boundary conditions. At the external computational boundary, the density is assumed to be equal to the free-stream density. SUBROUTINE NRO is called from SUBROUTINES NSOLVE and NPRINT.

NROCO. This subroutine is used to calculate the modified density coefficients at the ξ, η, and ζ half-points in the computational mesh. The

modified density coefficients are computed by forming the appropriate averages of the physical density coefficients calculated by SUBROUTINE NRO. If the flow is locally supersonic, then upwinding is effected by forming a weighted average of the physical density at the point in consideration and the density at a point in the upwind direction along the corresponding curvilinear coordinate. Upwinding is always performed along the ξ wraparound coordinate. Upwinding in the η circumferential direction and in the ζ radial direction are user-defeatable options. SUBROUTINE NROCO is called from SUBROUTINE NSOLVE.

NRESID. This subroutine is used to apply the full-potential equation residual operator to the current velocity potential field to obtain the mass residuals at all points in the computational mesh except for those points on the outer computational boundary. The mass residual at a given point is computed by forming the sum of the finite-difference derivatives of the mass fluxes in the ξ, η , and ζ coordinate directions. Central difference expressions are used at interior field points while special procedures are used at the body surface and at the internal and external outflow surfaces. SUBROUTINE NRESID employs the modified density coefficients calculated by SUBROUTINE NROCO. SUBROUTINE NRESID is called from SUBROUTINE NSOLVE.

NSOLVE. This subroutine is the main flow field integration control routine and is used to apply the AF2 approximate factorization scheme to determine the inviscid flow solution. The AF2 scheme is applied in an iterative manner with the iteration sequence being terminated by either achieving convergence or by reaching a maximum permissible number of iterations. Per iteration, a three-step process is used to obtain the potential function correction. The first two steps calculate intermediate potential function corrections arising from solving systems of factorized difference equations in the ξ-wraparound and η-circumferential directions. The third step calculates the actual potential correction by solving a system of factorized difference equations for the ζ-radial coordinate. Steps 1 and 2 require sweeping the computational mesh from the body surface outwards. The third step sweeps from the outer computational boundary towards the body surface. SUBROUTINE NSOLVE calls SUBROUTINES NRO, NROCO, and NRESID for calculation of the physical density coefficients, modified density coefficients, and mass residuals, respectively. SUBROUTINES NTRIC and NTRIP are called in the course of applying the AF2 scheme to solve systems of tridiagonal simultaneous linear equations with fixed and periodic boundary conditions, respectively. SUBROUTINE NPRINT is called to print the computed surface solution. If plots of the surface Mach number and/or pressure coefficient distributions are required, SUBROUTINE RESPLOT is then called by SUBROUTINE NSOLVE. SUBROUTINE NSOLVE is called by routine NACELLE.

NTRIC. This subroutine is used to solve a system of simultaneous linear equations with a tridiagonal coefficient matrix and fixed boundary conditions. This routine is used in the AF2 iteration algorithm to obtain the potential function intermediate correction in the ξ-wraparound coordinate direction. SUBROUTINE NTRIC is called from SUBROUTINE NSOLVE.

NTRIP. This subroutine is used to solve a system of simultaneous linear equations with a tridiagonal coefficient matrix and periodic boundary

conditions. This routine is used in the AF2 iteration algorithm to obtain the potential function intermediate correction in the η-circumferential coordinate direction. SUBROUTINE NTRIP is called from SUBROUTINE NSOLVE.

NPRINT. This subroutine is used to print the computed surface solution when convergence has been attained, or when the maximum permissible number of iterations has been reached, or throughout the computation at user-specified iteration counts. SUBROUTINE NRO is applied at the body surface to calculate the physical density coefficients at mesh mid-points on the surface. From the computed density distribution, the surface Mach number and pressure coefficient distributions are determined. SUBROUTINE NPRINT is called from SUBROUTINE NSOLVE.

RESPLOT. This subroutine is used to plot the surface Mach number and pressure coefficient distributions at user-selected meridional stations. Options exist to defeat the plot option, or to plot just the surface Mach number distribution or the pressure coefficient distribution. The plotting routines use the ISSCO-DISSPLA[9] Fortran library of plot functions. If this subroutine library is not available, then the plotting section of the code will have to be modified to be compatible with the user's particular installation. SUBROUTINE RESPLOT is called from SUBROUTINE NPRINT.

SECTION IV

INPUT PARAMETERS AND OUTPUT INTERPRETATION

1. INTRODUCTION

In this section, the input parameters are defined for both the NGRIDA grid generation program and the NACELLE flow solution program. Where applicable, both the default value and typical value of each input parameter are given. Discussions on interpretation of the output, PARAMETER statement specification, and file usage for both programs are also provided.

2. NGRIDA GRID GENERATION PROGRAM INPUT PARAMETERS

The input data required for execution of the NGRIDA grid generation computer program are entered by namelist input. In all cases, the four NAMELISTS LIST1, LIST2, LIST3, and LIST4 are entered. All of the input parameters have assigned default values. A suitable grid can often be generated by retaining many of the input parameters at their default values.

2.1 NAMELIST LIST1

The input parameters specified in NAMELIST LIST1 specify the number of mesh points, outer boundary shape, grid point distribution stretching factors, and print and plot options.

The following three parameters specify the number of grid points.

IMAX — A positive integer denoting the number of ξ-wraparound stations in the computational grid, as shown in Figure 18. The specified value of IMAX must be less than or equal to 140, and should be of the form (3m+1) if grid sequencing is to be used in the GRAPE algorithm, where m is an integer. A default value of 67 is specified for IMAX.

JMAX — A positive integer denoting the number of η-circumferential stations in the computational grid, as shown in Figure 19. Stations J=1 and J=JMAX are coincident with the (x-y)-plane. The remaining meridional stations are spaced in equal angular increments around the body. The specified value of JMAX must be odd. A default value of 13 is specified for JMAX.

KMAX — A positive integer denoting the number of ζ-radial stations in the computational grid, as shown in Figure 18. The specified value of KMAX must be less than or equal to 60, and should be of the form (3n+1) if grid sequencing is to be used in the GRAPE algorithm, where n is an integer. A default value of 13 is specified for KMAX.

The next three parameters specify the outer computational boundary.

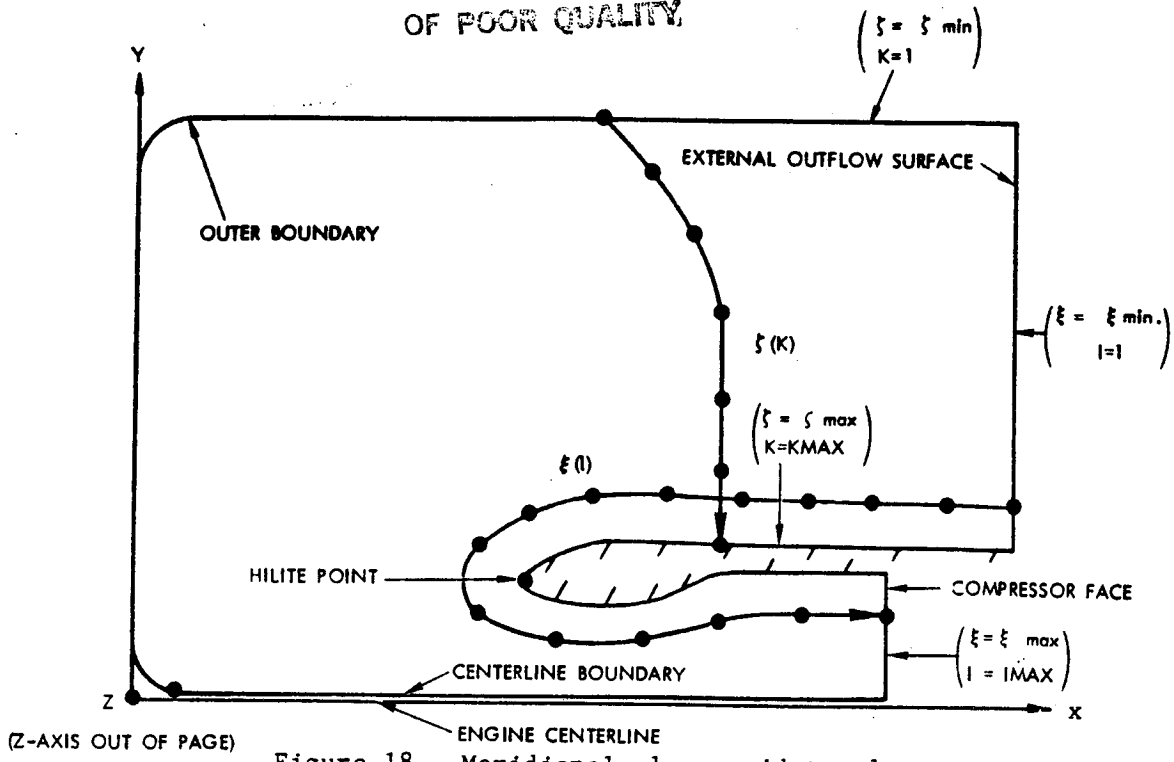

Figure 18. Meridional plane grid topology.

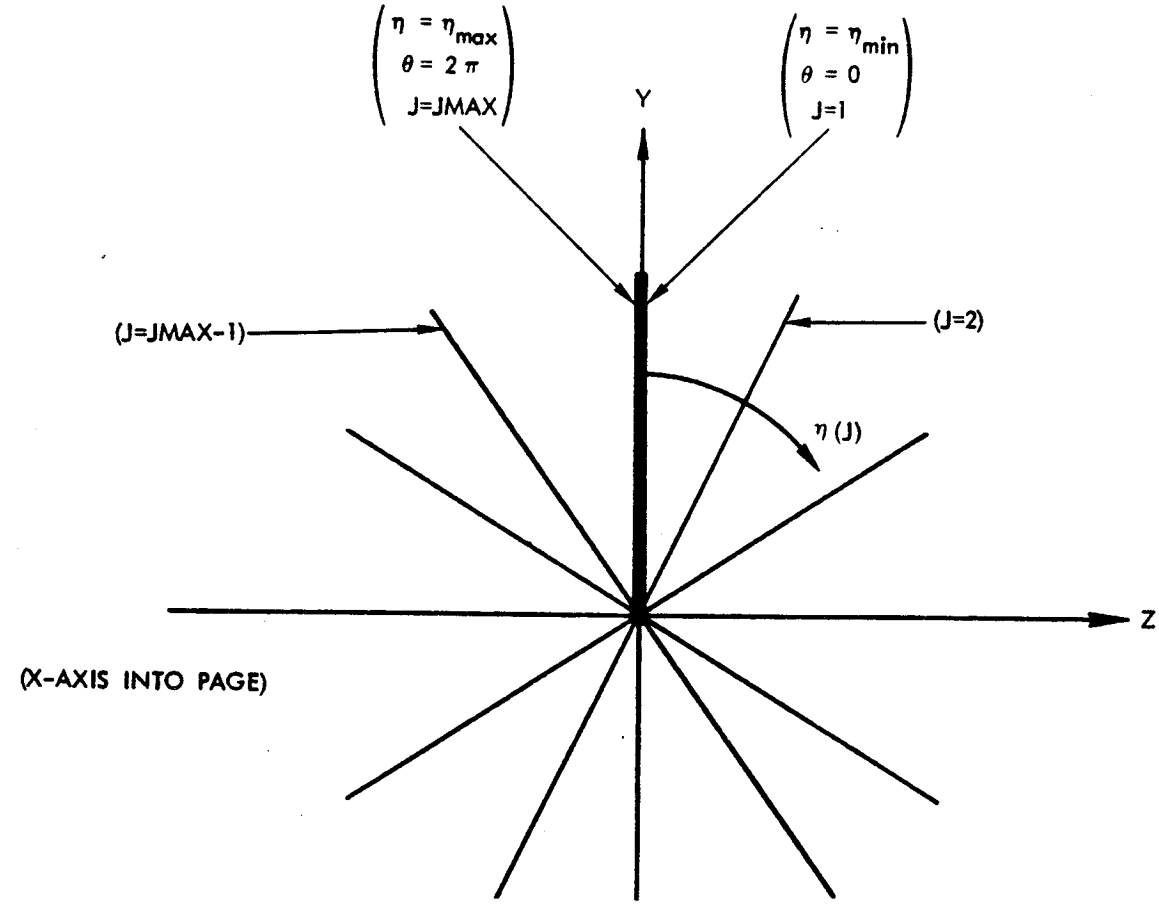

Figure 19. Grid as viewed along the longitudinal (X) axis.

XLEFT A real variable denoting the x-coordinate value of the left-hand side of the outer computational boundary, as shown in Figure 20. XLEFT is specified in the units of the input geometry, and typically is negative. A default value of -30.0 is specified for XLEFT.

RADOUT A positive real variable denoting the radius of the outer computational boundary, as shown in Figure 20. RADOUT is specified in the units of the input geometry. A default value of 50.0 is specified for RADOUT.

DELTA A positive real variable denoting the offset distance between the computational boundary and the x-axis, as shown in Figure 20. DELTA is specified in the units of the input geometry and must not be zero. A value of approximately 5% of the compressor face radius is recommended for DELTA. A default value of 0.5 is specified for DELTA.

The next four parameters control the grid point distribution on the body surface.

IOUTER A positive integer denoting the number of grid points desired on the outer portion of the nacelle surface ranging from the hilite point to the external outflow surface, as shown in Figure 20. A default value of 38 is specified for IOUTER.

IINNER A positive integer denoting the number of grid points desired on the inner portion of the nacelle surface ranging from the hilite point to the compressor face outflow surface, as shown in Figure 20. The specified values for IOUTER and IINNER must satisfy the relation

$$IMAX = IINNER + IOUTER - 1 \qquad (35)$$

A default value of 30 is specified for IINNER.

ALPHAO A positive real variable denoting the stretching factor used in determining the grid point distribution on the nacelle external surface. Entering ALPHAO=1.0 produces a point distribution with uniform arc length between the points [see equation (1)]. Entering ALPHAO > 1.0 clusters points near the nacelle hilite. A default value of 1.1 is specified for ALPHAO.

ALPHAI A positive real variable denoting the stretching factor used in determining the grid point distribution on the nacelle internal surface. Entering ALPHAI=1.0 produces a point distribution with uniform arc length between the points [see equation (1)]. Entering ALPHAI > 1.0 clusters points near the nacelle hilite. A default value of 1.1 is specified for ALPHAI.

The next five parameters determine the outer boundary grid point distribution. Generally, the outer boundary points near both the external and internal outflow surfaces are found by equating the axial coordinate of

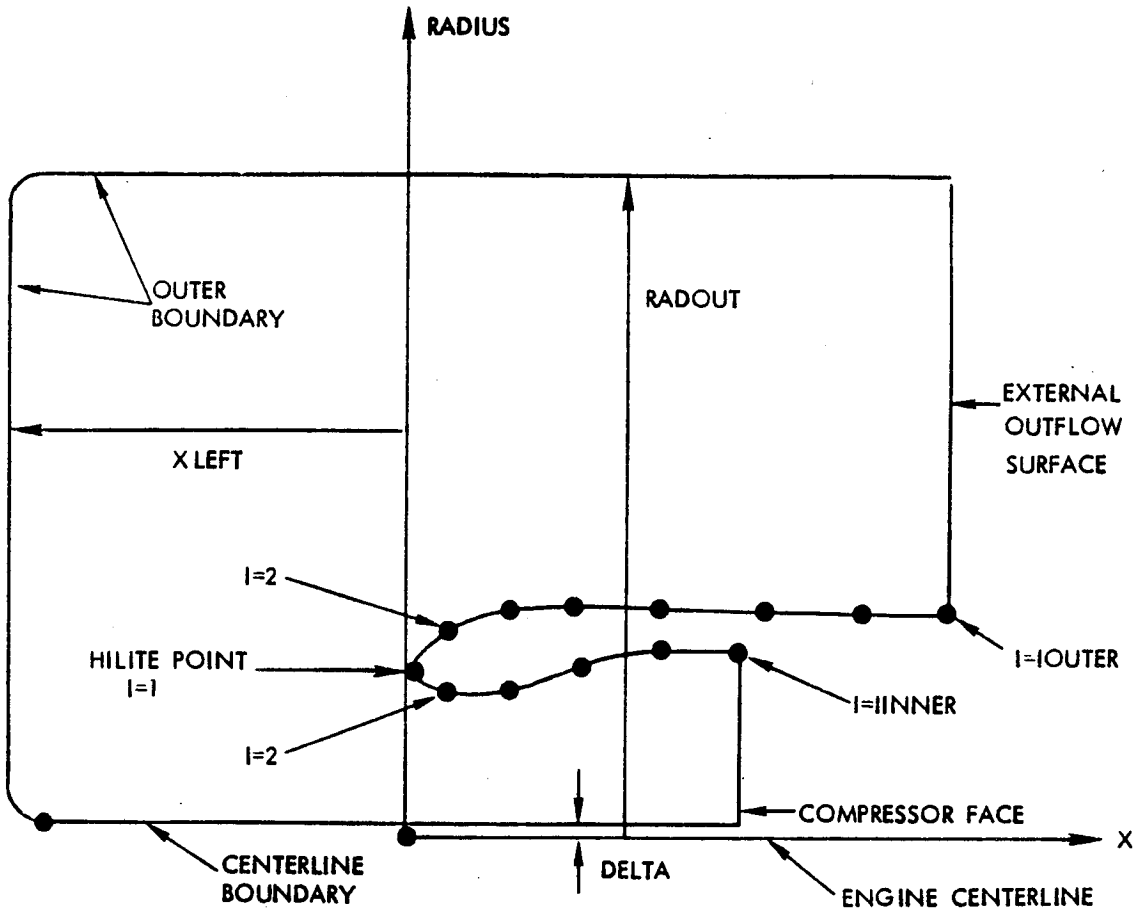

Figure 20. Specification of outer boundary and point distribution on surface.

a given boundary point to the axial coordinate of the corresponding body point (see Figure 21). The remaining boundary points are found by either using an angular distribution or an arc-length distribution.

IAA — A positive integer denoting the wraparound coordinate station up to which the points on the computational boundary near the centerline have their axial coordinates equated to the respective values of the corresponding points on the internal nacelle surface, as illustrated in Figure 21. IAA is specified in terms of the GRAPE algorithm point-ordering scheme in which the wraparound coordinate initiates at the compressor face and terminates at the external outflow surface (see Figure 21). A default value of 12 is specified for IAA.

IDD — A positive integer denoting the wraparound coordinate station after which the points on the outer computational boundary have their axial coordinates equated to the respective values of the corresponding points on the nacelle external surface, as shown in Figure 21. IDD is specified in terms of the GRAPE algorithm point-ordering scheme in which the wraparound coordinate initiates at the compressor face and terminates at the external outflow surface (see Figure 21). Note that IDD must satisfy the relation IAA < IDD < IMAX. A default value of 57 is specified for IDD.

KOUTER — An integer denoting whether the outer boundary grid points between points IAA and IDD are to be determined by an angular distribution or by an arc-length distribution. If KOUTER=0, the grid points are determined by an angular distribution with the grid points being spaced at equal angular increments around the nacelle hilite. If KOUTER=1, the grid points are determined by an arc-length distribution with respective stretching factors being specified by the user. A default value of 0 is specified for KOUTER.

If KOUTER=1 is specified, then the following two parameters must be entered.

ALPHBO — A positive real variable denoting the stretching factor used in determining the outer boundary grid point distribution for the portion of the boundary between points C and IDD, as shown in Figure 21. Entering ALPHBO=1.0 produces a point distribution with uniform arc length between the points [see equation (1)]. Entering ALPHBO > 1.0 clusters points near point C. A default value of 1.0 is specified for ALPHBO.

ALPHBI — A positive real variable denoting the stretching factor used in determining the outer boundary grid point distribution for the portion of the outer boundary between point C and IAA, as shown in Figure 21. Entering ALPHBI=1.0 produces a point distribution with uniform arc length between the points [see equation (1)]. Entering ALPHBI > 1.0 clusters points near point C. A default value of 1.0 is specified for ALPHBI.

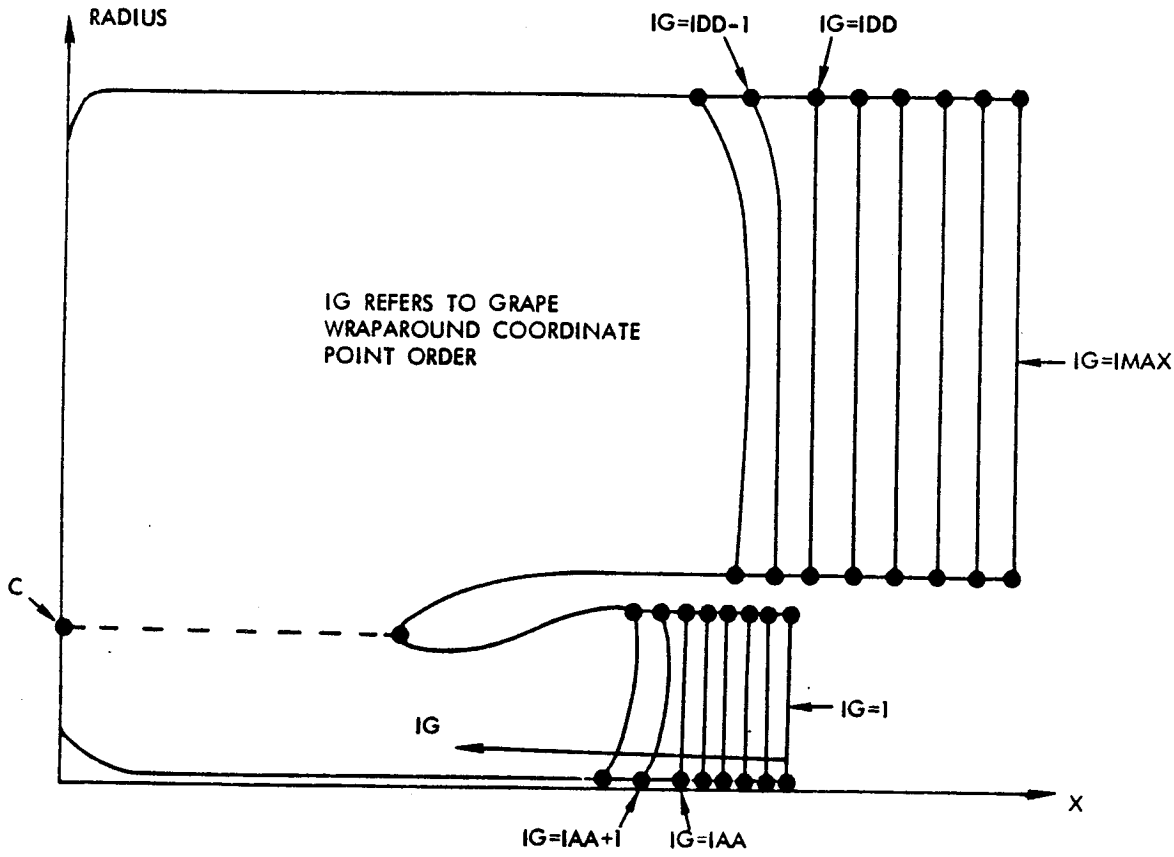

Figure 21. Definition of points IAA and IDD.

The next three parameters control the grid spacing adjacent to the body surface in the direction normal to the surface. Generally, the normal distance DS, as shown in Figure 22, is computed by the relation

$$DS = (RCF - DELTA)/(KMAX - 1) \qquad (36)$$

where RCF is the compressor face radius. For isolated nacelle grids, it is generally preferable to adjust DS near the external outflow surface to make the radial point distribution uniform as shown in Figure 22. This point distribution produces a more favorable cell aspect ratio at the outflow surface, and thereby enhances stability and convergence in the flow solution algorithm.

DSFACT — A positive real variable used as a multiplier for DS which is defined by equation (36). A default value of 1.0 is specified for DSFACT.

KRAMP — An integer denoting whether or not the DS distribution is to be altered to produce a uniform radial point distribution at the external outflow surface. If KRAMP=1, the DS distribution is altered to produce the uniform radial point distribution. If KRAMP=0, the DS distribution is not altered, and the grid points will be packed towards the nacelle surface. If an isolated nacelle grid is being generated, then the KRAMP=1 option is recommended. A default value of 1 is specified for KRAMP.

IRAMP — A positive integer denoting the wraparound station after which the DS distribution is altered to produce a uniform radial point distribution at the external outflow surface, as shown in Figure 22. IRAMP must be entered only if KRAMP=1. IRAMP is specified in terms of the GRAPE algorithm point ordering scheme in which the wraparound coordinate initiates at the compressor face and terminates at the external outflow surface. Note that IRAMP must satisfy the relation IRAMP < IMAX. A default value of 57 is specified for IRAMP.

The next three parameters specify the scaling and smoothing function parameters.

SCALE — A positive real variable denoting the scaling multiplier used in obtaining the final grid. Entering SCALE=1.0 produces a grid in terms of the original input units. Setting SCALE=1.0/RCF, where RCF is the compressor face radius, produces a grid with a compressor face radius of 1.0. This option is recommended as it allows for more easily determining the optimum acceleration parameters in the flow solution code. A default value of 0.11904762=1.0/8.4 is specified for SCALE.

KTIME — An integer denoting the number of times smoothing polynomials are applied in determining the outer boundary axial coordinate distribution in the vicinity of point IDD, and the DS distribution in the vicinity of point IRAMP if the KRAMP=1 option is specified. If KTIME=0 is entered, no smoothing is performed.

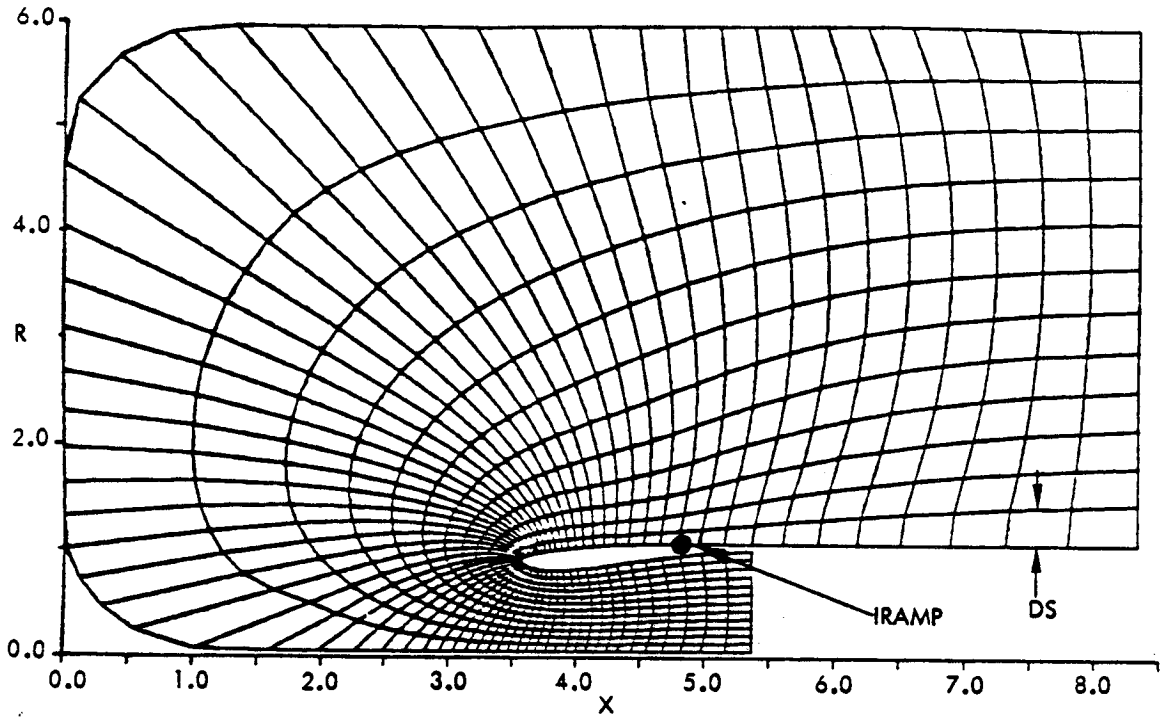

Figure 22. Normal mesh spacing and definition of point IRAMP.

The default and recommended value for KTIME is 3.

NDEL — A positive integer denoting the number of points to the left of point IDD at which the smoothing is initiated for the outer boundary point axial locations if KTIME > 0 is specified. NDEL must be entered only if KTIME > 0 is specified. A default value of 5 is specified for NDEL.

The next two parameters specify the print options.

KDUMP — An integer denoting whether or not detailed nacelle surface and outer boundary coordinate data are to be printed. If KDUMP=0, the data are not printed. If KDUMP=1, the printout is performed. A default value of 1 is specified for KDUMP.

KPRINT — A one-dimensional integer array consisting of JMAX elements. Each element of KPRINT specifies whether or not a meridional plane grid point distribution is to be printed. Specifying KPRINT(J)=1 (J=1,...,JMAX) causes the grid point coordinates to be printed for the Jth meridional plane. If KPRINT(J)=0 is entered, the printout is skipped for the Jth plane. A default value of KPRINT(1)=1 is specified, while the remaining elements of KPRINT are specified as 0.

The next two parameters specify the plot options.

KPLOT — An integer denoting whether or not the J=1 meridional plane grid is to be plotted. Specifying KPLOT=1 causes the grid to be plotted for the J=1 meridional plane. If KPLOT=0 is entered, the plotting is not performed. A default value of KPLOT=1 is specified.

KDEV — An integer denoting the plotting device. KDEV must be specified only if KPLOT=1 is entered. If KDEV=1, the plot device is the VERSATEC electrostatic plotter. If KDEV=2, the plot device is the HP ink plotter. A default value of 1 is specified for KDEV. (Note that the plot device specification can be altered by modifying SUBROUTINE CONVERT).

The next parameter specifies the tape number (disk file) on which the grid coordinate data are written.

ITAPE — An integer denoting the tape (file) number on which the grid coordinate data are written. ITAPE can be entered as either 10 or 14. For the present code version, ITAPE should be retained at its default value of 10.

2.2 NAMELIST LIST2

The input parameters entered in NAMELIST LIST2 specify the nacelle/inlet geometry which is described by tabular input. A default axisymmetric nacelle/inlet geometry has been loaded onto DATA statements within the program. The default geometry data are for the Lockheed-Georgia GELAC1 axisymmetric nacelle/inlet configuration.

The following three parameters specify the internal surface contour for axisymmetric nacelles.

NI — A positive integer denoting the number of tabular data points used in defining the internal surface contour, as shown in Figure 23. A default value of 60 is specified for NI.

XIN — A one-dimensional real variable array consisting of NI elements. XIN(I) (I=1,...,NI) denotes the axial coordinate of the Ith point used in defining the internal surface contour, as shown in Figure 23. Successive elements of XIN must be monotonically increasing. XIN(1) denotes the axial station of the nacelle hilite, and XIN(NI) denotes the compressor face axial station. Default values for XIN(I) (I=1,...,60) are specified.

RIN — A one-dimensional real variable array consisting of NI elements. RIN(I) (I=1,...,NI) denotes the radius of the Ith point used in defining the internal surface contour, as shown in Figure 23. RIN(1) denotes the nacelle hilite radius, and RIN(NI) denotes the compressor face radius. Default values for RIN(I) (I=1,...,60) are specified.

The next three parameters specify the external surface contour for axisymmetric nacelles.

NO — A positive integer denoting the number of tabular data points used in defining the external surface contour, as shown in Figure 23. A default value of 100 is specified for NO.

XOUT — A one-dimensional real variable array consisting of NO elements. XOUT(I) (I=1,...,NO) denotes the axial coordinate of the Ith point used in defining the external surface contour, as shown in Figure 23. The successive elements of XOUT must be monotonically increasing. XOUT(1) denotes the nacelle hilite axial station, and XOUT(NO) denotes the axial station of the external outflow surface. The relation XOUT(1) = XIN(1) must be satisfied. Default values for XOUT(I) (I=1,...,100) are specified.

ROUT — A one-dimensional real variable array consisting of NO elements. ROUT(I) (I=1,...,NO) denotes the radius of the Ith point used in defining the external surface contour, as shown in Figure 23. ROUT(1) denotes the nacelle hilite radius, and ROUT(NO) denotes the nacelle radius at the external outflow surface. The relation ROUT(1)=RIN(1) must be satisfied. Default values for ROUT(I) (I=1,...,100) are specified.

2.3 NAMELIST LIST3

The input parameters entered in NAMELIST LIST3 specify the convergence criteria, iteration limits, and print options used in the GRAPE algorithm. These parameters are given only cursory descriptions herein, but are more fully discussed in Reference 6. Generally, the program is executed by retaining all of the parameters in NAMELIST LIST3 at their default values.

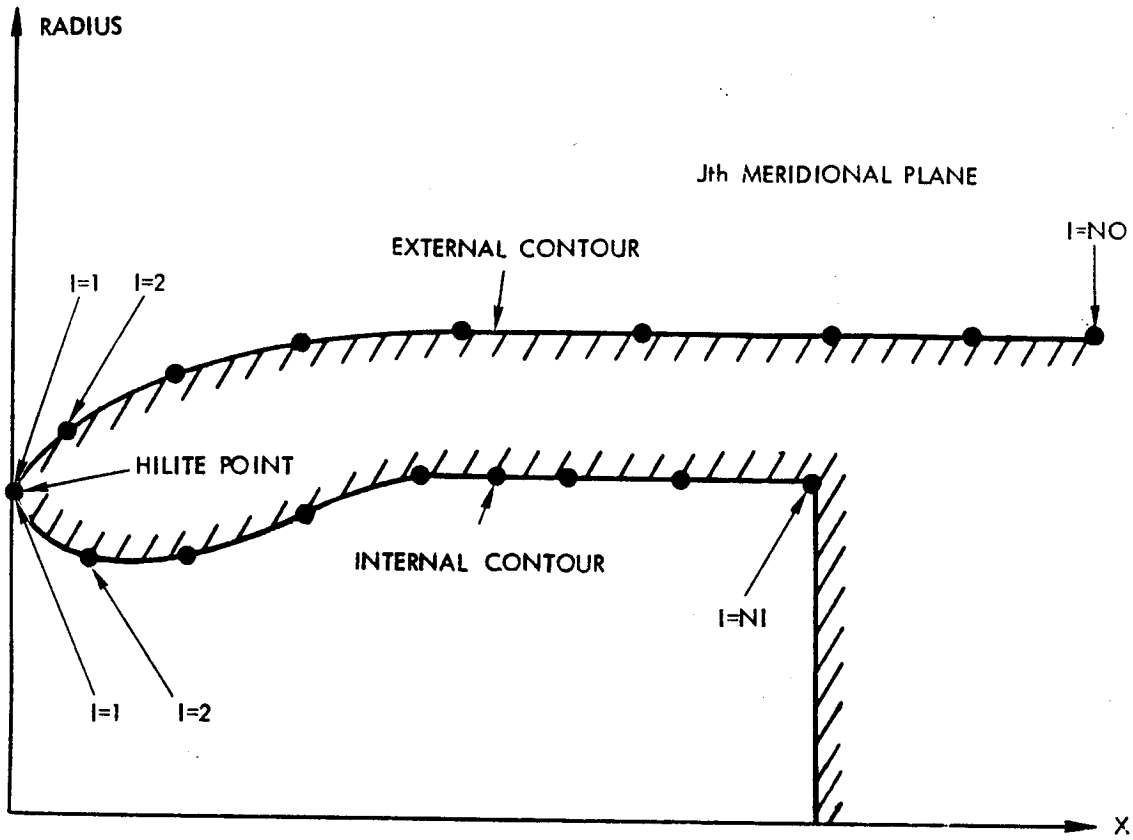

Figure 23. Surface geometry specification.

NORDA — A one-dimensional integer array consisting of two elements which denote the convergence criteria for the coarse-mesh and the fine-mesh GRAPE solutions. NORDA(1) and NORDA(2) denote the numbers of order of magnitude by which the maximum correction is to be reduced for the coarse-mesh and fine-mesh solutions, respectively. Default values of NORDA(1)=6 and NORDA(2)=3 are specified.

MAXITA — A one-dimensional integer array consisting of two elements which denote the iteration limits for the coarse-mesh and fine-mesh GRAPE solutions. MAXITA(1) and MAXITA(2) denote the iteration limits for the coarse-mesh and fine-mesh solutions, respectively. The MAXITA array is used in conjunction with the NORDA array. Default values of MAXITA(1)=400 and MAXITA(2)=200 are specified.

JPRT — An integer denoting the print option to be used in the GRAPE algorithm. If JPRT < 0, no printing is performed except for error warning messages. If JPRT=1, a detailed printout will be performed. A default value of -1 is specified for JPRT.

2.4 NAMELIST LIST4

The input parameters entered in NAMELIST LIST4 specify the grid control functions and convergence parameters used in the GRAPE algorithm. Again, only cursory descriptions are provided herein, with detailed definitions being available in Reference 6. Generally, the program is executed by retaining all of the parameters in NAMELIST LIST4 at their default values.

AAAI, BBBI — Positive real variables which control the enforcement of grid orthogonality and normal mesh spacing at the nacelle surface. Small values (i.e., 0.2) cause these effects to be propagated far into the field, whereas larger values (i.e., 0.6) cause these effects to diminish more rapidly. A default value of 0.6 is specified for both AAAI and BBBI.

CCCI, DDDI — Positive real variables which control the enforcement of grid orthogonality and normal mesh spacing at the outer boundary. Small values (i.e., 0.2) cause these effects to be propagated far into the field, whereas larger values (i.e., 0.6) cause these effects to diminish more rapidly. A default value of 0.6 is specified for both CCCI and DDDI.

OMEGA — A positive real variable used in the GRAPE successive-line-over-relaxation scheme to obtain the grid point distribution. OMEGA must be in the range of $0.0 < \text{OMEGA} < 2.0$. A default value of 1.3 is specified for OMEGA.

OMEGP, OMEGQ — Real variables used as relaxation parameters in obtaining the body surface forcing functions that are used in the Poisson equations. The effects of controlling grid spacing and orthogonality at the nacelle surface can be eliminated by entering OMEGP = OMEGQ = 0.0. OMEGP and OMEGQ must be in the

range of 0.0 to 2.0. A default value of 0.1 is specified for both OMEGP and OMEGQ.

OMEGR
OMEGS — Real variables used as relaxation parameters in obtaining the outer boundary forcing functions that are used in the Poisson equations. The effects of controlling grid spacing and orthogonality at the outer boundary can be eliminated by entering OMEGR = OMEGS = 0.0. OMEGR and OMEGS must be in the range of 0.0 to 2.0. A default value of 0.0 is specified for both OMEGR and OMEGS.

PLIM
QLIM
RLIM
SLIM — Real variables used as limitation factors in solving for the Poisson equation forcing functions. The range for each of these parameters is 0.0 to 100.0. A default value of 0.5 is specified for PLIM, QLIM, RLIM, and SLIM.

DSOBI — A positive real variable denoting the normal distance to be imposed between the radial stations KMAX and KMAX-1. DSOBI has units of the input geometry. A default value of 0.2 is specified for DSOBI.

2.5 PARAMETER STATEMENT SPECIFICATION

The NGRIDA grid generation program uses variable array dimensions. The respective array sizes are fixed by specification of the following dimension parameters on the PARAMETER statement:

Parameter		Allowed Values
NX	$\geq$	IMAX
NY	=	1
NYG	$\geq$	JMAX
NZ	$\geq$	KMAX
NXO	$\geq$	NO
NXI	$\geq$	NI
NXON	$\geq$	IOUTER
NXIN	$\geq$	IINNER
NXO2	$\geq$	NO*NO
NXI2	$\geq$	NI*NI

The array dimensions will be fixed at the time of compilation.

2.6 FILE USAGE

The following files are used by the NGRIDA grid generation code.

File No.	Usage
TAPE 5	input file
TAPE 6	printed output file
TAPE 10	file on which the finished grid coordinate data are stored (output)
TAPES 1,4,7	scratch files (should be deleted after computation)

3. NGRIDA PROGRAM OUTPUT INTERPRETATION

The initial portion of the computer printout for the NGRIDA program consists of the NAMELIST input data. Then if the KDUMP=1 option is specified, detailed nacelle surface and outer boundary coordinate data are listed. After this, the GRAPE algorithm output is printed. The finished grid point coordinates are then printed for selected meridional planes as specified by the KPRINT array. Finally, certain index parameters are printed (whose definitions are given in the flow solution algorithm user's manual).

The output parameters for the GRAPE algorithm are discussed in Reference 6. The remaining output parameters are defined below.

I	ξ-wraparound point index
J	η-circumferential point index
K	ζ-radial point index
X	x-coordinate of point in finished grid, (scaled units)
Y	y-coordinate of point in finished grid, (scaled units)
Z	z-coordinate of point in finished grid, (scaled units)
XOUT	x-coordinate of input point on external surface, (original units)
ROUT	radius of input point on external surface, (original units)
XIN	x-coordinate of input point on internal surface, (original units)
RIN	radius of input point on internal surface, (original units)
ARC-LENGTH	arc length measured from hilite point, (original units)
XBO	x-coordinate of redistributed point on external surface, (original units)
RBO	radius of redistributed point on external surface, (original units)
XBI	x-coordinate of redistributed point on internal surface, (original units)
RBI	radius of redistributed point on internal surface, (original units)
XSURF	surface point x-coordinate used as input for GRAPE code, (original units)
RSURF	surface point radius used as input for GRAPE code, (original units)
XBOUND	outer boundary point x-coordinate used as input for GRAPE code, (original units)
RBOUND	outer boundary point radius used as input for GRAPE code, (original units)

4. NACELLE FLOW SOLUTION PROGRAM INPUT PARAMETERS

The input data required for execution of the NACELLE flow analysis computer program are entered by namelist input. In all cases, the four NAMELISTS LIST1, LIST2, LIST3, and LIST4 are entered. Most of the input

parameters have assigned default values. In many cases, the flow solution can be obtained by retaining most of the input parameters at their default values. The coordinate data for the computational mesh are entered through a binary read of TAPE10.

4.1 NAMELIST LIST1

The input parameters entered in NAMELIST LIST1 specify the inlet orientation, free-stream and compressor face Mach numbers, convergence criterion, iteration limit, and initialization, print, and plot options.

The following six parameters specify the inlet orientation, free-stream Mach number, compressor face Mach number, and specific heat ratio.

PITCH — A real variable denoting the angle, in degrees, subtended by the free-stream velocity vector and the projection of that vector on the (x-z)-plane, as shown in Figure 24. A default value of 1.0 degree is specified for PITCH.

YAW — A real variable denoting the angle, in degrees, subtended by the x-axis and the projection of the free-stream velocity vector on the (x-z)-plane, as shown in Figure 24. A default value of 0.0 degrees is specified for YAW.

XMFS — A real variable denoting the free-stream Mach number. A default value of 0.8 is specified for XMFS.

XMCF — A real variable denoting the effective Mach number at the compressor face. XMCF must be entered only if the inlet capture ratio (CRATIO) is not entered. A default value of 0.3516 is specified for XMCF.

CRATIO — A real variable denoting the inlet capture ratio, which is defined by

$$\text{CRATIO} = \text{AINF}/\text{AHL} \tag{37}$$

where AINF is the cross-sectional area of the capture streamtube far upstream of the inlet, and AHL is the effective hilite area (see Figure 25). If CRATIO≠0.0, then the compressor face Mach number XMCF will be internally computed from the supplied value of CRATIO. If CRATIO = 0.0, then XMCF must be entered directly. A default value of 0.0 is specified for CRATIO.

GAMMA — A real variable denoting the specific heat ratio. A default value of 1.4 is specified for GAMMA.

The next three parameters specify the metric calculation and potential function initialization options.

KORDER — An integer which denotes whether second-order or fourth-order accurate finite-difference formulae are used in obtaining the metric parameters. If KORDER=0, second-order accurate formulae are used. If KORDER = 1, fourth-order accurate formulae are

$$u_\infty = |\overline{V}_\infty| \cos (\text{PITCH}) \cos (\text{YAW})$$

$$v_\infty = |\overline{V}_\infty| \sin (\text{PITCH})$$

$$w_\infty = |\overline{V}_\infty| \cos (\text{PITCH}) \sin (\text{YAW})$$

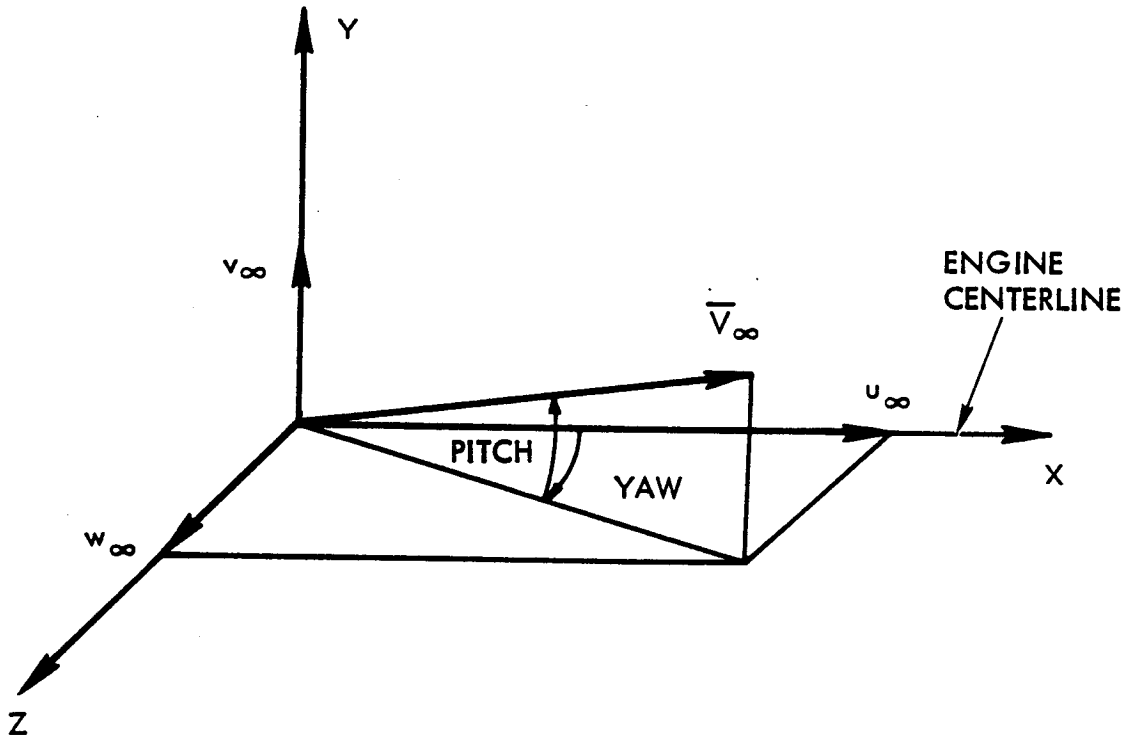

Figure 24. Definition of PITCH and YAW angles.

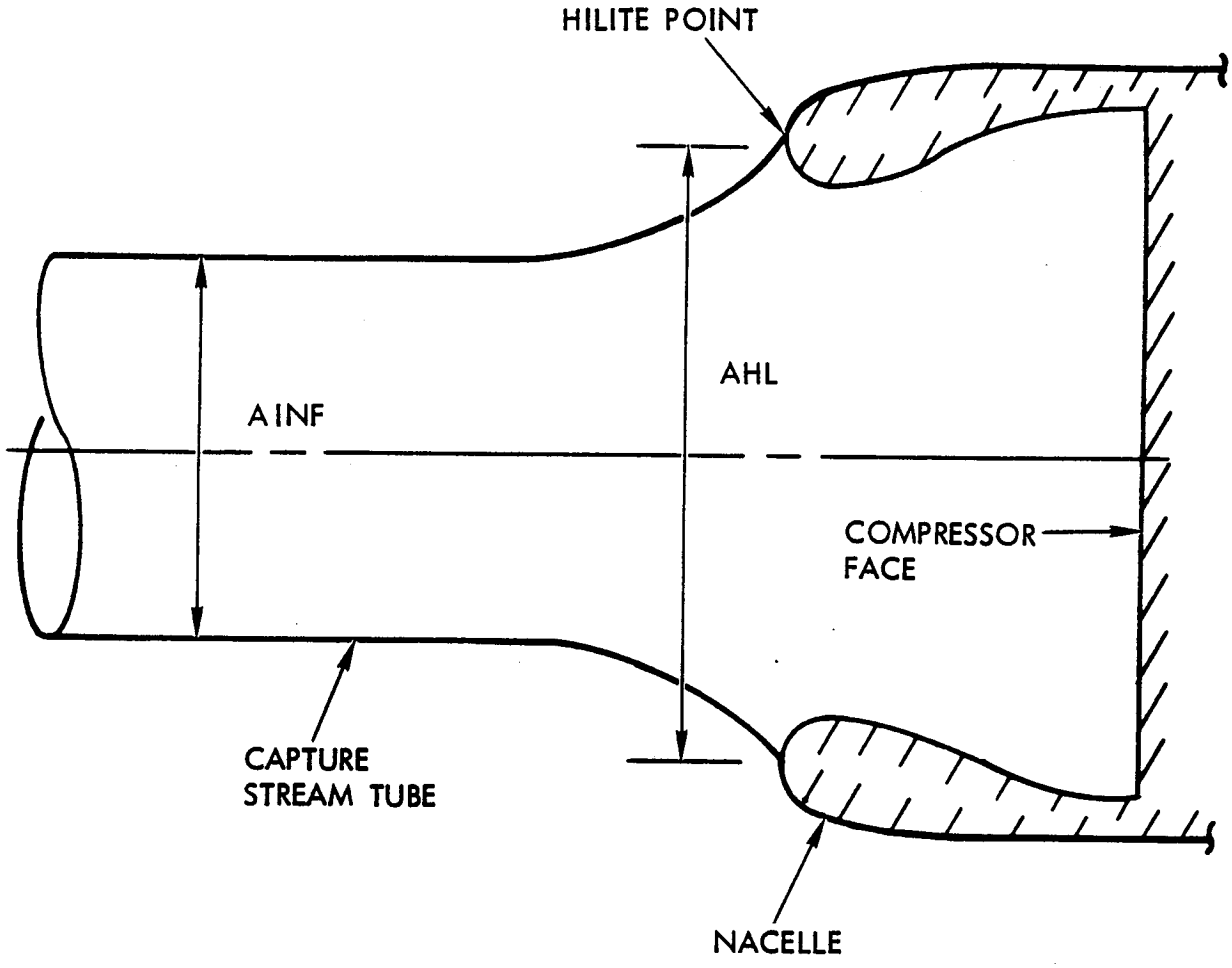

Figure 25. Definition of AINF and AHL areas.

used. The default and recommended value for KORDER is 0.

KINIT — An integer denoting the potential function initialization option. If KINIT = 0, the potential function initialization is performed using free-stream velocity components for each point in the computational mesh. If KINIT = 1, the potential function initialization is performed using free-stream velocity components for the external flow mesh points, and using velocity components calculated from one-dimensional gas dynamic formulae for the internal flow mesh points. The local internal flow Mach number is calculated using the compressor face Mach number and the ratio between the local flow area and the compressor face area. Setting KINIT = 1 generally significantly improves convergence speed. The default and recommended value for KINIT is 1.

XMULM — A positive real variable used as a Mach number multiplier for the internal flow points if the KINIT = 1 initialization option is specified. XMULM must be entered only if KINIT = 1, and generally is in the range of 0.6 to 0.8. The default value for XMULM is 0.7.

The next two parameters specify the convergence criterion and iteration limit.

CRIT — A real variable denoting the convergence criterion used for terminating the calculation. Convergence is attained if the following relation is satisfied

$$|R^{n}_{max}| / |R^{1}_{max}| \leq \text{CRIT} \qquad (38)$$

where R^{1}_{max} is the maximum residual on the first iteration, and R^{n}_{max} is the maximum residual on the nth iteration. A default value of 0.001 is specified for CRIT.

ITMAX — A positive integer denoting the maximum number of iterations permissible. A default value of 200 is specified for ITMAX.

The next three parameters control the program output.

KPRCOR — An integer denoting whether or not the supplied grid point coordinates are to be printed. If KPRCOR=0, the mesh coordinates are not printed. If KPRCOR=1, the coordinate data are printed. A default value of 0 is specified for KPRCOR.

KPRINT — A positive integer denoting the number of iterations between which the surface solution is printed. If KPRINT=1, the surface solution will be printed for each iteration. If KPRINT=50, the solution will be printed every 50 iterations, etc. If KPRINT is equated to a large number (i.e., 1000), then the solution will be printed only if convergence has been attained or if the iteration limit has been reached. A default value of 1000 is specified for KPRINT.

SCALE — A positive real variable used as a multiplier for the surface

coordinates when the solution is printed. This parameter allows the original coordinate units to be recovered if scaling was performed in generating the computational grid. A default value of 8.4 is specified for SCALE.

The next five parameters control the program plot options.

KPLOT An integer denoting whether or not plotting of the surface solution is to be performed. If KPLOT=0, no plotting is performed. If KPLOT=1, plotting will be performed. A default value of 1 is specified for KPLOT.

If KPLOT=1 is entered, the following four parameters must be specified.

KDEV An integer denoting the plot device. If KDEV=1, the plot device is the VERSATEC electrostatic plotter. If KDEV=2, the plot device is the HP ink plotter. A default value of 1 is specified for KDEV. (Note that the plot device specification can be altered by modifying SUBROUTINE RESPLOT.)

KMACH A one-dimensional integer array consisting of JMAX elements, where JMAX is the number of circumferential stations in the computational grid (see NAMELIST LIST2). KMACH(J) (J=1,...,JMAX) specifies whether or not the surface Mach number distribution is to be plotted for the Jth meridional plane. If KMACH(J)=1, the Mach number distribution is plotted for the Jth meridional plane. If KMACH(J)=0, the plotting is not performed. All elements of KMACH have 0 specified as a default value except for KMACH(1), KMACH(4), and KMACH(7) which each have a default value of 1.

XMTOP A positive real variable denoting the maximum Mach number to be used in defining the ordinate axis for the Mach number plotting. XMTOP must be entered only if an element of KMACH is specified as nonzero. A default value of 1.5 is specified for XMTOP.

KCP A one-dimensional integer array consisting of JMAX elements. KCP(J) (J=1,...,JMAX) specifies whether or not the surface pressure coefficient distribution is to be plotted for the Jth meridional plane. If KCP(J)=1, the pressure coefficient distribution is plotted for the Jth meridional plane. If KCP(J)=0, the plotting is not performed. All elements of KCP have 0 specified as a default value except for KCP(1), KCP(4), and KCP(7) which each have a default value of 1.

The following parameter controls storage of the completed solution for use in post-processing or ensuing computations.

ITDUMP An integer denoting whether or not the potential function field is to be loaded onto a disk file at the end of the computation. If ITDUMP=0, the file write is not performed. If ITDUMP=1, the potential function values are loaded onto TAPE 12 (see SUBROUTINE NPRINT for the format of the write statement). A default value of 0 is specified for ITDUMP.

4.2 NAMELIST LIST2

The input parameters entered in NAMELIST LIST2 specify the number of points in the computational mesh and certain index values.

The following three parameters specify the number of mesh points. These parameters have the same definitions as noted in the grid generation algorithm user's manual.

IMAX — A positive integer denoting the number of ξ-wraparound stations in the computational grid. A default value of 67 is specified for IMAX.

JMAX — A positive integer denoting the number of η-circumferential stations in the computational grid. A default value of 13 is specified for JMAX.

KMAX — A positive integer denoting the number of ζ-radial stations in the computational grid. A default value of 13 is specified for KMAX.

The next parameter specifies whether certain index parameters are to be user specified or are to be read from the grid generator supplied disk file.

ITREAD — An integer denoting whether or not certain index parameters (defined later) are to be user specified or are to be read from the grid generator output disk file. If ITREAD=0, the index values must be user supplied. If ITREAD=1, the index values are read from the disk file created by the grid generation algorithm. A default value of 1 is specified for ITREAD.

If ITREAD=1 is specified, then no other input parameters must be entered in this namelist. If ITREAD=0, the following four parameters must be entered (this allows for an alternate grid generation algorithm to be used).

ITRAN1 — A one-dimensional integer array consisting of KMAX elements. ITRAN1(K) (K=1,...,KMAX) specifies the ξ-wraparound station that is closest to the radius of the nacelle hilite for the Kth radial station, as shown in Figure 26. The ITRAN1 array is used in determining the upwind direction for the ξ-wraparound coordinate. No default values are specified for the elements of ITRAN1.

ITRAN2 — A positive integer denoting the ξ-wraparound coordinate station at which the outer computational boundary becomes parallel to the inlet centerline, as shown in Figure 26. The ITRAN2 index is used to switch the boundary point treatment from that of a free-stream boundary to a centerline boundary. No default value is specified for ITRAN2.

ITRAN3 — A positive integer denoting the ξ-wraparound coordinate station at which the potential function under-relaxation (described later) is to be initiated. Generally, ITRAN3 is between ITRAN2

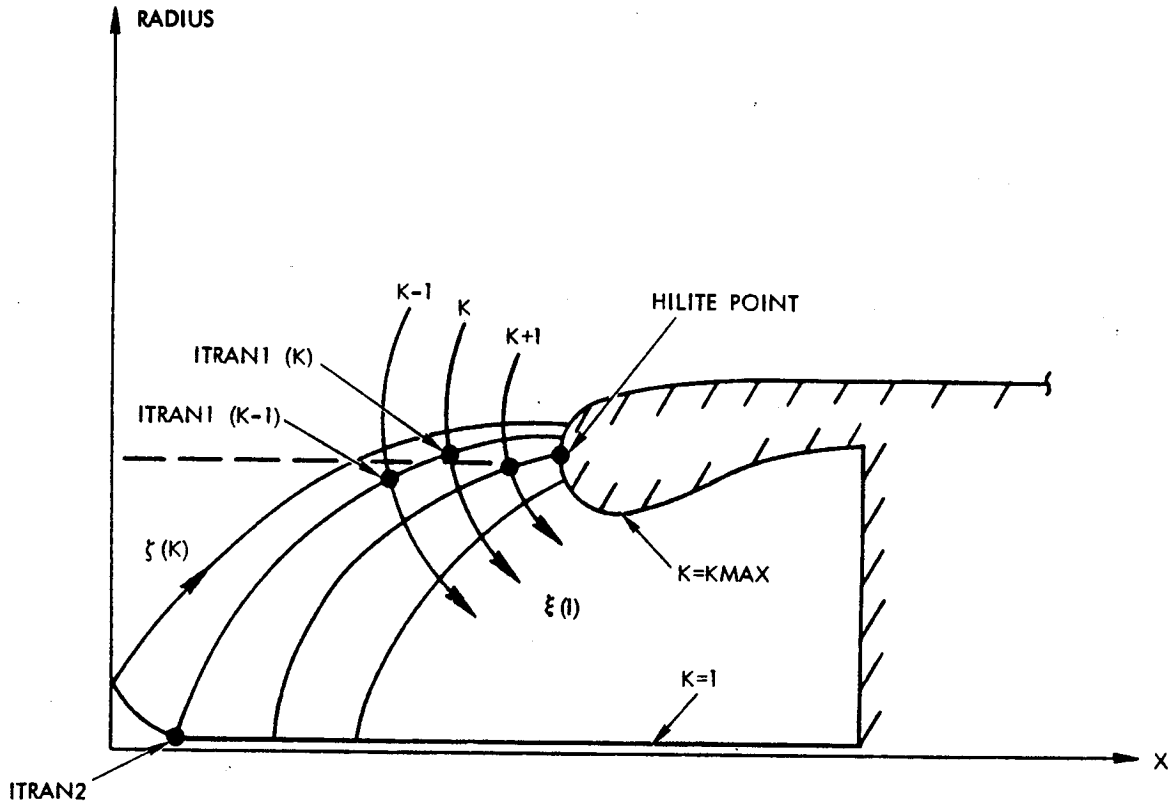

Figure 26. Definition of ITRAN1 and ITRAN2 points.

and IMAX. No default value is specified for ITRAN3.

IBEG — A positive integer denoting the ξ-wraparound coordinate station at which the internal flow potential function initialization is started if the KINIT=1 option is specified. No default value is specified for IBEG.

4.3 NAMELIST LIST3

The input parameters entered in NAMELIST LIST3 specify the acceleration parameters, relaxation factors, artificial viscosity and damping coefficients, under-relaxation parameters, and smoothing functions used in the flow solution algorithm.

The next four parameters specify the acceleration constants used in the AF2 iteration scheme. Two options have been incorporated into the program for calculating the acceleration parameter sequence. The first option employs the sequence

$$\alpha_K = \alpha_H \left(\alpha_L / \alpha_H\right)^{\frac{K-1}{M-1}} \qquad (K=1,2,3,\ldots,M) \tag{39}$$

where α_L is the lower limit for α, α_H is the upper limit for α, K is the sequence element number, and M is the number of elements in the sequence. The second option employs the sequence

$$\alpha_1 = \alpha_H$$

$$\alpha_K = \alpha_{K-1} - \left[\frac{\alpha_H - \alpha_L}{28}\right] (9-K) \quad (K=2,3,\ldots,7,8) \tag{40}$$

in which case M equals 8.

KALPHA — An integer denoting the α-sequence to be used in the computation. If KALPHA=1, the sequence given by equation (39) is used. If KALPHA=2, the sequence given by equation (40) is used. The default and recommended value for KALPHA is 1.

ALPHAL — A positive real variable denoting the α lower limit α_L. A default value of 0.175 is specified for ALPHAL.

ALPHAH — A positive real variable denoting the α upper limit α_H. A default value of 6.0 is specified for ALPHAH.

MD — A positive integer denoting the number of elements M of the sequence in equation (39). MD must be entered as 8 if the KALPHA=2 option is specified. A default value of 8 is specified for MD.

The following parameter specifies the standard relaxation factor used

in the AF2 iteration scheme.

OMEGA A positive real variable denoting the relaxation factor. For stability, OMEGA must be in the range 0.0 < OMEGA < 2.0. The default and recommended value for OMEGA is 1.0.

The next four parameters control the upwinding of the density and the amount of artificial viscosity and dissipation used in stabilizing the computations in regions of supersonic flow. Note that upwinding is always applied in the ξ-wraparound coordinate direction.

NJVIS An integer denoting whether or not upwinding in regions of supersonic flow is to be applied in the η-circumferential coordinate direction. If NJVIS=0, the upwinding is not applied. If NJVIS=1, upwinding of the density is applied in the η-direction. Upwinding in the η-direction is needed only in cases of high cross flow. A default value of 0 is specified for NJVIS.

NKVIS An integer denoting whether or not upwinding in regions of supersonic flow is to be applied in the ζ-radial coordinate direction. If NKVIS=0, the upwinding is not applied. If NKVIS=1, upwinding of the density is applied in the ζ-direction. A default value of 0 is specified for NKVIS.

CFACT A positive real variable denoting the artificial viscosity coefficient used in performing upwinding of the density in regions of supersonic flow. CFACT generally takes the values $1.0 \leq$ CFACT $<$ 2.0, with higher values of CFACT producing greater upwinding. High values of CFACT can decrease shock wave resolution. A default value of 1.2 is specified for CFACT.

BXIE A positive real variable denoting the timelike dissipation coefficient which is used in the AF2 algorithm to produce diagonal dominance in the ξ-difference equations and thereby enhance stability in regions of supersonic flow. Increasing BXIE increases the amount of dissipation. A default value of 0.1 is specified for BXIE.

The next three parameters control the smoothing operations performed in the computations.

KSMTH A positive integer denoting the ζ-radial station index K up to which smoothing is performed for the computed density in the ξ-wraparound coordinate direction in the vicinity of the ITRAN2 ξ-station. The density smoothing generally improves convergence speed. A default value of 4 is specified for KSMTH.

KTIME An integer denoting the number of times a smoothing polynomial is applied in smoothing the density values in the ξ-direction in the vicinity of the ITRAN2 ξ-station for the ζ-stations ranging from 1 to KSMTH. If KTIME=0 is entered, no smoothing is performed. The density smoothing generally improves convergence speed. A

default value of 3 is specified for KTIME.

NDEL — A positive integer denoting the number of ξ-stations to the left and to the right of point ITRAN2 at which the density is smoothed. Smoothing is performed from point (ITRAN2-NDEL) to point (ITRAN2+NDEL) for the ζ-stations ranging from 2 to KSMTH, and from point (ITRAN2+1) to point (ITRAN2+2*NDEL) for the 1st ζ-station. A default value of 3 is specified for NDEL.

The next two parameters specify the potential function under-relaxation factors.

CORFAT — A one-dimensional real variable array consisting of KMAX elements. CORFAT(K) (K=1,...,KMAX) specifies the potential function under-relaxation factor for the Kth ζ-station. This under-relaxation is necessary to maintain stability and enhance convergence for mesh points near the inlet centerline. Under-relaxation of the potential function is performed only for the ξ-stations which are in the range ITRAN3 $\leq$ I $\leq$ IMAX. The elements of CORFAT generally range from a low value at K = 1 to a value of 1.0 (no under-relaxation) as K approaches KMAX. The following default values have been assigned to the elements of CORFAT: CORFAT(K) = 0.2, 0.25, 0.30, 0.35, 0.40, 0.50, 0.60, 0.70, 0.80, 0.90, 1.0, 1.0, and 1.0 for K = 1 to 13, respectively.

ITCOR — A positive integer denoting the iteration number at which the potential function under-relaxation is terminated. For iteration numbers greater than ITCOR, the standard algorithm with no under-relaxation is applied. Generally, fastest convergence is obtained by using under-relaxation for all iterations. The default and recommended value for ITCOR is 10,000.

4.4 NAMELIST LIST4

The input parameters entered in NAMELIST LIST4 specify if debug output is to be printed.

KDUMP — A one-dimensional integer array consisting of nine elements. Each element of KDUMP specifies whether or not a particular subroutine is to have debug output printed. Specifying KDUMP(I)=1 (I=1,...,9) activates the debug output option for the corresponding subroutine. Specifying KDUMP(I) = 0 causes the debug printout to be skipped. The elements of KDUMP activate the debug printout for the following subroutines/computations and have the following default values.

KDUMP(I)	Activates Debug Output for (SUBROUTINE)	Default Value
KDUMP(1)	metric calculations (METRIC)	0
KDUMP(2)	initialization (NINIT)	0
KDUMP(3)	not presently used	0
KDUMP(4)	AF2 solution scheme (NSOLVE)	0

KDUMP(5)	physical density calculation (NRO)	0
KDUMP(6)	residual calculation (NRESID)	0
KDUMP(7)	modified density calculation (NROCO)	0
KDUMP(8)	not presently used	0
KDUMP(9)	amplification factors (METRIC)	0

ITSTRT An integer denoting the iteration number at which debug output is to be initiated. A default value of 1 is specified for ITSTRT.

4.5 PARAMETER STATEMENT SPECIFICATION

The NACELLE flow solution program uses variable array dimensions. The respective array sizes are fixed by specification of the following dimension parameters on the PARAMETER statement:

Parameter		Allowed Values
NX	$\geq$	IMAX
NY	$\geq$	JMAX
NZ	$\geq$	KMAX
NXP	$\geq$	IMAX + 1

The array dimensions will be fixed at the time of compilation.

4.6 FILE USAGE

The following files are used by the NACELLE flow solution code.

File No.	Usage
TAPE 5	input file
TAPE 6	printed output file
TAPE 10	input file for grid coordinate data (from grid generation code)
TAPE 12	potential function field (output)

5. NACELLE PROGRAM OUTPUT INTERPRETATION

The initial portion of the computer printout for the NACELLE flow analysis program consists of the NAMELIST input data. Then the transition point indices ITRAN1, ITRAN2, ITRAN3, and IBEG are printed. After this, a convergence history summary is printed. Finally, the computed surface solution is output. The surface solution is determined at points midway between the original grid points and at the grid end points.

The output parameters are defined below.

I	ξ-wraparound point index
J	η-circumferential point index
X	x-coordinate of surface solution point
Y	y-coordinate of surface solution point
Z	z-coordinate of surface solution point

DX	axial (x) distance between surface solution point and hilite point for a given meridional plane
RHO	density coefficient defined as the local density normalized by stagnation density
MACH	Mach number
CP	pressure coefficient
NSP	number of supersonic points
RMAX	maximum residual
RAVG	average residual
IRMAX	ξ-location of maximum residual
JRMAX	η-location of maximum residual
KRMAX	ζ-location of maximum residual

SECTION V

SAMPLE CASES AND SUGGESTIONS FOR USAGE

1. INTRODUCTION

In this section, a number of sample cases are presented to illustrate application of both the NGRIDA grid generation program and the NACELLE flow analysis program. For each sample case, a discussion of the problem is given, the required input data are presented, and selected portions of the computer output are listed. The input parameter discussions follow the order in which the input parameters are presented in Section IV. At the end of this section, suggestions are provided for use of the respective computer programs.

2. NGRIDA GRID GENERATION PROGRAM SAMPLE CASES

Four sample cases are presented in this section to illustrate application of the NGRIDA grid generation algorithm to determining the computational grid about axisymmetric nacelle/inlet configurations.

2.1 SAMPLE CASE NO. 1

This sample case is concerned with the grid generation for the Lockheed-Georgia GELAC1 axisymmetric nacelle/inlet configuration. This sample case represents the case being considered when all input parameters are retained at their default values.

The data deck for Sample Case No. 1 is illustrated in Figure 27. All parameters in NAMELIST LIST1 are retained at their default values. Consequently, a 67x13x13 (IMAX x JMAX x KMAX) computational mesh will be generated. The outer computational boundary will have an outer radius RADOUT of 50.0, a left-side coordinate XLEFT of -30.0, and an offset distance DELTA of 0.5. The surface grid point distribution will be determined by the stretching factors ALPHA0 and ALPHAI, which are both retained at their default values of 1.1, and by the distribution parameters IOUTER=38 and IINNER=30. The outer boundary grid point distribution is determined by retaining IAA and IDD at 12 and 57, respectively, and since KOUTER=0, an angular distribution will be used in locating the points between points IAA and IDD. Since KRAMP=1, the DS distribution will be adjusted to produce a uniform radial point distribution at the external outflow surface with IRAMP being retained at its default value of 57. All smoothing and plot options retain their default values. Since KDUMP=1 and KPRINT(1)=1, the nacelle and outer boundary grid points are printed along with the finished grid coordinates for the J=1 meridional plane. The meridional plane grid for the J=1 circumferential station will be plotted since KPLOT=1. The finished grid will be scaled by the factor SCALE=0.11904762 which is the reciprocal of the input compressor face radius. Since ITAPE=10, the grid point coordinate data will be loaded onto disk file TAPE 10 for use by the NACELLE flow analysis program.

All input parameters in NAMELIST LIST2 retain their default values. Consequently, the default nacelle/inlet geometry (Lockheed GELAC1 inlet) will be used which has 60 internal surface tabular data points and 100

```
$LIST1 $END
$LIST2 $END
$LIST3 $END
$LIST4 $END
```

Figure 27. Data deck for NGRIDA Sample Case No. 1.

external surface tabular data points. The XIN, RIN, XOUT, and ROUT arrays are specified using the default geometry.

All input parameters in NAMELIST LIST3 and NAMELIST LIST4, which specify the GRAPE algorithm parameters, are retained at their default values.

A plot of the completed grid is illustrated in Figure 28. Selected portions of the computer output for Sample Case No. 1 are presented in Figure 29.

2.2 SAMPLE CASE NO. 2

This sample case is concerned with the generation of a computational grid for the Lockheed-California CALAC4 axisymmetric nacelle.

The data deck for this sample case is illustrated in Figure 30. All input parameters in NAMELIST LIST1 are retained at their default values except for ALPHA0 and ALPHAI which are now set as ALPHA0=1.125 and ALPHAI=1.110. These larger values for the stretching factors enhance mesh resolution near the hilite. The nacelle/inlet geometry is entered in NAMELIST LIST2. For this case, 64 and 83 tabular points are used in defining the internal and external nacelle contours, respectively; hence, NI=64 and NO=83. The surface coordinate data are then entered by the XIN, RIN, XOUT, and ROUT arrays. All input parameters in NAMELIST LIST3 and NAMELIST LIST4 are left at their default values.

Selected portions of the computer output for Sample Case No. 2 are presented in Figure 31.

2.3 SAMPLE CASE NO. 3

This sample case is concerned with the grid generation for the Lockheed-California CALAC5 axisymmetric nacelle.

The data deck for this sample case is illustrated in Figure 32. All parameters in NAMELIST LIST1 retain their default values except for the mesh stretching factors which are again set as ALPHA0=1.125 and ALPHAI=1.110. The surface geometry is again entered in NAMELIST LIST2 with this case using 64 and 79 points in defining the internal and external contours, respectively. All input parameters in NAMELISTS LIST3 and LIST4 retain their default assignments.

Selected portions of the computer output for Sample Case No. 3 are presented in Figure 33.

2.4 SAMPLE CASE NO. 4

This sample case is concerned with generating a computational mesh for the CALAC4 inlet which has better mesh resolution than the grids generated in the previous sample cases.

The data deck for this sample case is illustrated in Figure 34. All input parameters in NAMELIST LIST1 retain their default values except for

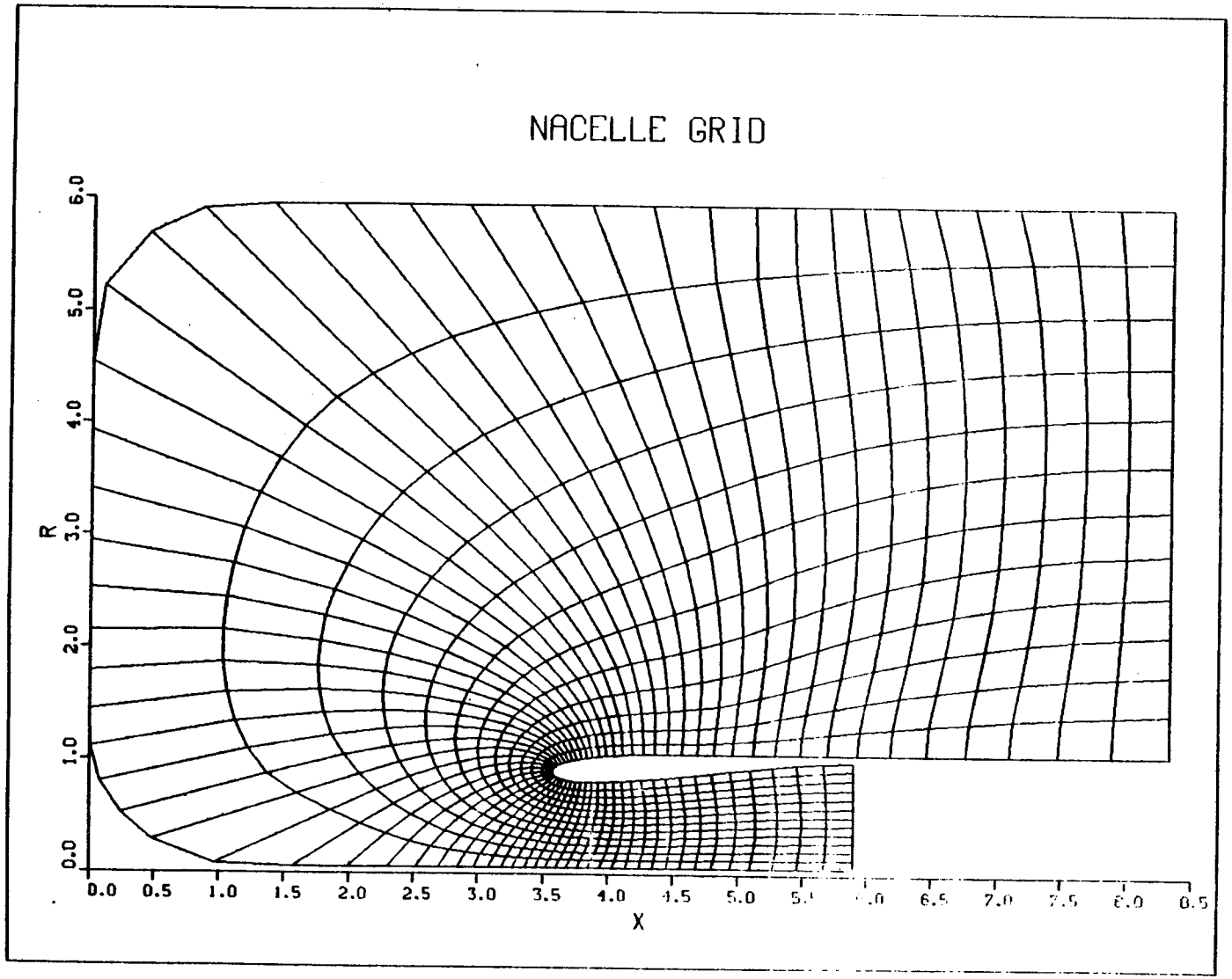

Figure 28. Grid for NGRIDA Sample Case No. 1.

LISTING OF INPUT DATA

```
$LIST1
IMAX    =          67,
JMAX    =          13,
KMAX    =          13,
XLEFT   =  -30.00000    ,
RADOUT  =   50.00000    ,
DELTA   =  0.5000000    ,
IOUTER  =          38,
IINNER  =          30,
ALPHAI  =   1.100000    ,
ALPHAO  =   1.100000    ,
KOUTER  =           0,
ALPHRI  =   1.000000    ,
ALPHRO  =   1.000000    ,
SCALE   =  0.1190476    ,
ITAPE   =          10,
KPLOT   =           1,
KDEV    =           1,
KDUMP   =           1,
IAA     =          12,
IDD     =          57,
KPRINT  =           1, 24*0,
KTIME   =           3,
NDEL    =           5,
DSFACT  =   1.000000    ,
KRAMP   =           1,
IRAMP   =          57
$END
$LIST2
NO      =         100,
XOUT    =  0.0000000E+00,  4.9999999E-03,  9.9999998E-03,  1.5000000E-02,
 2.0000000E-02,  2.5000000E-02,  2.9999999E-02,  3.5000000E-02,  3.9999999E-02,
 4.5000002E-02,  5.0000001E-02,  5.5000000E-02,  5.9999999E-02,  6.4999998E-02,
 7.0000000E-02,  7.9999998E-02,  9.0000004E-02,  0.1000000    ,  0.1100000    ,
```

Figure 29. Output for NGRIDA Sample Case No. 1.

GRID POINT COORDINATES FOR SELECTED MERIDIONAL PLANES

I= 1	J= 1	K= 1	X= 0.833333E+01	Y= 0.595238E+01	Z= 0.000000E+00
I= 2	J= 1	K= 1	X= 0.792466E+01	Y= 0.595238E+01	Z= 0.000000E+00
I= 3	J= 1	K= 1	X= 0.752527E+01	Y= 0.595238E+01	Z= 0.000000E+00
I= 4	J= 1	K= 1	X= 0.715054E+01	Y= 0.595238E+01	Z= 0.000000E+00
I= 5	J= 1	K= 1	X= 0.680709E+01	Y= 0.595238E+01	Z= 0.000000E+00
I= 6	J= 1	K= 1	X= 0.649343E+01	Y= 0.595238E+01	Z= 0.000000E+00
I= 7	J= 1	K= 1	X= 0.620492E+01	Y= 0.595238E+01	Z= 0.000000E+00
I= 8	J= 1	K= 1	X= 0.593510E+01	Y= 0.595238E+01	Z= 0.000000E+00
I= 9	J= 1	K= 1	X= 0.567372E+01	Y= 0.595238E+01	Z= 0.000000E+00
I= 10	J= 1	K= 1	X= 0.540402E+01	Y= 0.595238E+01	Z= 0.000000E+00
I= 11	J= 1	K= 1	X= 0.510106E+01	Y= 0.595238E+01	Z= 0.000000E+00
I= 12	J= 1	K= 1	X= 0.473751E+01	Y= 0.595238E+01	Z= 0.000000E+00
I= 13	J= 1	K= 1	X= 0.430742E+01	Y= 0.595238E+01	Z= 0.000000E+00
I= 14	J= 1	K= 1	X= 0.384002E+01	Y= 0.595238E+01	Z= 0.000000E+00
I= 15	J= 1	K= 1	X= 0.336708E+01	Y= 0.595238E+01	Z= 0.000000E+00
I= 16	J= 1	K= 1	X= 0.289572E+01	Y= 0.595238E+01	Z= 0.000000E+00
I= 17	J= 1	K= 1	X= 0.242287E+01	Y= 0.595238E+01	Z= 0.000000E+00
I= 18	J= 1	K= 1	X= 0.192223E+01	Y= 0.595238E+01	Z= 0.000000E+00
I= 19	J= 1	K= 1	X= 0.139033E+01	Y= 0.595238E+01	Z= 0.000000E+00
I= 20	J= 1	K= 1	X= 0.856567E+00	Y= 0.590459E+01	Z= 0.000000E+00
I= 21	J= 1	K= 1	X= 0.439945E+00	Y= 0.568599E+01	Z= 0.000000E+00
I= 22	J= 1	K= 1	X= 0.888817E-01	Y= 0.521326E+01	Z= 0.000000E+00
I= 23	J= 1	K= 1	X= 0.000000E+00	Y= 0.454335E+01	Z= 0.000000E+00
I= 24	J= 1	K= 1	X= 0.000000E+00	Y= 0.392977E+01	Z= 0.000000E+00
I= 25	J= 1	K= 1	X= 0.000000E+00	Y= 0.340506E+01	Z= 0.000000E+00
I= 26	J= 1	K= 1	X= 0.000000E+00	Y= 0.294392E+01	Z= 0.000000E+00
I= 27	J= 1	K= 1	X= 0.000000E+00	Y= 0.252883E+01	Z= 0.000000E+00
I= 28	J= 1	K= 1	X= 0.000000E+00	Y= 0.214705E+01	Z= 0.000000E+00
I= 29	J= 1	K= 1	X= 0.000000E+00	Y= 0.178888E+01	Z= 0.000000E+00
I= 30	J= 1	K= 1	X= 0.000000E+00	Y= 0.144657E+01	Z= 0.000000E+00

Figure 29. Continued.

```
$LIST1 ALPHAO=1.125, ALPHAI=1.11 $END
$LIST2 NI=64, NO=83,
 XIN(  1)=  0.0000     ,RIN(  1)=  7.6822,
 XIN(  2)=  0.0016     ,RIN(  2)=  7.6498,
 XIN(  3)=  0.0065     ,RIN(  3)=  7.6173,
 XIN(  4)=  0.0147     ,RIN(  4)=  7.5849,
 XIN(  5)=  0.0261     ,RIN(  5)=  7.5525,
 XIN(  6)=  0.0410     ,RIN(  6)=  7.5200,
 XIN(  7)=  0.0593     ,RIN(  7)=  7.4876,
 XIN(  8)=  0.0811     ,RIN(  8)=  7.4551,
 XIN(  9)=  0.1066     ,RIN(  9)=  7.4227,
 XIN( 10)=  0.1359     ,RIN( 10)=  7.3903,
 XIN( 11)=  0.1693     ,RIN( 11)=  7.3578,
 XIN( 12)=  0.2068     ,RIN( 12)=  7.3254,
 XIN( 13)=  0.2488     ,RIN( 13)=  7.2929,
 XIN( 14)=  0.2957     ,RIN( 14)=  7.2605,
 XIN( 15)=  0.3477     ,RIN( 15)=  7.2281,
 XIN( 16)=  0.4055     ,RIN( 16)=  7.1956,
 XIN( 17)=  0.4696     ,RIN( 17)=  7.1632,
 XIN( 18)=  0.5409     ,RIN( 18)=  7.1307,
 XIN( 19)=  0.6205     ,RIN( 19)=  7.0983,
 XIN( 20)=  0.7098     ,RIN( 20)=  7.0659,
```

(Note - Complete listing of data not shown)

```
 XOUT( 82)= 35.0000     ,ROUT( 82)=  9.0000,
 XOUT( 83)=40.0000      ,ROUT( 83)=  9.0000 $END
$LIST3 $END
$LIST4 $END
```

Figure 30. Data deck for NGRIDA Sample Case No. 2.

```
LISTING OF INPUT DATA

$LIST1
IMAX    =          67,
JMAX    =          13,
KMAX    =          13,
XLEFT   =  -30.00000    ,
RADOUT  =   50.00000    ,
DELTA   =  0.5000000    ,
IOUTER  =          38,
IINNER  =          30,
ALPHAI  =   1.110000    ,
ALPHAO  =   1.125000    ,
KOUTER  =           0,
ALPHRI  =   1.000000    ,
ALPHRO  =   1.000000    ,
SCALE   =  0.1190476    ,
ITAPE   =          10,
KPLOT   =           1,
KDEV    =           1,
KDUMP   =           1,
IAA     =          12,
IDD     =          57,
KPRINT  =           1, 24*0,
KTIME   =           3,
NDFL    =           5,
DSFACT  =   1.000000    ,
KRAMP   =           1,
IRAMP   =          57
$END
$LIST2
NO      =          83,
XOUT    =  0.0000000E+00,  1.6000000E-03,  6.3000000E-03,  1.4200000E-02,
 2.5300000E-02,  3.9600000E-02,  5.7100002E-02,  7.7799998E-02,  0.1017000    ,
 0.1290000    ,  0.1596000    ,  0.1935000    ,  0.2308000    ,  0.2716000    ,
 0.3159000    ,  0.3638000    ,  0.4153000    ,  0.4705000    ,  0.5295000    ,
```

Figure 31. Output for NGRIDA Sample Case No. 2.

GRID POINT COORDINATES FOR SELECTED MERIDIONAL PLANES

I= 1	J= 1	K= 1	X= 0.833333E+01	Y= 0.595238E+01	Z= 0.000000E+00
I= 2	J= 1	K= 1	X= 0.785318E+01	Y= 0.595238E+01	Z= 0.000000E+00
I= 3	J= 1	K= 1	X= 0.738629E+01	Y= 0.595238E+01	Z= 0.000000E+00
I= 4	J= 1	K= 1	X= 0.695455E+01	Y= 0.595238E+01	Z= 0.000000E+00
I= 5	J= 1	K= 1	X= 0.656706E+01	Y= 0.595238E+01	Z= 0.000000E+00
I= 6	J= 1	K= 1	X= 0.622129E+01	Y= 0.595238E+01	Z= 0.000000E+00
I= 7	J= 1	K= 1	X= 0.591081E+01	Y= 0.595238E+01	Z= 0.000000E+00
I= 8	J= 1	K= 1	X= 0.562781E+01	Y= 0.595238E+01	Z= 0.000000E+00
I= 9	J= 1	K= 1	X= 0.536122E+01	Y= 0.595238E+01	Z= 0.000000E+00
I= 10	J= 1	K= 1	X= 0.509418E+01	Y= 0.595238E+01	Z= 0.000000E+00
I= 11	J= 1	K= 1	X= 0.480232E+01	Y= 0.595238E+01	Z= 0.000000E+00
I= 12	J= 1	K= 1	X= 0.445877E+01	Y= 0.595238E+01	Z= 0.000000E+00
I= 13	J= 1	K= 1	X= 0.405558E+01	Y= 0.595238E+01	Z= 0.000000E+00
I= 14	J= 1	K= 1	X= 0.361676E+01	Y= 0.595238E+01	Z= 0.000000E+00
I= 15	J= 1	K= 1	X= 0.316990E+01	Y= 0.595238E+01	Z= 0.000000E+00
I= 16	J= 1	K= 1	X= 0.272192E+01	Y= 0.595238E+01	Z= 0.000000E+00
I= 17	J= 1	K= 1	X= 0.227077E+01	Y= 0.595238E+01	Z= 0.000000E+00
I= 18	J= 1	K= 1	X= 0.178964E+01	Y= 0.595238E+01	Z= 0.000000E+00
I= 19	J= 1	K= 1	X= 0.127777E+01	Y= 0.595238E+01	Z= 0.000000E+00
I= 20	J= 1	K= 1	X= 0.781369E+00	Y= 0.587989E+01	Z= 0.000000E+00
I= 21	J= 1	K= 1	X= 0.389639E+00	Y= 0.564275E+01	Z= 0.000000E+00
I= 22	J= 1	K= 1	X= 0.762491E-01	Y= 0.518111E+01	Z= 0.000000E+00
I= 23	J= 1	K= 1	X= 0.000000E+00	Y= 0.455083E+01	Z= 0.000000E+00
I= 24	J= 1	K= 1	X= 0.000000E+00	Y= 0.396637E+01	Z= 0.000000E+00
I= 25	J= 1	K= 1	X= 0.000000E+00	Y= 0.346323E+01	Z= 0.000000E+00
I= 26	J= 1	K= 1	X= 0.000000E+00	Y= 0.301925E+01	Z= 0.000000E+00
I= 27	J= 1	K= 1	X= 0.000000E+00	Y= 0.261881E+01	Z= 0.000000E+00
I= 28	J= 1	K= 1	X= 0.000000E+00	Y= 0.225048E+01	Z= 0.000000E+00
I= 29	J= 1	K= 1	X= 0.000000E+00	Y= 0.190550E+01	Z= 0.000000E+00
I= 30	J= 1	K= 1	X= 0.000000E+00	Y= 0.157687E+01	Z= 0.000000E+00

Figure 31. Continued.

```
$LIST1 ALPHAO=1.125, ALPHAI=1.11 $END
$LIST2 NI=64, NO=79,
 XIN(  1)=  0.0000      ,RIN(  1)=  7.6822,
 XIN(  2)=  0.0016      ,RIN(  2)=  7.6498,
 XIN(  3)=  0.0065      ,RIN(  3)=  7.6173,
 XIN(  4)=  0.0147      ,RIN(  4)=  7.5849,
 XIN(  5)=  0.0261      ,RIN(  5)=  7.5525,
 XIN(  6)=  0.0410      ,RIN(  6)=  7.5200,
 XIN(  7)=  0.0593      ,RIN(  7)=  7.4876,
 XIN(  8)=  0.0811      ,RIN(  8)=  7.4551,
 XIN(  9)=  0.1066      ,RIN(  9)=  7.4227,
 XIN( 10)=  0.1359      ,RIN( 10)=  7.3903,
 XIN( 11)=  0.1693      ,RIN( 11)=  7.3578,
 XIN( 12)=  0.2068      ,RIN( 12)=  7.3254,
 XIN( 13)=  0.2488      ,RIN( 13)=  7.2929,
 XIN( 14)=  0.2957      ,RIN( 14)=  7.2605,
 XIN( 15)=  0.3477      ,RIN( 15)=  7.2281,
 XIN( 16)=  0.4055      ,RIN( 16)=  7.1956,
 XIN( 17)=  0.4696      ,RIN( 17)=  7.1632,
 XIN( 18)=  0.5409      ,RIN( 18)=  7.1307,
 XIN( 19)=  0.6205      ,RIN( 19)=  7.0983,
 XIN( 20)=  0.7098      ,RIN( 20)=  7.0659,
```

(Note - Complete listing of data not shown)

```
 XOUT( 78)= 35.0000      ,ROUT( 78)=  9.0000,
 XOUT( 79)= 40.0000      ,ROUT( 79)=  9.0000 $END
$LIST3 $END
$LIST4 $END
```

Figure 32. Data deck for NGRIDA Sample Case No. 3.

```
LISTING OF INPUT DATA

$LIST1
IMAX    =          67,
JMAX    =          13,
KMAX    =          13,
XLEFT   =  -30.00000    ,
RADOUT  =   50.00000    ,
DELTA   =  0.5000000    ,
IOUTER  =          38,
IINNER  =          30,
ALPHAI  =   1.110000    ,
ALPHAO  =   1.125000    ,
KOUTER  =           0,
ALPHRI  =   1.000000    ,
ALPHRO  =   1.000000    ,
SCALE   =  0.1190476    ,
ITAPE   =          10,
KPLOT   =           1,
KDEV    =           1,
KDUMP   =           1,
IAA     =          12,
IDD     =          57,
KPRINT  =           1, 24*0,
KTIME   =           3,
NDEL    =           5,
DSFACT  =   1.000000    ,
KRAMP   =           1,
IRAMP   =          57
$END
$LIST2
NO      =          79,
XOUT    =  0.0000000E+00,  2.0000001E-03,  7.8999996E-03,  1.7700000E-02,
 3.1500001E-02,  4.9300000E-02,  7.1099997E-02,  9.6900001E-02,  0.1268000    ,
 0.1608000    ,  0.1988000    ,  0.2411000    ,  0.2877000    ,  0.3385000    ,
 0.3937000    ,  0.4533000    ,  0.5175000    ,  0.5863000    ,  0.6599000    ;
```

Figure 33. Output for NGRIDA Sample Case No. 3.

GRID POINT COORDINATES FOR SELECTED MERIDIONAL PLANES

I= 1	J= 1	K= 1	X= 0.833333E+01	Y= 0.595238E+01	Z= 0.000000E+00
I= 2	J= 1	K= 1	X= 0.785363E+01	Y= 0.595238E+01	Z= 0.000000E+00
I= 3	J= 1	K= 1	X= 0.738719E+01	Y= 0.595238E+01	Z= 0.000000E+00
I= 4	J= 1	K= 1	X= 0.695585E+01	Y= 0.595238E+01	Z= 0.000000E+00
I= 5	J= 1	K= 1	X= 0.656873E+01	Y= 0.595238E+01	Z= 0.000000E+00
I= 6	J= 1	K= 1	X= 0.622328E+01	Y= 0.595238E+01	Z= 0.000000E+00
I= 7	J= 1	K= 1	X= 0.591309E+01	Y= 0.595238E+01	Z= 0.000000E+00
I= 8	J= 1	K= 1	X= 0.563034E+01	Y= 0.595238E+01	Z= 0.000000E+00
I= 9	J= 1	K= 1	X= 0.536396E+01	Y= 0.595238E+01	Z= 0.000000E+00
I= 10	J= 1	K= 1	X= 0.509707E+01	Y= 0.595238E+01	Z= 0.000000E+00
I= 11	J= 1	K= 1	X= 0.480529E+01	Y= 0.595238E+01	Z= 0.000000E+00
I= 12	J= 1	K= 1	X= 0.446174E+01	Y= 0.595238E+01	Z= 0.000000E+00
I= 13	J= 1	K= 1	X= 0.405849E+01	Y= 0.595238E+01	Z= 0.000000E+00
I= 14	J= 1	K= 1	X= 0.361958E+01	Y= 0.595238E+01	Z= 0.000000E+00
I= 15	J= 1	K= 1	X= 0.317272E+01	Y= 0.595238E+01	Z= 0.000000E+00
I= 16	J= 1	K= 1	X= 0.272466E+01	Y= 0.595238E+01	Z= 0.000000E+00
I= 17	J= 1	K= 1	X= 0.227350E+01	Y= 0.595238E+01	Z= 0.000000E+00
I= 18	J= 1	K= 1	X= 0.179245E+01	Y= 0.595238E+01	Z= 0.000000E+00
I= 19	J= 1	K= 1	X= 0.128071E+01	Y= 0.595238E+01	Z= 0.000000E+00
I= 20	J= 1	K= 1	X= 0.783893E+00	Y= 0.586080E+01	Z= 0.000000E+00
I= 21	J= 1	K= 1	X= 0.391860E+00	Y= 0.564477E+01	Z= 0.000000E+00
I= 22	J= 1	K= 1	X= 0.774078E-01	Y= 0.518418E+01	Z= 0.000000E+00
I= 23	J= 1	K= 1	X= 0.000000E+00	Y= 0.455397E+01	Z= 0.000000E+00
I= 24	J= 1	K= 1	X= 0.000000E+00	Y= 0.396895E+01	Z= 0.000000E+00
I= 25	J= 1	K= 1	X= 0.000000E+00	Y= 0.346541E+01	Z= 0.000000E+00
I= 26	J= 1	K= 1	X= 0.000000E+00	Y= 0.302113E+01	Z= 0.000000E+00
I= 27	J= 1	K= 1	X= 0.000000E+00	Y= 0.262047E+01	Z= 0.000000E+00
I= 28	J= 1	K= 1	X= 0.000000E+00	Y= 0.225197E+01	Z= 0.000000E+00
I= 29	J= 1	K= 1	X= 0.000000E+00	Y= 0.190685E+01	Z= 0.000000E+00
I= 30	J= 1	K= 1	X= 0.000000E+00	Y= 0.157812E+01	Z= 0.000000E+00

Figure 33. Continued.

```
$LIST1 ALPHAO=1.125, ALPHAI=1.11, JMAX=25, KMAX=16 $END
$LIST2 NI=64, NO=83,
 XIN(  1)=  0.0000      ,RIN(  1)=  7.6822,
 XIN(  2)=  0.0016      ,RIN(  2)=  7.6498,
 XIN(  3)=  0.0065      ,RIN(  3)=  7.6173,
 XIN(  4)=  0.0147      ,RIN(  4)=  7.5849,
 XIN(  5)=  0.0261      ,RIN(  5)=  7.5525,
 XIN(  6)=  0.0410      ,RIN(  6)=  7.5200,
 XIN(  7)=  0.0593      ,RIN(  7)=  7.4876,
 XIN(  8)=  0.0811      ,RIN(  8)=  7.4551,
 XIN(  9)=  0.1066      ,RIN(  9)=  7.4227,
 XIN( 10)=  0.1359      ,RIN( 10)=  7.3903,
 XIN( 11)=  0.1693      ,RIN( 11)=  7.3578,
 XIN( 12)=  0.2068      ,RIN( 12)=  7.3254,
 XIN( 13)=  0.2488      ,RIN( 13)=  7.2929,
 XIN( 14)=  0.2957      ,RIN( 14)=  7.2605,
 XIN( 15)=  0.3477      ,RIN( 15)=  7.2281,
 XIN( 16)=  0.4055      ,RIN( 16)=  7.1956,
 XIN( 17)=  0.4696      ,RIN( 17)=  7.1632,
 XIN( 18)=  0.5409      ,RIN( 18)=  7.1307,
 XIN( 19)=  0.6205      ,RIN( 19)=  7.0983,
 XIN( 20)=  0.7098      ,RIN( 20)=  7.0659,


( Note - Complete listing of data not shown )


 XOUT( 82)= 35.0000      ,ROUT( 82)=  9.0000,
 XOUT( 83)=40.0000       ,ROUT( 83)=  9.0000 $END
$LIST3 $END
$LIST4 $END
```

Figure 34. Data deck for NGRIDA Sample Case No. 4.

ALPHAO, ALPHAI, JMAX, and KMAX. ALPHAO=1.125 and ALPHAI=1.110 are again specified as before. In this case, however, the mesh resolution in the circumferential direction will be enhanced by entering JMAX=25 instead of the default value JMAX=13. Likewise the radial direction mesh resolution will be enhanced by specifying KMAX=16 instead of the default value KMAX=13. The nacelle/inlet geometry data are again entered as before in NAMELIST LIST2. All parameters in NAMELISTS LIST3 and LIST4 are retained at their assigned default values.

Selected portions of the computer output for Sample Case No. 4 are presented in Figure 35.

3. NACELLE FLOW ANALYSIS PROGRAM SAMPLE CASES

Four sample cases are presented in this section to illustrate application of the NACELLE flow solution algorithm to determining the flow field about realistic axisymmetric nacelle/inlet configurations. The computational grid for each sample case is generated using the NGRIDA grid generation code.

3.1 SAMPLE CASE NO. 1

This sample case is concerned with determining the flow field solution for the Lockheed-Georgia GELAC1 axisymmetric nacelle/inlet configuration at angle of attack. This sample case represents the case being considered when all input parameters in both the NACELLE flow solution algorithm and in the NGRIDA grid generation algorithm are retained at their default values. Consequently, the computational mesh for this sample case is generated by executing Sample Case No. 1 for the NGRIDA program.

The data deck for Sample Case No. 1 is illustrated in Figure 36. All input parameters in NAMELIST LIST1 are retained at their default values. Consequently, this case considers the flow computation for an angle of attack PITCH of 1.0 degree, a free-stream Mach number XMFS of 0.8, a compressor face Mach number XMCF of 0.3516, and a specific heat ratio GAMMA of 1.4. The computation will use second-order metrics and an internal flow Mach number initialization based on area ratio, as noted by the default values of KORDER=0 and KINIT=1. The internal flow Mach number multiplier XMULM is left at its default value of 0.7. The solution algorithm will stop when either the residual ratio reaches the value of 0.001 or when the iteration count reaches 200. The grid point coordinates will not be printed since KPRCOR=0, and the surface solution will be printed when either the convergence criterion has been satisfied or when the iteration count reaches ITMAX, since KPRINT=1000. The printed surface coordinates will be up-scaled by the factor 8.4, since SCALE=8.4. This recaptures the original dimensions since scaling was performed in generating the grid. The Mach number and pressure coefficient distributions will be plotted for the J=1, J=4, and J=7 meridional planes, since KPLOT, KMACH, and KCP retain their default values. Since ITDUMP=0, the converged potential function field will not be loaded onto a disk file.

All input parameters in NAMELIST LIST2 retain their default values. Consequently, the program assumes that a 67 x 13 x 13 (IMAX x JMAX x KMAX) computational mesh will be used. Since ITREAD=1, the transition point

LISTING OF INPUT DATA

```
$LIST1
IMAX    =          67,
JMAX    =          25,
KMAX    =          16,
XLEFT   =  -30.00000    ,
RADOUT  =   50.00000    ,
DELTA   =  0.5000000    ,
IOUTFR  =          38,
IINNER  =          30,
ALPHAI  =   1.110000    ,
ALPHAO  =   1.125000    ,
KOUTER  =           0,
ALPHBI  =   1.000000    ,
ALPHBO  =   1.000000    ,
SCALE   =  0.1190476    ,
ITAPE   =          10,
KPLOT   =           1,
KDEV    =           1,
KDUMP   =           1,
IAA     =          12,
IDD     =          57,
KPRINT  =           1, 24*0,
KTIME   =           3,
NDEL    =           5,
DSFACT  =   1.000000    ,
KRAMP   =           1,
IRAMP   =          57
$END
$LIST2
NO      =          83,
XOUT    =  0.0000000E+00,  1.6000000E-03,  6.3000000E-03,  1.4200000E-02,
 2.5300000E-02,  3.9600000E-02,  5.7100002E-02,  7.7799998E-02,  0.1017000    ,
 0.1290000    ,  0.1596000    ,  0.1935000    ,  0.2308000    ,  0.2716000    ,
 0.3159000    ,  0.3638000    ,  0.4153000    ,  0.4705000    ,  0.5295000    ,
```

Figure 35. Output for NGRIDA Sample Case No. 4.

```
I= 36  J=  1  K= 16  X= 0.357618E+01  Y= 0.929976E+00  Z= 0.000000E+00
I= 37  J=  1  K= 16  X= 0.357256E+01  Y= 0.922037E+00  Z= 0.000000E+00
I= 38  J=  1  K= 16  X= 0.357143E+01  Y= 0.914548E+00  Z= 0.000000E+00
I= 39  J=  1  K= 16  X= 0.357279E+01  Y= 0.904527E+00  Z= 0.000000E+00
I= 40  J=  1  K= 16  X= 0.357706E+01  Y= 0.893885E+00  Z= 0.000000E+00
I= 41  J=  1  K= 16  X= 0.358431E+01  Y= 0.883444E+00  Z= 0.000000E+00
I= 42  J=  1  K= 16  X= 0.359437E+01  Y= 0.873508E+00  Z= 0.000000E+00
I= 43  J=  1  K= 16  X= 0.360697E+01  Y= 0.864134E+00  Z= 0.000000E+00
I= 44  J=  1  K= 16  X= 0.362207E+01  Y= 0.855415E+00  Z= 0.000000E+00
I= 45  J=  1  K= 16  X= 0.363965E+01  Y= 0.847324E+00  Z= 0.000000E+00
I= 46  J=  1  K= 16  X= 0.365982E+01  Y= 0.839918E+00  Z= 0.000000E+00
I= 47  J=  1  K= 16  X= 0.368272E+01  Y= 0.833222E+00  Z= 0.000000E+00
I= 48  J=  1  K= 16  X= 0.370857E+01  Y= 0.827498E+00  Z= 0.000000E+00
I= 49  J=  1  K= 16  X= 0.373759E+01  Y= 0.822837E+00  Z= 0.000000E+00
I= 50  J=  1  K= 16  X= 0.377005E+01  Y= 0.819539E+00  Z= 0.000000E+00
I= 51  J=  1  K= 16  X= 0.380623E+01  Y= 0.818074E+00  Z= 0.000000E+00
I= 52  J=  1  K= 16  X= 0.384643E+01  Y= 0.818563E+00  Z= 0.000000E+00
I= 53  J=  1  K= 16  X= 0.389101E+01  Y= 0.820622E+00  Z= 0.000000E+00
I= 54  J=  1  K= 16  X= 0.394041E+01  Y= 0.824257E+00  Z= 0.000000E+00
I= 55  J=  1  K= 16  X= 0.399514E+01  Y= 0.829568E+00  Z= 0.000000E+00
I= 56  J=  1  K= 16  X= 0.405574E+01  Y= 0.836790E+00  Z= 0.000000E+00
I= 57  J=  1  K= 16  X= 0.412286E+01  Y= 0.846024E+00  Z= 0.000000E+00
I= 58  J=  1  K= 16  X= 0.419719E+01  Y= 0.857407E+00  Z= 0.000000E+00
I= 59  J=  1  K= 16  X= 0.427954E+01  Y= 0.871029E+00  Z= 0.000000E+00
I= 60  J=  1  K= 16  X= 0.437084E+01  Y= 0.886809E+00  Z= 0.000000E+00
I= 61  J=  1  K= 16  X= 0.447213E+01  Y= 0.904633E+00  Z= 0.000000E+00
I= 62  J=  1  K= 16  X= 0.458462E+01  Y= 0.924076E+00  Z= 0.000000E+00
I= 63  J=  1  K= 16  X= 0.470969E+01  Y= 0.944478E+00  Z= 0.000000E+00
I= 64  J=  1  K= 16  X= 0.484889E+01  Y= 0.964600E+00  Z= 0.000000E+00
I= 65  J=  1  K= 16  X= 0.500399E+01  Y= 0.982443E+00  Z= 0.000000E+00
I= 66  J=  1  K= 16  X= 0.517676E+01  Y= 0.995676E+00  Z= 0.000000E+00
I= 67  J=  1  K= 16  X= 0.536905E+01  Y= 0.100000E+01  Z= 0.000000E+00
```

Figure 35. Continued.

```
$LIST1 $END
$LIST2 $END
$LIST3 $END
$LIST4 $END
```

Figure 36. Data deck for NACELLE Sample Case No. 1.

indices ITRAN1, ITRAN2, ITRAN3, and IBEG are read from the binary file produced by the grid generation algorithm.

All input parameters in NAMELIST LIST3 retain their default values. Consequently, the α sequence is based on equation (39), α_L=0.175, and α_H=6.0. The relaxation factor OMEGA will be 1.0, and, since NJVIS=NKVIS=0, upwinding will only be performed in the wraparound coordinate direction. CFACT and BXIE are left at their default values of 1.2 and 0.1, respectively. The smoothing function parameters KSMTH, KTIME, and NDEL are retained at their default values of 4, 3, and 3, respectively. The elements of the under-relaxation factor array CORFAT are maintained at their monotonically increasing default values, starting at 0.2 and ending at 1.0.

No debug output is to be printed, hence all input parameters in NAMELIST LIST4 maintain their default values.

Selected portions of the computer output for Sample Case No. 1 are presented in Figure 37. Results for the GELAC1 nacelle are presented in Section II.

3.2 SAMPLE CASE NO. 2

This sample case is concerned with determining the flow field solution for the Lockheed-California CALAC4 axisymmetric nacelle/inlet configuration at incidence. The computational mesh for this case is generated by executing Sample Case No. 2 for the NGRIDA program.

The data deck for this sample case is illustrated in Figure 38. All input parameters in NAMELISTS LIST2 and LIST4 retain their default values. In this case the angle of attack is 2.0 degrees, hence PITCH=2.0 is specified in NAMELIST LIST1. The remaining parameters in NAMELIST LIST1 are left at their default values. All parameters in NAMELIST LIST3 retain their default values except for CFACT, which has now been slightly increased to 1.3.

Selected portions of the computer output for Sample Case No. 2 are presented in Figure 39. Results for the CALAC4 nacelle are presented in Section II.

3.3 SAMPLE CASE NO. 3

This sample case is concerned with the flow field computation for the Lockheed-California CALAC5 axisymmetric nacelle geometry. This solution is for zero incidence, hence the flow field will be axisymmetric. The grid for this case is determined by executing Sample Case No. 3 for the NGRIDA program.

The data deck for this sample case is illustrated in Figure 40. All input parameters retain their default values except for PITCH in NAMELIST LIST1. PITCH is now equated to 0.0.

Selected portions of the computer output for Sample Case No. 3 are presented in Figure 41.

LISTING OF INPUT DATA

```
 $LIST1
 PITCH   =   1.000000     ,
 YAW     =  0.0000000E+00,
 XMFS    =  0.8000000     ,
 XMCF    =  0.3516000     ,
 CRATIO  =  0.0000000E+00,
 GAMMA   =   1.400000     ,
 KPLOT   =             1,
 ITDUMP  =             0,
 KORDER  =             0,
 KINIT   =             1,
 KPRCOR  =             0,
 KPRINT  =          1000,
 ITMAX   =           200,
 CRIT    =  1.0000000E-03,
 KDEV    =             1,
 KMACH   =             1, 2*0,          1, 2*0,          1, 18*0,
 KCP     =             1, 2*0,          1, 2*0,          1, 18*0,
 XMTOP   =   1.500000     ,
 XMULT   =  0.7000000     ,
 SCALE   =   8.400000
 $END
 $LIST2
 IMAX    =            97,
 JMAX    =            13,
 KMAX    =            13,
 ITREAD  =             1,
 ITRAN1  =  16*0,
 ITRAN2  =             0,
 ITRAN3  =             0,
 IBFG    =             0
 $END
 $LIST3
 KALPHA  =             1,
 ALPHAL  =  0.1750000     ,
 ALPHAH  =   6.000000
```

Figure 37. Output for NACELLE Sample Case No. 1.

SURFACE SOLUTION FOR ITERATION NO.= 158

I= 0	J= 1	X= 70.0000	DX= 40.0000	Y= 9.0000	Z= 0.0000	RHO= 0.7400	MACH= 0.8000	CP= 0.0000
I= 1	J= 1	X= 68.1102	DX= 38.1102	Y= 9.0000	Z= 0.0000	RHO= 0.7419	MACH= 0.7964	CP= 0.0079
I= 2	J= 1	X= 64.5023	DX= 34.5023	Y= 9.0000	Z= 0.0000	RHO= 0.7439	MACH= 0.7926	CP= 0.0163
I= 3	J= 1	X= 61.2225	DX= 31.2225	Y= 9.0000	Z= 0.0000	RHO= 0.7416	MACH= 0.7969	CP= 0.0068
I= 4	J= 1	X= 58.2408	DX= 28.2408	Y= 9.0000	Z= 0.0000	RHO= 0.7393	MACH= 0.8014	CP= -0.0030
I= 5	J= 1	X= 55.5302	DX= 25.5302	Y= 9.0000	Z= 0.0000	RHO= 0.7375	MACH= 0.8048	CP= -0.0106
I= 6	J= 1	X= 53.0660	DX= 23.0660	Y= 9.0000	Z= 0.0000	RHO= 0.7358	MACH= 0.8079	CP= -0.0176
I= 7	J= 1	X= 50.8258	DX= 20.8258	Y= 9.0000	Z= 0.0000	RHO= 0.7336	MACH= 0.8122	CP= -0.0270
I= 8	J= 1	X= 48.7892	DX= 18.7892	Y= 9.0000	Z= 0.0000	RHO= 0.7311	MACH= 0.8169	CP= -0.0375
I= 9	J= 1	X= 46.9379	DX= 16.9379	Y= 9.0000	Z= 0.0000	RHO= 0.7282	MACH= 0.8223	CP= -0.0494
I= 10	J= 1	X= 45.2548	DX= 15.2548	Y= 9.0000	Z= 0.0000	RHO= 0.7252	MACH= 0.8282	CP= -0.0624
I= 11	J= 1	X= 43.7247	DX= 13.7247	Y= 9.0000	Z= 0.0000	RHO= 0.7221	MACH= 0.8340	CP= -0.0754
I= 12	J= 1	X= 42.3337	DX= 12.3337	Y= 9.0000	Z= 0.0000	RHO= 0.7192	MACH= 0.8395	CP= -0.0874
I= 13	J= 1	X= 41.0692	DX= 11.0692	Y= 9.0000	Z= 0.0000	RHO= 0.7164	MACH= 0.8448	CP= -0.0991
I= 14	J= 1	X= 39.9196	DX= 9.9196	Y= 9.0000	Z= 0.0000	RHO= 0.7130	MACH= 0.8511	CP= -0.1130
I= 15	J= 1	X= 38.8746	DX= 8.8746	Y= 9.0000	Z= 0.0000	RHO= 0.7081	MACH= 0.8603	CP= -0.1334
I= 16	J= 1	X= 37.9245	DX= 7.9245	Y= 8.9995	Z= 0.0000	RHO= 0.6999	MACH= 0.8758	CP= -0.1674
I= 17	J= 1	X= 37.0608	DX= 7.0608	Y= 8.9960	Z= 0.0000	RHO= 0.6877	MACH= 0.8988	CP= -0.2178
I= 18	J= 1	X= 36.2758	DX= 6.2758	Y= 8.9854	Z= 0.0000	RHO= 0.6745	MACH= 0.9235	CP= -0.2715
I= 19	J= 1	X= 35.5623	DX= 5.5623	Y= 8.9657	Z= 0.0000	RHO= 0.6634	MACH= 0.9444	CP= -0.3166
I= 20	J= 1	X= 34.9140	DX= 4.9140	Y= 8.9375	Z= 0.0000	RHO= 0.6558	MACH= 0.9587	CP= -0.3472
I= 21	J= 1	X= 34.3252	DX= 4.3252	Y= 8.9017	Z= 0.0000	RHO= 0.6614	MACH= 0.9483	CP= -0.3248
I= 22	J= 1	X= 33.7906	DX= 3.7906	Y= 8.8595	Z= 0.0000	RHO= 0.6674	MACH= 0.9370	CP= -0.3005
I= 23	J= 1	X= 33.3054	DX= 3.3054	Y= 8.8124	Z= 0.0000	RHO= 0.5620	MACH= 1.1385	CP= -0.7135
I= 24	J= 1	X= 32.8652	DX= 2.8652	Y= 8.7610	Z= 0.0000	RHO= 0.5312	MACH= 1.1998	CP= -0.8287
I= 25	J= 1	X= 32.4661	DX= 2.4661	Y= 8.7063	Z= 0.0000	RHO= 0.5117	MACH= 1.2397	CP= -0.9005
I= 26	J= 1	X= 32.1043	DX= 2.1043	Y= 8.6489	Z= 0.0000	RHO= 0.4975	MACH= 1.2690	CP= -0.9515
I= 27	J= 1	X= 31.7768	DX= 1.7768	Y= 8.5891	Z= 0.0000	RHO= 0.4876	MACH= 1.2900	CP= -0.9873
I= 28	J= 1	X= 31.4806	DX= 1.4806	Y= 8.5268	Z= 0.0000	RHO= 0.4820	MACH= 1.3020	CP= -1.0075
I= 29	J= 1	X= 31.2132	DX= 1.2132	Y= 8.4619	Z= 0.0000	RHO= 0.4814	MACH= 1.3033	CP= -1.0096
I= 30	J= 1	X= 30.9725	DX= 0.9725	Y= 8.3940	Z= 0.0000	RHO= 0.4872	MACH= 1.2910	CP= -0.9890
I= 31	J= 1	X= 30.7567	DX= 0.7567	Y= 8.3226	Z= 0.0000	RHO= 0.5008	MACH= 1.2622	CP= -0.9398
I= 32	J= 1	X= 30.5646	DX= 0.5646	Y= 8.2464	Z= 0.0000	RHO= 0.5229	MACH= 1.2167	CP= -0.8594
I= 33	J= 1	X= 30.3960	DX= 0.3960	Y= 8.1640	Z= 0.0000	RHO= 0.5563	MACH= 1.1497	CP= -0.7351
I= 34	J= 1	X= 30.2516	DX= 0.2516	Y= 8.0734	Z= 0.0000	RHO= 0.6158	MACH= 1.0344	CP= -0.5062
I= 35	J= 1	X= 30.1348	DX= 0.1348	Y= 7.9724	Z= 0.0000	RHO= 0.7629	MACH= 0.7560	CP= 0.0975
I= 36	J= 1	X= 30.0520	DX= 0.0520	Y= 7.8600	Z= 0.0000	RHO= 0.8600	MACH= 0.5576	CP= 0.5227
I= 37	J= 1	X= 30.0101	DX= 0.0101	Y= 7.7416	Z= 0.0000	RHO= 0.9308	MACH= 0.3814	CP= 0.8455
I= 38	J= 1	X= 30.0133	DX= 0.0133	Y= 7.6173	Z= 0.0000	RHO= 0.9787	MACH= 0.2681	CP= 1.0693
I= 39	J= 1	X= 30.0646	DX= 0.0646	Y= 7.4899	Z= 0.0000	RHO= 0.9995	MACH= 0.0302	CP= 1.1682
I= 40	J= 1	X= 30.1610	DX= 0.1610	Y= 7.3715	Z= 0.0000	RHO= 0.9900	MACH= 0.1419	CP= 1.1228
I= 41	J= 1	X= 30.2936	DX= 0.2936	Y= 7.2664	Z= 0.0000	RHO= 0.9587	MACH= 0.2917	CP= 0.9753
I= 42	J= 1	X= 30.4557	DX= 0.4557	Y= 7.1742	Z= 0.0000	RHO= 0.9199	MACH= 0.4120	CP= 0.7952
I= 43	J= 1	X= 30.6446	DX= 0.6446	Y= 7.0934	Z= 0.0000	RHO= 0.8830	MACH= 0.5091	CP= 0.6264
I= 44	J= 1	X= 30.8594	DX= 0.8594	Y= 7.0230	Z= 0.0000	RHO= 0.8509	MACH= 0.5776	CP= 0.4820
I= 45	J= 1	X= 31.1011	DX= 1.1011	Y= 6.9618	Z= 0.0000	RHO= 0.8248	MACH= 0.6328	CP= 0.3662

Figure 37. Continued.

```
$LIST1 PITCH=2.0 $END
$LIST2 $END
$LIST3 CFACT=1.3 $END
$LIST4 $END
```

Figure 38. Data deck for NACELLE Sample Case No. 2.

LISTING OF INPUT DATA

```
$LIST1
PITCH   =   2.000000    ,
YAW     =  0.0000000E+00,
XMFS    =  0.8000000    ,
XMCF    =  0.3516000    ,
CHATIO  =  0.0000000E+00,
GAMMA   =   1.400000    ,
KPLOT   =             1,
ITDUMP  =             0,
KORDER  =             0,
KINIT   =             1,
KPRCOR  =             0,
KPRINT  =          1000,
ITMAX   =           200,
CRIT    =  1.0000000E-03,
KDEV    =             1,
KMACH   =             1, 2*0,          1, 2*0,          1, 18*0,
KCP     =             1, 2*0,          1, 2*0,          1, 18*0,
XMTOP   =   1.500000    ,
XMULM   =  0.7000000    ,
SCALE   =   8.400000
$END
$LIST2
IMAX    =            67,
JMAX    =            13,
KMAX    =            13,
ITREAD  =             1,
ITRAN1  = 16*0,
ITRAN2  =             0,
ITRAN3  =             0,
IBEG    =             0
$END
$LIST3
KALPHA  =             1,
ALPHAL  =  0.1750000    ,
ALPHAH  =   6.000000
```

Figure 39. Output for NACELLE Sample Case No. 2.

SURFACE SOLUTION FOR ITERATION NO.= 166

I=	0	J=	1	X=	70.0000	DX=	40.0000	Y=	9.0000	Z=	0.0000	RHO=	0.7400	MACH=	0.8000	CP=	0.0000
I=	1	J=	1	X=	67.7331	DX=	37.7331	Y=	9.0000	Z=	0.0000	RHO=	0.7432	MACH=	0.7939	CP=	0.0136
I=	2	J=	1	X=	63.4511	DX=	33.4511	Y=	9.0000	Z=	0.0000	RHO=	0.7451	MACH=	0.7903	CP=	0.0216
I=	3	J=	1	X=	59.6449	DX=	29.6449	Y=	9.0000	Z=	0.0000	RHO=	0.7423	MACH=	0.7956	CP=	0.0098
I=	4	J=	1	X=	56.2616	DX=	26.2616	Y=	9.0000	Z=	0.0000	RHO=	0.7395	MACH=	0.8009	CP=	-0.0020
I=	5	J=	1	X=	53.2542	DX=	23.2542	Y=	9.0000	Z=	0.0000	RHO=	0.7370	MACH=	0.8057	CP=	-0.0127
I=	6	J=	1	X=	50.5810	DX=	20.5810	Y=	9.0000	Z=	0.0000	RHO=	0.7345	MACH=	0.8102	CP=	-0.0227
I=	7	J=	1	X=	48.2048	DX=	18.2048	Y=	9.0000	Z=	0.0000	RHO=	0.7315	MACH=	0.8162	CP=	-0.0360
I=	8	J=	1	X=	46.0926	DX=	16.0926	Y=	9.0000	Z=	0.0000	RHO=	0.7279	MACH=	0.8230	CP=	-0.0511
I=	9	J=	1	X=	44.2151	DX=	14.2151	Y=	9.0000	Z=	0.0000	RHO=	0.7236	MACH=	0.8312	CP=	-0.0691
I=	10	J=	1	X=	42.5463	DX=	12.5463	Y=	9.0000	Z=	0.0000	RHO=	0.7184	MACH=	0.8409	CP=	-0.0905
I=	11	J=	1	X=	41.0628	DX=	11.0628	Y=	9.0000	Z=	0.0000	RHO=	0.7125	MACH=	0.8522	CP=	-0.1154
I=	12	J=	1	X=	39.7442	DX=	9.7442	Y=	9.0000	Z=	0.0000	RHO=	0.7053	MACH=	0.8657	CP=	-0.1451
I=	13	J=	1	X=	38.5721	DX=	8.5721	Y=	9.0000	Z=	0.0000	RHO=	0.6951	MACH=	0.8848	CP=	-0.1872
I=	14	J=	1	X=	37.5302	DX=	7.5302	Y=	8.9960	Z=	0.0000	RHO=	0.6773	MACH=	0.9183	CP=	-0.2601
I=	15	J=	1	X=	36.6043	DX=	6.6043	Y=	8.9842	Z=	0.0000	RHO=	0.6582	MACH=	0.9542	CP=	-0.3375
I=	16	J=	1	X=	35.7817	DX=	5.7817	Y=	8.9536	Z=	0.0000	RHO=	0.6472	MACH=	0.9750	CP=	-0.3818
I=	17	J=	1	X=	35.0513	DX=	5.0513	Y=	8.9113	Z=	0.0000	RHO=	0.6378	MACH=	0.9926	CP=	-0.4192
I=	18	J=	1	X=	34.4029	DX=	4.4029	Y=	8.8606	Z=	0.0000	RHO=	0.6283	MACH=	1.0106	CP=	-0.4568
I=	19	J=	1	X=	33.8275	DX=	3.8275	Y=	8.8036	Z=	0.0000	RHO=	0.6261	MACH=	1.0149	CP=	-0.4658
I=	20	J=	1	X=	33.3173	DX=	3.3173	Y=	8.7427	Z=	0.0000	RHO=	0.6311	MACH=	1.0054	CP=	-0.4459
I=	21	J=	1	X=	32.8648	DX=	2.8648	Y=	8.6798	Z=	0.0000	RHO=	0.6051	MACH=	1.0549	CP=	-0.5482
I=	22	J=	1	X=	32.4639	DX=	2.4639	Y=	8.6159	Z=	0.0000	RHO=	0.5735	MACH=	1.1159	CP=	-0.6699
I=	23	J=	1	X=	32.1087	DX=	2.1087	Y=	8.5518	Z=	0.0000	RHO=	0.5530	MACH=	1.1563	CP=	-0.7475
I=	24	J=	1	X=	31.7942	DX=	1.7942	Y=	8.4862	Z=	0.0000	RHO=	0.5377	MACH=	1.1868	CP=	-0.8047
I=	25	J=	1	X=	31.5161	DX=	1.5161	Y=	8.4254	Z=	0.0000	RHO=	0.5251	MACH=	1.2123	CP=	-0.8515
I=	26	J=	1	X=	31.2702	DX=	1.2702	Y=	8.3658	Z=	0.0000	RHO=	0.5142	MACH=	1.2346	CP=	-0.8914
I=	27	J=	1	X=	31.0532	DX=	1.0532	Y=	8.3033	Z=	0.0000	RHO=	0.5053	MACH=	1.2529	CP=	-0.9236
I=	29	J=	1	X=	30.8619	DX=	0.8619	Y=	8.2439	Z=	0.0000	RHO=	0.4989	MACH=	1.2662	CP=	-0.9467
I=	29	J=	1	X=	30.6938	DX=	0.6938	Y=	8.1855	Z=	0.0000	RHO=	0.4952	MACH=	1.2740	CP=	-0.9601
I=	30	J=	1	X=	30.5463	DX=	0.5463	Y=	8.1261	Z=	0.0000	RHO=	0.4942	MACH=	1.2762	CP=	-0.9638
I=	31	J=	1	X=	30.4175	DX=	0.4175	Y=	8.0717	Z=	0.0000	RHO=	0.4959	MACH=	1.2726	CP=	-0.9577
I=	32	J=	1	X=	30.3054	DX=	0.3054	Y=	8.0164	Z=	0.0000	RHO=	0.5023	MACH=	1.2591	CP=	-0.9344
I=	33	J=	1	X=	30.2089	DX=	0.2089	Y=	7.9616	Z=	0.0000	RHO=	0.5162	MACH=	1.2304	CP=	-0.8839
I=	34	J=	1	X=	30.1286	DX=	0.1286	Y=	7.9046	Z=	0.0000	RHO=	0.7305	MACH=	0.8181	CP=	-0.0402
I=	35	J=	1	X=	30.0663	DX=	0.0663	Y=	7.8435	Z=	0.0000	RHO=	0.8027	MACH=	0.6778	CP=	0.2692
I=	36	J=	1	X=	30.0247	DX=	0.0247	Y=	7.7785	Z=	0.0000	RHO=	0.8654	MACH=	0.5456	CP=	0.5470
I=	37	J=	1	X=	30.0048	DX=	0.0048	Y=	7.7137	Z=	0.0000	RHO=	0.9065	MACH=	0.4424	CP=	0.7426
I=	38	J=	1	X=	30.0057	DX=	0.0057	Y=	7.6401	Z=	0.0000	RHO=	0.9475	MACH=	0.3303	CP=	0.9228
I=	39	J=	1	X=	30.0294	DX=	0.0294	Y=	7.5533	Z=	0.0000	RHO=	0.9803	MACH=	0.1996	CP=	1.0772
I=	40	J=	1	X=	30.0778	DX=	0.0778	Y=	7.4648	Z=	0.0000	RHO=	0.9961	MACH=	0.0621	CP=	1.1612
I=	41	J=	1	X=	30.1505	DX=	0.1505	Y=	7.3792	Z=	0.0000	RHO=	0.9974	MACH=	0.0721	CP=	1.1581
I=	42	J=	1	X=	30.2456	DX=	0.2456	Y=	7.2961	Z=	0.0000	RHO=	0.9811	MACH=	0.1959	CP=	1.0806
I=	43	J=	1	X=	30.3620	DX=	0.3620	Y=	7.2221	Z=	0.0000	RHO=	0.9550	MACH=	0.3048	CP=	0.9581
I=	44	J=	1	X=	30.4992	DX=	0.4992	Y=	7.1515	Z=	0.0000	RHO=	0.9251	MACH=	0.3976	CP=	0.8192
I=	45	J=	1	X=	30.6578	DX=	0.6578	Y=	7.0864	Z=	0.0000	RHO=	0.8954	MACH=	0.4753	CP=	0.6828

Figure 39. Continued.

```
$LIST1 PITCH=0.0 $END
$LIST2 $END
$LIST3 $END
$LIST4 $END
```

Figure 40. Data deck for NACELLE Sample Case No. 3.

LISTING OF INPUT DATA

```
$LIST1
PITCH   =  0.0000000E+00,
YAW     =  0.0000000E+00,
XMFS    =  0.8000000    ,
XMCF    =  0.3516000    ,
CRATIO  =  0.0000000E+00,
GAMMA   =   1.400000    ,
KPLOT   =             1,
ITDUMP  =             0,
KORDER  =             0,
KINIT   =             1,
KPRCOR  =             0,
KPRINT  =          1000,
ITMAX   =           200,
CRIT    =  1.0000000E-03,
KDEV    =             1,
KMACH   =             1, 2*0,          1, 2*0,          1, 18*0,
KCP     =             1, 2*0,          1, 2*0,          1, 18*0,
XMTOP   =   1.500000    ,
XMULM   =  0.7000000    ,
SCALE   =   8.400000
$END
$LIST2
IMAX    =            67,
JMAX    =            13,
KMAX    =            13,
ITREAD  =             1,
ITRAN1  = 16*0,
ITRAN2  =             0,
ITRAN3  =             0,
IBEG    =             0
$END
$LIST3
KALPHA  =             1,
ALPHAL  =  0.1750000    ,
ALPHAH  =   6.000000
```

Figure 41. Output for NACELLE Sample Case No. 3.

SURFACE SOLUTION FOR ITERATION NO.= 165

I=	0	J=	1	X=	70.0000	DX=	40.0000	Y=	9.0000	Z=	0.0000	RHO=	0.7400	MACH=	0.8000	CP=	0.0000
I=	1	J=	1	X=	67.7352	DX=	37.7352	Y=	9.0000	Z=	0.0000	RHO=	0.7424	MACH=	0.7954	CP=	0.0102
I=	2	J=	1	X=	63.4573	DX=	33.4573	Y=	9.0000	Z=	0.0000	RHO=	0.7444	MACH=	0.7916	CP=	0.0185
I=	3	J=	1	X=	59.6547	DX=	29.6547	Y=	9.0000	Z=	0.0000	RHO=	0.7415	MACH=	0.7971	CP=	0.0064
I=	4	J=	1	X=	56.2746	DX=	26.2746	Y=	9.0000	Z=	0.0000	RHO=	0.7367	MACH=	0.8075	CP=	-0.0056
I=	5	J=	1	X=	53.2701	DX=	23.2701	Y=	9.0000	Z=	0.0000	RHO=	0.7362	MACH=	0.8073	CP=	-0.0161
I=	6	J=	1	X=	50.5994	DX=	20.5994	Y=	9.0000	Z=	0.0000	RHO=	0.7337	MACH=	0.8119	CP=	-0.0264
I=	7	J=	1	X=	48.2255	DX=	18.2255	Y=	9.0000	Z=	0.0000	RHO=	0.7305	MACH=	0.8180	CP=	-0.0400
I=	8	J=	1	X=	46.1153	DX=	16.1153	Y=	9.0000	Z=	0.0000	RHO=	0.7267	MACH=	0.8252	CP=	-0.0558
I=	9	J=	1	X=	44.2396	DX=	14.2396	Y=	9.0000	Z=	0.0000	RHO=	0.7221	MACH=	0.8340	CP=	-0.0752
I=	10	J=	1	X=	42.5723	DX=	12.5723	Y=	9.0000	Z=	0.0000	RHO=	0.7163	MACH=	0.8450	CP=	-0.0995
I=	11	J=	1	X=	41.0903	DX=	11.0903	Y=	9.0000	Z=	0.0000	RHO=	0.7086	MACH=	0.8595	CP=	-0.1315
I=	12	J=	1	X=	39.7729	DX=	9.7729	Y=	8.9996	Z=	0.0000	RHO=	0.6963	MACH=	0.8827	CP=	-0.1825
I=	13	J=	1	X=	38.6020	DX=	8.6020	Y=	8.9968	Z=	0.0000	RHO=	0.6822	MACH=	0.9090	CP=	-0.2400
I=	14	J=	1	X=	37.5614	DX=	7.5614	Y=	8.9664	Z=	0.0000	RHO=	0.6735	MACH=	0.9254	CP=	-0.2756
I=	15	J=	1	X=	36.6370	DX=	6.6370	Y=	8.9291	Z=	0.0000	RHO=	0.6684	MACH=	0.9350	CP=	-0.2962
I=	16	J=	1	X=	35.8159	DX=	5.8159	Y=	8.8829	Z=	0.0000	RHO=	0.6640	MACH=	0.9434	CP=	-0.3143
I=	17	J=	1	X=	35.0868	DX=	5.0868	Y=	8.8303	Z=	0.0000	RHO=	0.6597	MACH=	0.9513	CP=	-0.3314
I=	18	J=	1	X=	34.4395	DX=	4.4395	Y=	8.7733	Z=	0.0000	RHO=	0.6553	MACH=	0.9597	CP=	-0.3492
I=	19	J=	1	X=	33.8650	DX=	3.8650	Y=	8.7139	Z=	0.0000	RHO=	0.6501	MACH=	0.9694	CP=	-0.3701
I=	20	J=	1	X=	33.3552	DX=	3.3552	Y=	8.6534	Z=	0.0000	RHO=	0.6442	MACH=	0.9805	CP=	-0.3936
I=	21	J=	1	X=	32.9029	DX=	2.9029	Y=	8.5925	Z=	0.0000	RHO=	0.6366	MACH=	0.9912	CP=	-0.4161
I=	22	J=	1	X=	32.5017	DX=	2.5017	Y=	8.5321	Z=	0.0000	RHO=	0.6298	MACH=	1.0078	CP=	-0.4510
I=	23	J=	1	X=	32.1461	DX=	2.1461	Y=	8.4727	Z=	0.0000	RHO=	0.6206	MACH=	1.0253	CP=	-0.4874
I=	24	J=	1	X=	31.8309	DX=	1.8309	Y=	8.4143	Z=	0.0000	RHO=	0.6185	MACH=	1.0293	CP=	-0.4956
I=	25	J=	1	X=	31.5518	DX=	1.5518	Y=	8.3572	Z=	0.0000	RHO=	0.6270	MACH=	1.0132	CP=	-0.4623
I=	26	J=	1	X=	31.3047	DX=	1.3047	Y=	8.3016	Z=	0.0000	RHO=	0.6212	MACH=	1.0242	CP=	-0.4852
I=	27	J=	1	X=	31.0863	DX=	1.0863	Y=	8.2472	Z=	0.0000	RHO=	0.5875	MACH=	1.0888	CP=	-0.6164
I=	28	J=	1	X=	30.8934	DX=	0.8934	Y=	8.1941	Z=	0.0000	RHO=	0.5575	MACH=	1.1475	CP=	-0.7307
I=	29	J=	1	X=	30.7233	DX=	0.7233	Y=	8.1422	Z=	0.0000	RHO=	0.5333	MACH=	1.1957	CP=	-0.8212
I=	30	J=	1	X=	30.5736	DX=	0.5736	Y=	8.0913	Z=	0.0000	RHO=	0.5146	MACH=	1.2338	CP=	-0.8900
I=	31	J=	1	X=	30.4421	DX=	0.4421	Y=	8.0418	Z=	0.0000	RHO=	0.5021	MACH=	1.2595	CP=	-0.9351
I=	32	J=	1	X=	30.3270	DX=	0.3270	Y=	7.9934	Z=	0.0000	RHO=	0.4961	MACH=	1.2679	CP=	-0.9497
I=	33	J=	1	X=	30.2273	DX=	0.2273	Y=	7.9448	Z=	0.0000	RHO=	0.5037	MACH=	1.2563	CP=	-0.9295
I=	34	J=	1	X=	30.1433	DX=	0.1433	Y=	7.8935	Z=	0.0000	RHO=	0.7518	MACH=	0.7775	CP=	0.0498
I=	35	J=	1	X=	30.0763	DX=	0.0763	Y=	7.8377	Z=	0.0000	RHO=	0.8173	MACH=	0.6482	CP=	0.3332
I=	36	J=	1	X=	30.0295	DX=	0.0295	Y=	7.7765	Z=	0.0000	RHO=	0.8769	MACH=	0.5148	CP=	0.6078
I=	37	J=	1	X=	30.0058	DX=	0.0058	Y=	7.7134	Z=	0.0000	RHO=	0.9203	MACH=	0.4109	CP=	0.7971
I=	38	J=	1	X=	30.0057	DX=	0.0057	Y=	7.6401	Z=	0.0000	RHO=	0.9564	MACH=	0.2998	CP=	0.9647
I=	39	J=	1	X=	30.0294	DX=	0.0294	Y=	7.5533	Z=	0.0000	RHO=	0.9862	MACH=	0.1670	CP=	1.1048
I=	40	J=	1	X=	30.0778	DX=	0.0778	Y=	7.4648	Z=	0.0000	RHO=	0.9996	MACH=	0.0265	CP=	1.1687
I=	41	J=	1	X=	30.1505	DX=	0.1505	Y=	7.3792	Z=	0.0000	RHO=	0.9939	MACH=	0.1105	CP=	1.1415
I=	42	J=	1	X=	30.2456	DX=	0.2456	Y=	7.2961	Z=	0.0000	RHO=	0.9725	MACH=	0.2369	CP=	1.0400
I=	43	J=	1	X=	30.3620	DX=	0.3620	Y=	7.2221	Z=	0.0000	RHO=	0.9420	MACH=	0.3477	CP=	0.8975
I=	44	J=	1	X=	30.4992	DX=	0.4992	Y=	7.1515	Z=	0.0000	RHO=	0.9067	MACH=	0.4417	CP=	0.7438
I=	45	J=	1	X=	30.6578	DX=	0.6578	Y=	7.0864	Z=	0.0000	RHO=	0.8767	MACH=	0.5198	CP=	0.5979

Figure 41. Continued.

3.4 SAMPLE CASE NO. 4

This sample case is concerned with the flow field computation for the CALAC4 nacelle using a (67 X 25 X 16)-point grid. The computational mesh for this case is generated by executing Sample Case No. 4 for the NGRIDA program.

The data deck for this sample case is illustrated in Figure 42. All input parameters in NAMELIST LIST1 retain their default values except for XMFS, CRATIO, PITCH, ITMAX, KMACH, and KCP. For this case, the free-stream Mach number XMFS is 0.6, the capture ratio CRATIO is 0.505, and the angle of attack PITCH is 1.083 degrees. To ensure convergence, ITMAX has been increased to 300. The surface solution is to be plotted for the meridians at 0.0 degrees, 90.0 degrees, and 180.0 degrees; hence, KMACH(1)=1,5*0,1,5*0,1,12*0 and KCP(1)=1,5*0,1,5*0,1,12*0 are entered in NAMELIST LIST1.

Since a (67 X 25 X 16)-point grid will be employed, JMAX=25 and KMAX=16 are entered in NAMELIST LIST2. IMAX is retained at its default value of 67.

All input parameters in NAMELIST LIST3 retain their default values except for ALPHAL, ALPHAH, and CORFAT. To optimize convergence speed, ALPHAL=0.4 and ALPHAH=4.0 are entered. These values were obtained by numerical experiment. Since 16 radial stations are to be used, the elements of the CORFAT array need to be altered from their default values. This array is now specified as CORFAT(K)=.2, .25, .3, .35, .4, .45, .5, .6, .7, .8, .9, and 5*1.0 for K=1 to K=16, respectively. Note that CORFAT(1)=.2 and CORFAT(KMAX)=1.0 as in the default assignment.

All parameters in NAMELIST LIST4 retain their default assignments since no debug output is to be printed.

Selected portions for the computer output for Sample Case No. 4 are presented in Figure 43. Results for the CALAC4 nacelle are presented in Section II.

4. SUGGESTIONS FOR USAGE

4.1 PARAMETER STATEMENT USAGE

The NGRIDA grid generation program and the NACELLE flow analysis program have been executed on the VAX-11/780 and CRAY-1 computers. Both the NGRIDA and NACELLE programs employ PARAMETER statements which fix the respective array dimensions at the time of compilation. This provides an effective means of changing program core storage requirements. The VAX version of each program employs an INCLUDE statement which inserts the respective PARAMETER statement at the appropriate locations within the code. The NGRIDA and NACELLE programs employ the 'INCLUDE 'NGRID.DIM'' and 'INCLUDE 'NACELLE.DIM'' statements, respectively. If the codes are executed on a VAX, then the NGRID.DIM and NACELLE.DIM files must reside in the user's directory. For execution on the CRAY-1 or CDC computers, the PARAMETER statement is edited into the code by use of a COMDECK. For use

```
$LIST1 XMFS=0.6, CRATIO=0.505, PITCH=1.083, ITMAX=300,
KMACH(1)=1, 5*0, 1, 5*0, 1, 12*0,
KCP(1)=1, 5*0, 1, 5*0, 1, 12*0 $END
$LIST2 KMAX=16, JMAX=25 $END
$LIST3 ALPHAL=0.4, ALPHAH=4.0,
CORFAT(1)= .2, .25, .3, .35, .4, .45, .5, .6, .7, .8, .9, 5*1.0 $END
$LIST4 $END
```

Figure 42. Data deck for NACELLE Sample Case No. 4.

LISTING OF INPUT DATA

```
$LIST1
PITCH   =   1.083000    ,
YAW     =  0.0000000E+00,
XMFS    =  0.6000000    ,
XMCF    =  0.3516000    ,
CRATIO  =  0.5050000    ,
GAMMA   =   1.400000    ,
KPLOT   =             1,
ITDUMP  =             0,
KORDER  =             0,
KINIT   =             1,
KPRCOR  =             0,
KPRINT  =          1000,
ITMAX   =           300,
CRIT    =  1.0000000E-03,
KDFV    =             1,
KMACH   =             1, 5*0,          1, 5*0,          1, 12*0,
KCP     =             1, 5*0,          1, 5*0,          1, 12*0,
XMTOP   =   1.500000    ,
XMULM   =  0.7000000    ,
SCALE   =   8.400000
$END
$LIST2
IMAX    =            67,
JMAX    =            25,
KMAX    =            16,
ITREAD  =             1,
ITRAN1  =  16*0,
ITRAN2  =             0,
ITRAN3  =             0,
IBEG    =             0
$END
$LIST3
KALPHA  =             1,
ALPHAL  =  0.4000000    ,
ALPHAH  =   4.000000    ,
```

Figure 43. Output for NACELLE Sample Case No. 4

SURFACE SOLUTION FOR ITERATION NO.= 227

I=	0	J=	1	X=	70.0000	DX=	40.0000	Y=	9.0000	Z=	0.0000	RHO=	0.8405	MACH=	0.6000	CP=	0.0000
I=	1	J=	1	X=	67.7331	DX=	37.7331	Y=	9.0000	Z=	0.0000	RHO=	0.8417	MACH=	0.5974	CP=	0.0082
I=	2	J=	1	X=	63.4511	DX=	33.4511	Y=	9.0000	Z=	0.0000	RHO=	0.8425	MACH=	0.5957	CP=	0.0133
I=	3	J=	1	X=	59.6449	DX=	29.6449	Y=	9.0000	Z=	0.0000	RHO=	0.8408	MACH=	0.5993	CP=	0.0022
I=	4	J=	1	X=	56.2616	DX=	26.2616	Y=	9.0000	Z=	0.0000	RHO=	0.8392	MACH=	0.6027	CP=	-0.0085
I=	5	J=	1	X=	53.2542	DX=	23.2542	Y=	9.0000	Z=	0.0000	RHO=	0.8376	MACH=	0.6061	CP=	-0.0190
I=	6	J=	1	X=	50.5810	DX=	20.5810	Y=	9.0000	Z=	0.0000	RHO=	0.8360	MACH=	0.6093	CP=	-0.0291
I=	7	J=	1	X=	48.2048	DX=	18.2048	Y=	9.0000	Z=	0.0000	RHO=	0.8340	MACH=	0.6136	CP=	-0.0424
I=	8	J=	1	X=	46.0926	DX=	16.0926	Y=	9.0000	Z=	0.0000	RHO=	0.8317	MACH=	0.6184	CP=	-0.0577
I=	9	J=	1	X=	44.2151	DX=	14.2151	Y=	9.0000	Z=	0.0000	RHO=	0.8289	MACH=	0.6243	CP=	-0.0761
I=	10	J=	1	X=	42.5463	DX=	12.5463	Y=	9.0000	Z=	0.0000	RHO=	0.8256	MACH=	0.6312	CP=	-0.0980
I=	11	J=	1	X=	41.0628	DX=	11.0628	Y=	9.0000	Z=	0.0000	RHO=	0.8216	MACH=	0.6394	CP=	-0.1240
I=	12	J=	1	X=	39.7442	DX=	9.7442	Y=	9.0000	Z=	0.0000	RHO=	0.8167	MACH=	0.6494	CP=	-0.1558
I=	13	J=	1	X=	38.5721	DX=	8.5721	Y=	9.0000	Z=	0.0000	RHO=	0.8101	MACH=	0.6629	CP=	-0.1992
I=	14	J=	1	X=	37.5302	DX=	7.5302	Y=	8.9980	Z=	0.0000	RHO=	0.8003	MACH=	0.6827	CP=	-0.2631
I=	15	J=	1	X=	36.6043	DX=	6.6043	Y=	8.9842	Z=	0.0000	RHO=	0.7905	MACH=	0.7021	CP=	-0.3259
I=	16	J=	1	X=	35.7817	DX=	5.7817	Y=	8.9536	Z=	0.0000	RHO=	0.7838	MACH=	0.7153	CP=	-0.3693
I=	17	J=	1	X=	35.0513	DX=	5.0513	Y=	8.9113	Z=	0.0000	RHO=	0.7778	MACH=	0.7271	CP=	-0.4079
I=	18	J=	1	X=	34.4029	DX=	4.4029	Y=	8.8606	Z=	0.0000	RHO=	0.7719	MACH=	0.7387	CP=	-0.4458
I=	19	J=	1	X=	33.8275	DX=	3.8275	Y=	8.8036	Z=	0.0000	RHO=	0.7661	MACH=	0.7498	CP=	-0.4825
I=	20	J=	1	X=	33.3173	DX=	3.3173	Y=	8.7427	Z=	0.0000	RHO=	0.7604	MACH=	0.7610	CP=	-0.5191
I=	21	J=	1	X=	32.8648	DX=	2.8648	Y=	8.6798	Z=	0.0000	RHO=	0.7541	MACH=	0.7730	CP=	-0.5588
I=	22	J=	1	X=	32.4639	DX=	2.4639	Y=	8.6159	Z=	0.0000	RHO=	0.7474	MACH=	0.7859	CP=	-0.6011
I=	23	J=	1	X=	32.1087	DX=	2.1087	Y=	8.5518	Z=	0.0000	RHO=	0.7403	MACH=	0.7995	CP=	-0.6460
I=	24	J=	1	X=	31.7942	DX=	1.7942	Y=	8.4882	Z=	0.0000	RHO=	0.7328	MACH=	0.8136	CP=	-0.6926
I=	25	J=	1	X=	31.5161	DX=	1.5161	Y=	8.4254	Z=	0.0000	RHO=	0.7251	MACH=	0.8283	CP=	-0.7410
I=	26	J=	1	X=	31.2702	DX=	1.2702	Y=	8.3638	Z=	0.0000	RHO=	0.7174	MACH=	0.8428	CP=	-0.7887
I=	27	J=	1	X=	31.0532	DX=	1.0532	Y=	8.3033	Z=	0.0000	RHO=	0.7120	MACH=	0.8530	CP=	-0.8220
I=	28	J=	1	X=	30.8619	DX=	0.8619	Y=	8.2439	Z=	0.0000	RHO=	0.7148	MACH=	0.8477	CP=	-0.8049
I=	29	J=	1	X=	30.6938	DX=	0.6938	Y=	8.1855	Z=	0.0000	RHO=	0.7148	MACH=	0.8098	CP=	-0.6801
I=	30	J=	1	X=	30.5463	DX=	0.5463	Y=	8.1281	Z=	0.0000	RHO=	0.6815	MACH=	0.9103	CP=	-1.0091
I=	31	J=	1	X=	30.4175	DX=	0.4175	Y=	8.0717	Z=	0.0000	RHO=	0.4903	MACH=	1.2842	CP=	-2.1019
I=	32	J=	1	X=	30.3054	DX=	0.3054	Y=	8.0164	Z=	0.0000	RHO=	0.4624	MACH=	1.3443	CP=	-2.2491
I=	33	J=	1	X=	30.2089	DX=	0.2089	Y=	7.9616	Z=	0.0000	RHO=	0.4522	MACH=	1.3668	CP=	-2.3020
I=	34	J=	1	X=	30.1286	DX=	0.1286	Y=	7.9046	Z=	0.0000	RHO=	0.4588	MACH=	1.3521	CP=	-2.2677
I=	35	J=	1	X=	30.0663	DX=	0.0663	Y=	7.8435	Z=	0.0000	RHO=	0.4766	MACH=	1.3135	CP=	-2.1749
I=	36	J=	1	X=	30.0247	DX=	0.0247	Y=	7.7785	Z=	0.0000	RHO=	0.7722	MACH=	0.7380	CP=	-0.4435
I=	37	J=	1	X=	30.0048	DX=	0.0048	Y=	7.7137	Z=	0.0000	RHO=	0.8227	MACH=	0.6371	CP=	-0.1166
I=	38	J=	1	X=	30.0057	DX=	0.0057	Y=	7.6401	Z=	0.0000	RHO=	0.8830	MACH=	0.5052	CP=	0.2838
I=	39	J=	1	X=	30.0294	DX=	0.0294	Y=	7.5533	Z=	0.0000	RHO=	0.9361	MACH=	0.3659	CP=	0.6462
I=	40	J=	1	X=	30.0778	DX=	0.0778	Y=	7.4648	Z=	0.0000	RHO=	0.9744	MACH=	0.2286	CP=	0.9125
I=	41	J=	1	X=	30.1505	DX=	0.1505	Y=	7.3792	Z=	0.0000	RHO=	0.9946	MACH=	0.1046	CP=	1.0547
I=	42	J=	1	X=	30.2456	DX=	0.2456	Y=	7.2981	Z=	0.0000	RHO=	1.0000	MACH=	0.0011	CP=	1.0933
I=	43	J=	1	X=	30.3620	DX=	0.3620	Y=	7.2221	Z=	0.0000	RHO=	0.9962	MACH=	0.0870	CP=	1.0665
I=	44	J=	1	X=	30.4992	DX=	0.4992	Y=	7.1515	Z=	0.0000	RHO=	0.9880	MACH=	0.1559	CP=	1.0081
I=	45	J=	1	X=	30.6578	DX=	0.6578	Y=	7.0864	Z=	0.0000	RHO=	0.9782	MACH=	0.2106	CP=	0.9392

Figure 43. Continued.

on other computer systems, the PARAMETER statements will have to be inserted in the respective programs at the locations noted by the INCLUDE statements.

4.2 NGRIDA PROGRAM USAGE

The NGRIDA grid generation program often can be executed by retaining most of the input parameters at their respective default values. Maintaining the outer computational boundary at the same distance from the body, relative to the compressor face radius (RCF), as was done in the supplied sample cases should be sufficient for most new applications of the program. This can be accomplished by maintaining the ratios RADOUT/RCF, XLEFT/RCF, and DELTA/RCF the same as in the sample cases provided herein.

For transonic flow computations, supercritical flow occurs generally in the external flow region that is slightly downstream of the inlet lip. The mesh resolution can be enhanced in this region by increasing the mesh stretching parameter ALPHAO beyond its default value of 1.1. The ξ-mesh spacing is quite sensitive to ALPHAO and only a small increase beyond its default value is usually required. Increasing the number of circumferential stations, denoted by JMAX, generally improves the ability of the flow analysis program to predict the Mach number distribution peaks, especially on the external surface of the leeward meridian.

In the sample cases provided herein, the grid coordinates are down-scaled by setting the SCALE input parameter equal to the reciprocal of the compressor face radius. This practice is recommended as it produces a computational mesh with a compressor radius of unity and thereby sizes the grid so that the default AF2 algorithm acceleration parameters, denoted by ALPHAL and ALPHAH in the NACELLE program input, are approximately optimum. The original coordinates can then be recovered in the NACELLE flow solution program by setting the SCALE input parameter in that code equal to the compressor face radius.

Generally, the GRAPE algorithm input parameters specified in NAMELISTS LIST3 and LIST4 of the NGRIDA program are retained at their default values. If a nacelle with a very sharp inlet lip is to be analyzed, however, it may be necessary to reduce or equate to 0.0 the values of OMEGP and OMEGQ in NAMELIST LIST4. This relaxes the enforcement of the grid spacing and orthogonality conditions at the nacelle surface and should permit a converged grid solution to be obtained.

4.3 NACELLE PROGRAM USAGE

The NACELLE flow analysis program often can be executed by retaining most of the input parameters at their respective default values. For cases with very strong shocks or high local supersonic Mach numbers, the artificial viscosity parameter CFACT and the time-like dissipation factor BXIE will probably have to be increased over their default values of 1.2 and 0.1, respectively. Increasing CFACT while holding BXIE at its default value for a typical case can decrease the number of iterations required for convergence. However, increasing CFACT generally decreases shock wave resolution which is indicated by a slight smearing of the surface pressure distribution in the vicinity of the shock. Increasing BXIE generally

decreases convergence speed but ensures numerical stability by maintaining diagonal dominance in the ξ-factorized difference equations.

The AF2 acceleration parameters ALPHAL and ALPHAH and the potential correction under-relaxation array CORFAT will require input values different from the default values if different size grids are employed. The default values of ALPHAL=0.175 and ALPHAH=6.0 were obtained by numerical experiment to produce the optimum convergence speed on the (67 x 13 x 13)-point default computational mesh. If finer meshes are to be used, ALPHAL and ALPHAH will have to be altered. For a (67 x 25 x 16)-point grid, ALPHAL=0.4 and ALPHAH=4.0 provided good convergence speed. Because of the non-linear nature of the analysis, it is not possible to predetermine the optimum values of the α parameters, hence they generally are determined by numerical experiment for a given grid size. Minor alterations in the surface geometry generally have little effect on convergence speed once the acceleration parameters are optimized for a given grid size.

If the number of radial stations, denoted by KMAX, is changed then so must the CORFAT potential correction under-relaxation array. It is recommended that CORFAT(1) $\simeq$ .15, .2 and that CORFAT(KMAX)=1.0. The remaining elements of the CORFAT array should vary between these extremes and should monotonically increase with increasing K-index. Generally, fastest convergence is attained if the maximum residual occurs on the body surface and not near the centerline. If it occurs near the centerline, then slightly increasing the first few elements of the CORFAT array should move it to the body.

REFERENCES

1. Ballhaus, W. F., Jameson, A., and Albert, J., "Implicit Approximate-Factorization Schemes for Steady Transonic Flow Problems," AIAA Journal, Vol. 16, June 1978, pp. 573-579.

2. Holst, T. L., "An Implicit Algorithm for the Conservative Transonic Full Potential Equation Using an Arbitrary Mesh," AIAA Journal, Vol. 17, Oct. 1979, pp. 1038-1045.

3. Holst, T. L., and Thomas, S. D., "Numerical Solution of Transonic Wing Flow Fields," AIAA Paper No. 82-0105, Jan. 1982.

4. Atta, E. H., and Vadyak, J., "A Grid Interfacing Zonal Algorithm for Three-Dimensional Transonic Flows About Aircraft Configurations," AIAA Paper No. 82-1017, June 1982; see also: "A Grid Overlapping Scheme for Flowfield Computations About Multicomponent Configurations," AIAA Journal, Vol. 21, September 1983, pp. 1271-1277.

5. Atta, E. H., and Vadyak, J., "A Grid Embedding Transonic Flow Analysis Computer Program for Wing/Nacelle Configurations", NASA CR-166529, 1983.

6. Sorensen, R. L., "A Computer Program to Generate Two-Dimensional Grids About Airfoils and Other Shapes by Use of Poisson's Equation," NASA TM-81198, 1980.

7. Jameson, A., "Transonic Flow Analysis for Axially Symmetric Inlets with Centerbodies," Report No. 2, Antony Jameson and Associates, Inc., Princeton, New Jersey, Dec. 1981.

8. Results from the Joint NASA/Industry Subsonic Inlet Design Technology Testing Program conducted at NASA-Langley, 1982.

9. DISSPLA MANUAL, Integrated Software Systems Corporation, San Diego, California, Dec. 1980.